The Dissertation Committee for Joshua Morgan Woodruff
certifies that this is the approved version of the following dissertation:

Discretization in decision analysis

Committee:

Dr. J. Eric Bickel, Supervisor

Dr. Benjamin Leibowicz

Dr. Ofodike Ezekoye

Dr. John Hasenbein

Discretization in decision analysis

by

Joshua Morgan Woodruff, B.S., M.S.

DISSERTATION

Presented to the Faculty of the Graduate School of

The University of Texas at Austin

in Partial Fulfillment

of the Requirements

for the Degree of

DOCTOR OF PHILOSOPHY

THE UNIVERSITY OF TEXAS AT AUSTIN

August 2020

Discretization in decision analysis

Publication No. ____________________

Joshua Morgan Woodruff, Ph.D.
The University of Texas at Austin, 2020

Supervisor: Dr. J. Eric Bickel

The choice of discretizations in Decision Analysis impacts the accuracy of the probabilistic analysis of the potential strategies. This dissertation introduces a novel method for creating discretizations for specific problems. Next, we introduce the distance metric, which is borrowed from stochastic optimization. This metric indicates how well two cumulative distribution functions match each other in terms of shape. Discretizations that better match the shape are more accurate in estimating the value of a cumulative distribution function at any given percentile. We determine under which conditions the distance is higher or lower, and which discretizations to choose. Finally, we show what happens to the accuracy of discretizations when there is assessment error and how this impacts the choice of discretizations.

Table of Contents

List of Tables

List of Figures

Chapter 1

Introduction

1.1 A Brief Review of Discretization

Decision analysis seeks to help people and companies make infrequent, high-value decisions and to refine the strategy of executing those decisions. One example of such a decision is whether to launch a product. Parts of the launch strategy might be whether to launch the product immediately or research the market more and whether to have local or international branding. In such a decision, there are uncertainties that will affect the outcome for the company. Some examples of the uncertainties are the potential market size, the potential market share, the arrival of the next competitor, and the costs of different marketing campaigns. Decision analysts use the distributions of these uncertainties to determine the highest value strategy. All the potential strategies and all the potential uncertainties could be simulated to provide a distribution of the potential results for each strategy. A challenge for the decision analyst is that it is impossible to know the functional form of an uncertainty when there is little to no data about the uncertainties from which to form an estimate of the parameters of the distributions.

If the decision analyst has the functional form of each uncertainty, then he or she could draw random samples from each uncertainty and simulate potential values for the different strategies. The process of drawing random project values from a strategy and random realizations of the uncertainties is called the value lottery. From the value lottery the decision analyst can calculate the mean, standard deviation, and performance at different percentiles and determine other relevant statistics that will help in the decision of which strategy to use. Using these statistics, the decision analyst helps the client determine the best strategy, or whether to continue researching the uncertainties or create a new strategy. But in making decisions about infrequent, potentially unique, strategic decisions, the functional form of the distributions of the uncertainties is unlikely to be available. This is the nature of making strategic decisions that will take a company into new territory.

In order to execute a probabilistic analysis of the strategies, the decision analyst needs a distribution for each uncertainty. These distributions come in the form of discretizations when the functional form is not available. A discretization reduces a larger, possibly continuous, distribution into a probability mass function of usually three points [19]. A discretization is a mapping of a continuous distribution to a smaller probability mass function. Each point is referred to by its percentile. For example, the 10^{th} percentile is the $P10$. In decision analysis, where there may be many uncertainties all with different functional forms, it is common to refer to the values by their percentile, such as the $P10$ of the market share and the $P50$ of the demand. More formally, if x_p is a value from the distribution X, where p is a percentile, then $p = CDF_X(x_p)$. The $P10$ of the standard normal distribution is -1.28. The number of points in a discretization is usually small because estimating more points may be expensive. Three points is enough to replicate the first five moments of an uncertainty [40], and is often used in practice.

In using a discretization decision analysts may lose many details of the original problem, and the accuracy of various metrics suffers. While computa-

Table 1.1: Commonly used discretization shortcuts

Shortcut	Percentile points	Probability weights
EPT	P5, P50, P95	0.185, 0.630, 0.185
ESM	P10, P50, P90	0.300, 0.400, 0.300
MCS	P10, P50, P90	0.250, 0.500, 0.250

Each shortcut has its proponents in industry and there are trade-offs to selecting one over another.

tional ease is no longer a concern, discretizations reduced the computational cost of calculating statistics, and also serve to simplify communication. When displaying large jumps in the value of a strategy, the decision analyst is able to point out which jump in the value of an uncertainty was responsible for the change in value. Discretizations significantly improve a decision analyst's ability to communicate with clients [25]. Even with an increase in computing power, discretizations allow for human-understandable assessment and evaluation of decisions.

In choosing a discretization a decision analyst seeks to preserve the mean, variance, or other metrics. There are several common shortcuts that are used in industry. The two most common methods are the McNamee-Celona Shortcut (MCS) and the Extended Swanson-Megill (ESM) method. These methods use the $P10, P50$, and $P90$. ESM is commonly used in the oil and gas industry [3]. These discretizations are described in [15]. Most discretizations use the $P50$, and in this dissertation we refer to the low and high values as the *extreme* percentiles. ESM places more weight on the extreme points than MCS. Keefer and Bodily [19] proposed the Extended Pearson-Tukey method which uses percentiles at the 5^{th}, 50^{th}, and 95^{th} percentiles. The percentiles and probabilities for these shortcut discretizations are given in Table 1.1.

The benefit of shortcut discretizations is that they require no knowledge of the functional forms of the underlying discretizations. In order to use the values at each percentile, decision analysts rely on assessments. These assessments are educated guesses as to the true value at the required percentiles. The percentiles that are closer to the 50^{th} percentile are usually easier to assess accurately than those that are at more extreme. Thus, it is easier to accurately assess the 10^{th} and 90^{th} percentiles than the $5th$ and 95^{th} percentiles. A person with less experience is not as likely to have seen as many extreme events as a more experienced expert. In decision analysis practice, $10-50-90$ discretizations are used more commonly.

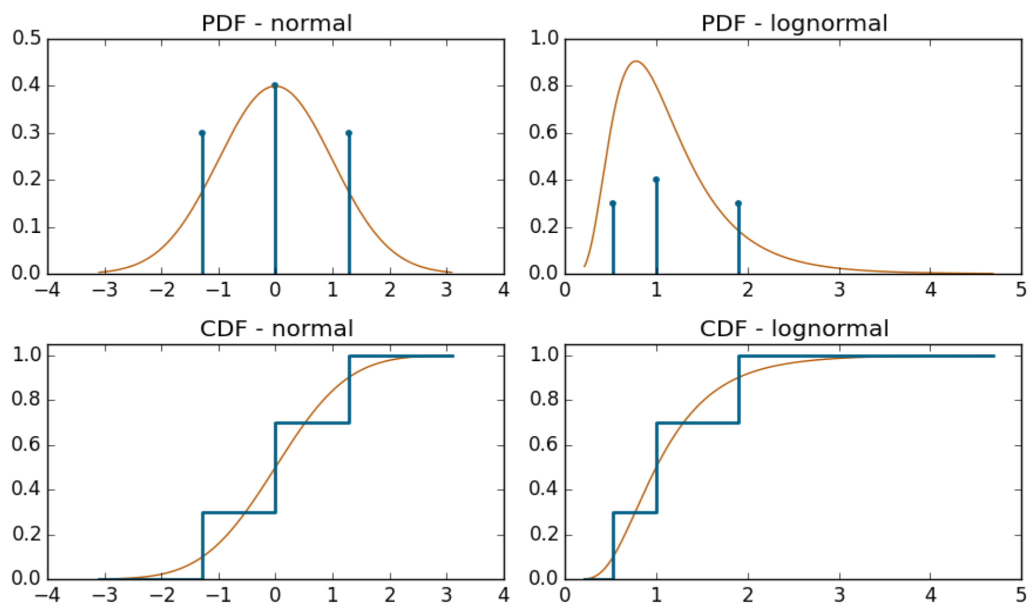

Figure 1.1: These are two examples of the same three-point discretization applied to a standard normal and a log-normal distribution. The placement of the points on the independent axis are determined by the percentiles of the discretization, and the height is based on the probabilities assigned.

The shortcut discretizations are based on calculating the optimal percentiles and probabilities for a few specific distributions, and they are applied to a larger set of distributions. When using a shortcut, the decision analyst and the experts he or she relies upon do not need to know the functional form, they just need to be able to assess a few specific percentiles. Another popular method for calculating discretizations is to use Gaussian quadrature (GQ). In GQ, the functional form of the discretization does not need to be known, but the first $2N - 1$ moments do need to be known. In this problem, N is the number of points in the discretization. Smith showed how this technique creates accurate discretizations [40] that when combined in a sample problem estimate the certain equivalent better than shortcuts such as EPT and MCS. To determine the GQ discretizations requires the use of linear algebra software to compute the values of the percentiles and probabilities.

There are a few considerations when considering GQ. The first is that the discretization is specific to the distribution that it is discretizing. This discretization matches the first $2N - 1$ moments and the more these values change from one uncertainty to another, the less reliable they will be for a different uncertainty. A second consideration is that the percentiles that come from GQ are neither intuitive nor easily assessable. For example, in [40], some sample values for the percentiles are 0.0416 and 0.9975. The assessment error on such specific and sometimes extreme values makes discretizations developed from GQ less practical, and may even require full knowledge of the underlying uncertainty. If the value of the underlying uncertainty is already known, various simulation methods may result in more accurate metrics and are not overly expensive to calculate. This is especially true as the number of uncertainties grows and the Cartesian combination of percentiles from each uncertainty grows exponentially.

In recent years, research by Hammond and Bickel produced a new class of discretizations [12]. These discretizations are shortcuts. They do not require any knowledge of the moments or the functional form of the uncertainty, but these discretizations do allow decision analysts to leverage additional information that is available about the uncertainty in selecting a discretization. This additional information yields more accurate discretizations. The Hammond and Bickel shortcuts (HB) require knowledge of the shape (bell, U, or J), the boundedness (unbounded, bounded on one side, or bounded), and the skewness (positive or negative). Based on the combination of the shape, boundedness, and skewness, the potential distribution falls into a region of the Pearson distribution system.

1.2 The Pearson Distribution System

The Pearson distribution system was first described by Karl Pearson in [30] and further expanded in [31] and [32]. A distribution in the Pearson system is the solution to the following differential equation:

$$\frac{1}{f} \cdot \frac{df}{dx} = \frac{b - x}{c_0 + c_1 \cdot x + c_2 \cdot x^2} \tag{1.1}$$

The parameters, b, c_0, c_1, c_2, determine the first four moments and consequently the shape of a distribution. A distribution may be described by the skewness, γ_1, and kurtosis, β_2. The distributions are symmetrical with respect to γ_1 and squared skewness, $\beta_1 = \gamma_1^2$, is used.

For any combination of β_1 and β_2 such that $\beta_2 \geq \beta_1 + 1$ the resulting distribution will fall into only one sub-family of distributions within the Pearson system. For this reason, it is possible to choose a distribution and consequently a discretization based on skewness and kurtosis. The result is that it is possible to use the Pearson system to approximate many of the uncertainties in a decision analysis problem.

Figure 1.2 shows a common representation of the Pearson distribution system. The type of distribution is dependent on the square of the skewness and the kurtosis of the uncertainty. Each of the regions also has a distinct shape and boundedness. Many common distributions can be modeled using the formulas from the Pearson system. One of the few commonly used distributions in decision analysis that cannot be explicitly modeled using the Pearson system is the log-normal distribution. The log-normal's squared skewness and kurtosis values can be plotted on the Pearson system, but the exact distribution cannot be plotted with the Pearson system formulas. While this information is not likely to be known, a decision analyst and an expert on the uncertainty are likely to know whether or not the uncertainty is positively or negatively skewed, and whether or not it is bounded on both sides, or one side. In decision analysis uncertainties are rarely unbounded. Experts are also likely to know whether the uncertainty is bell-shaped, J-shaped, or U-shaped. Knowing this information is enough to also determine the region of the Pearson distribution system into which an uncertainty may be placed.

When using the Pearson system, there are a few tests that determine the underlying distribution and the most appropriate discretization. If the distribution is bounded on both sides, then the distribution is a beta distribution. The type of beta distribution may be further refined by the knowledge that the distribution is bell-shaped, U-shaped, or J-shaped. Two examples of bounded uncertainties are market share and the oil extraction percentage. Both are percentage numbers that cannot go higher than 100% or lower than 0%. The other meaningful area for decision analysts is the beta prime area (Pearson VI). This

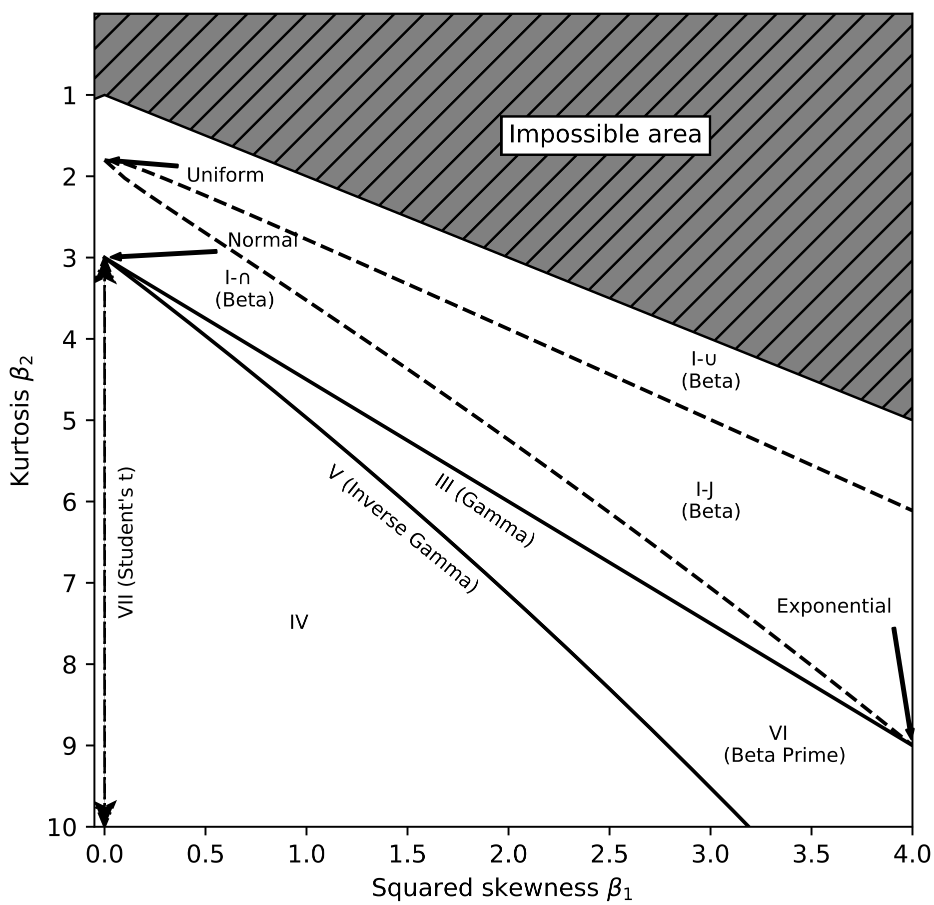

Figure 1.2: The distributions of the Pearson system are defined by the skew and kurtosis values. Given some properties of an uncertainty, it is possible to determine the region or regions where the distribution might lie.

area represents uncertainties that are bounded on one side, but unbounded on the other. For example, project development time or reservoir size are examples of uncertainties that are likely to be bounded from below but whose upper bounds may be extremely large and may be modeled as unbounded on one side. A case could be made that all uncertainties are bounded on both sides and that decision analysts should only consider uncertainties from the beta distribution, but the semi-bounded nature helps incorporate values that might be outside the expected bounds of a person making an assessment.

The benefit of being able to determine the zone in the Pearson systems where an uncertainty lies is that it is possible to find a discretization tailored to that part of the Pearson system. Table 1.2 shows a selection of the non-symmetric discretizations described in [12]. These discretization were created with the objective of minimizing the error of the discretization to that of the true mean and variance of a sampling of the distributions that make up the given Pearson region. This provides a more-specialized discretization without having to know the moments of functional form of the uncertainty. For discretizations with negative skewness, the decision analyst selects the $1 - P$ values and uses the probabilities in reverse order.

1.3 Problem-specific Discretizations

Most work on discretizations has focused on discretizing individual distributions. Researchers have sought to match one or more moments of potential distributions. When value lottery is transformed by a utility function, which often involves exponential values or log value, some accuracy may be lost. In addition to requiring more knowledge regarding the uncertainty, [4] found that moment matching did not accurately match the certain equivalent (CE). The

Table 1.2: A Selection of Discretization from [12]

Distribution type	Percentile points	Probability weights
I-∪ Beta	P1, P50, P85	0.216, 0.491, 0.293
I-J Beta	P2, P50, P94	0.184, 0.615, 0.201
I-∩ Beta	P5, P50, P95	0.184, 0.632, 0.184
Pearson IV	P7, P50, P94	0.231, 0.551, 0.218
VI Beta Prime	P4, P50, P96	0.164, 0.672, 0.164

This sampling of the [12] discretizations show the asymmetric, positively skewed discretizations for the most common areas of the Pearson systems that are of interest to decision anaylsis. The discretizations for the negatively skewed distributions use $1-P$ for the percentile points and reverse the order for the probabilities.

certain equivalent is a risk adjusted mean. For example, most people would value a bet with equal chances of a \$0 payout or a \$2 payout at the expected value of \$1. But as the value of the payoff rises, fewer people would be willing to wager the expected value. If the payout were $\$2,000,000$, few people would be willing to put all their life savings into a single bet that could wipe out their life savings and keep them in debt for life. Both individuals and companies may feel this risk aversion as the required investment increases. As a result, a decision analyst may need to apply a utility function to the results. Utility functions weigh negative results more heavily than positive results. In general three-point approximations produce “substantial” errors in the CE values they produce [18] (P. 763).

In industry, there are often problems that repeat themselves while still remaining unique. Oil and gas companies are constantly developing oil fields, and consumer and packaged goods (CPG) and pharmaceutical companies are constantly developing and launching new products or drugs. Each oil field, product or drug is different. When the quantity and type of uncertainties is the same from decision to decision, it is possible to use problem-specific discretizations. These discretizations are similar to other N-point discretizations in that they determine a N percentiles and corresponding probabilities for each uncertainty. They differ in that the discretizations act in unison to minimize the error of the problem's CE.

The benefit of problem-specific discretizations and that they are more accurate in determining the CE of a decision and use easy-to-assess percentiles. The drawback is that each problem-specific discretization must be calculated based on a the results of a large Cartesian combination of potential uncertainties. Once this up-front calculation is complete, the problem-specific discretization functions like a shortcut designed for the repeated decision.

1.4 Shape-matching Discretizations

When using shortcuts such as EPT and HB [12], academic analysis focuses on the accuracy of the mean of the results. In a decision problem where the decision maker is risk neutral, a positive mean for the net present value indicates that the decision maker should undertake the project. Even though though a company might be close to risk-neutral when making a decision, the individual making the decision is likely to be more concerned with the downside risks of a decision.

The individual will want to know the investment risk, the probability the net present value (NPV) is negative, or want to know the NPV at a certain P value. Investment risk is the probability the net present value of a decision is less than or equal to a safe alternative. We call these types of metrics shape-matching metrics. These metrics benefit when the CDF of the discretized value lottery is the same as the CDF of the true value lottery. When they are not equal, the absolute difference between the true and the discretized CDF is the distance. The distance is the average absolute difference (horizontal distance) in the value of the CDF between the true and discretized CDFs integrated in the probability range from 0 to 1,

$$d = \mathbb{E}\left|X - \tilde{X}\right|, \tag{1.2}$$

where X is the true value lottery and $\tilde{X}$ is the discretization of X. Distance tells a decision maker what is the mean difference in present values between a discretized value and the true value across all P values. An example of the distance can be seen in Figure 1.3. The true CDF is derived from a version of the Eagle Airlines problem described by [6] and later [36].

1.5 The Effect of Assessment Error on Discretizations

Most analysis of discretizations have assumed assessments are perfectly accurate. With these perfectly accurate assessments, certain discretizations outperform others. But there is little research on which discretization to use when assessment error is considered. The previously mentioned analysis includes errors of the mean, the variance, and the distance. Another type of error is *assessment error*. In assessments an expert is asked to give the values of different p values for each uncertainty. But the expert's assessment may have an error, e_p, that is dependent upon the percentile, p, being assessed. Instead of assessing p, the assessed percentile is actually q_p, and the relation between p and q is $p = q_p - e_p$. This form of assessment error is described in [13].

In this analysis the value of e_p can depend on p. This distinction allows for the difficulty that experts have in assessing extreme events. An expert with

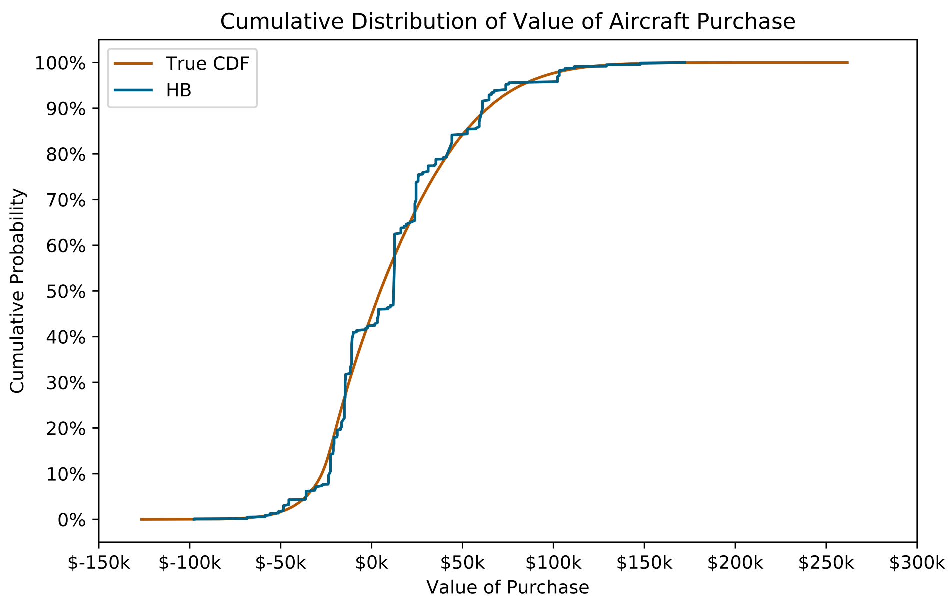

Figure 1.3: A slight perturbation in the value of the safe alternative, and the difference between the true and the discretized value of the investment risk changes drastically. The distance metric is the mean value of the absolute value of the horizontal distance between the true distribution and the discretized distribution at each cumulative probability.

20 years of experience is more likely to have seen events in the 5^{th} and 95^{th} percentiles than someone who only has 10 years of experience. So we can say that the assessed percentile, q_p, is a random distribution dependent on p:

$$p + e_p = q_p, \tag{1.3}$$

and the distribution of e_p is given as a random variable.

Given different assumptions regarding the distributions and correlations of each e_p in a discretization, it is possible to determine when to apply different discretizations depending on the assessment error. We propose to determine the effects of bias, and skewness in the assessment errors and to test the effects of different variances in the assessment errors.

1.6 Organization of the Dissertation

In this chapter, there is a brief introduction to the problems considered in the dissertation. In the following chapters a more-detailed review of the problems, the literature, and the approach taken to solve these problems. We begin with a detailed review of discretization approaches from the literature in Chapter 2. In Chapter 3 we describe a methodology for generating problem-specific discretizations. In Chapter 4 we present new shape-matching discretizations and the methodology for generating them. In chapter 5 we discuss the role of assessment error on the accuracy of the mean and variance of the discretizations. Finally, in Chapter 6 we propose new research and conclude.

The contributions of this dissertation are:

- A novel method for creating problem-specific discretizations.

- The introduction of the distance metric to determine how well discretizations match the shape of a distribution.
- A novel method for modeling assessment error and the effects of different assumptions on discretization accuracy.

Chapter 2

Literature Review

2.1 Discretization Methods

The fields of decision analysis and stochastic optimization have created several approaches to discretization. Both have the end goal of making the correct decision, the decision that would have been made if all the information of the uncertainties had been known.

In decision analysis, discretizations are typically broken up into a few types. The first is a distribution-specific method, the user has knowledge of the functional form of the distribution. In distribution-specific discretizations, the decision analyst must calculate the discretization for each uncertainty. The resulting discretization matches some of the qualities of the original distribution. The second is a shortcut, where the same discretization is applied regardless of what the true functional form might be. A third and more recent type of distribution is a hybrid approach. This approach uses some limited knowledge about the uncertainty's distribution to select the most appropriate discretization.

A common distribution-specific method for formulating discretizations is the bracket-mean method. It was first described by MacNamee and Celona in [23]. In this method, the regions are similarly partitioned by probability, but bracket-mean use the mean value of each region instead of the partition. In addition, [23] go on to recommend that instead of using equal weights for each region, the three-point regions should have probabilities of $0.25, 0.50$, and 0.25. The same probabilities are applied in the MacNamee-Celona Shortcut (MCS). Along with EPT and ESM, these are the three commonly used shortcuts in industry, with most companies either choosing ESM or MCS ([3]).

A second method for generating distribution-specific shortcuts is the Gaussian Quadrature (GQ). GQ chooses the percentiles and probabilities for an n-point discretization so that the first $2n - 1$ moments are matched. This method was first described by [25] and expanded by [40]. The logic, as explained by [40], is that if the present value, pv, of a project is dependent on an uncertainty, x, then its value can be approximated by a polynomial expansion, P. This gives the approximation,

$$pv(x) \approx P(x) = \sum_{i=0}^{n} a_i \cdot x^i. \tag{2.1}$$

In decision analysis, accurately determining the mean value of a decision strategy is important. With the approximation of (2.1), we can approximate the expected value with

$$E\left[pv(x)\right] \approx E\left[P(x)\right] = \sum_{i=0}^{n} a_i \cdot E\left[x^i\right]. \tag{2.2}$$

If $pv(x)$ is well-approximated by P, then $E\left[pv(x)\right]$ will be accurately calculated when the moments of x^i are accurately represented. The calculations of the probabilities and their percentiles requires heavy computation, and this method leveraged the advances in computing power available at the time. Today, scientific computing packages in R, Python, and many others can easily solve the discretization to match the moments. The shortfall of this method is that it requires the knowledge of the moments and the values at the specified percentiles. In his paper, [40] created estimates for the first ten moments of the value lottery that are more accurate than EPT and MCS. This increased accuracy also creates better estimates for the CE with various risk tolerances. The drawback is the percentiles required are quite extreme (e.g. $P95.84$, $P98.34$, and $P99.50$), and are unlikely to be assessed accurately, even if the first five moments of each uncertainty is known.

A common method in decision analysis for determining the relative merit of one strategy over another is to compare the mean net present value of all the potential strategies. As a result, ensuring that the mean and variance of an uncertainty are key goals. In order to graduate empirical data and to generate potential distributions for use with statistical procedures, Pearson and Tukey, [29], created a method to approximate means and standard deviations. They experimented with various percentiles, which they then converted to values for 29 "common" (P. 535) distributions to determine the true value and the error of the approximation. Their primary focus was on the Pearson system of distributions, which provided the benefits of flexibility, the inclusion of several families of distributions including beta, normal, uniform, and student-t distributions, and that distributions may be classified based on their values of β_1 and β_2, which are their skewness and kurtosis values respectively. A key result is that they were able to determine the mean of an uncertainty to within a small tolerance of the standard deviation of the uncertainty based its classification within the Pearson system.

The methods of [29] and [24] multiply specific percentiles of the distributions with a probability. Later, [19] coined these two as the Extended Pearson

Tukey (EPT) method and the Extended Swanson Megill (ESM) method. Both of these shortcuts are commonly used today. In order to test the accuracy of EPT and ESM, [19] tested the discretizations against a set of 78 different beta distributions where the parameter for β was given each of the values of 2, 3, 4, 5, 6, 8, 10, 12, 15, 20, 30, and 60. The value for α was also any one of these values, as long as $\alpha \leq \beta$. In their comparison, [19] compared the mean, variance, and CDF approximation. In all these tests, EPT and ESM outperformed such discretizations as the five point bracket median and the three and five point Brown-Kahr-Peterson discretizations as described in [5].

The bracket median discretization, as described in [6] is another shortcut method that does not require knowledge of the underlying distribution to select the percentiles and their probabilities. In the bracket median approach, a distribution is to be discretized by n probability masses. Each p value has the same probability of $\frac{1}{n}$. The percentile for each point, i, is $\frac{(i-1)}{n} + \frac{1}{2n}$. For example, a three-point bracket median discretization will have three points, each with probability of 0.333, and the percentiles will be $0.166, 0.5,$ and 0.833. Both [40] and [19] found bracket median to under-perform other more advanced methods.

A more recent approach to discretization is a hybrid approach that combines the convenience and generality of shortcuts with the the additional information that an expert may lend to the process, but that does not require knowledge of the moments or the functional form. Using the ability to classify distributions within the Pearson system that were leveraged by [19], [12] to create symmetrical and asymmetrical discretizations for each region of the Pearson system. They created a grid with approximately 2800 points. For all the points within each region of the Pearson system, they calculate a discretization that minimizes the error in the mean and variance across the entire set of points of the region.

The benefit to this method is that the decision analyst can leverage more information regarding each uncertainty. The different regions have bell ($\cap$), $\cup$, or J shapes. The uncertainties may also be unbounded, bounded from one side, or bounded from both sides. For example, the market share of a product is going to be a value between 0% and 100%. The size of the market for a new product is going to be bounded from below at \$0, while the upper bound may unbounded.

2.2 Discretization in Stochastic Optimization

In the field of stochastic optimization the purpose of discretization is to solve a deterministic equivalent of the problem in a format that is tractable where the objective value and the decisions remain the same. To this end, [33] and later [34] created the following definitions: P and Q and scenarios Ω where P and Q belonging to $\mathcal{P}(\Omega)$, and $f \in \mathcal{F}$ where $\mathcal{F}$ is a class of measurable functions from Ω to $\mathbb{R}$, where the objective value, $v(P)$ and solution values, $S(P)$ defined as:

$$v(P) = \inf \{\mathbb{E}_P f(\omega, x) : x \in X\}, \tag{2.3}$$

$$S_\varepsilon = \{x \in X : \mathbb{E}_P f(\omega, x) \leq v(P) + \varepsilon\}. \tag{2.4}$$

They proposed the following theorem:

Theorem 2.1. *Let $P \in \mathcal{P}_f$ and $S(P)$ be bounded and nonempty. Then there* *exist constants* $\rho > 0$ *and* $\overline{\varepsilon} > 0$ *such that*

$$|v(P) - v(Q)| \leq d_{f,\rho}(P, Q), \tag{2.5}$$

$$\varnothing \neq S(Q) \subset S(P) + \Psi(d_{f,\rho}(P, Q))\mathbb{B} \tag{2.6}$$

whenever $Q \in \mathcal{P}_f$ *with* $d_{f,\rho}(P, Q) < \overline{\varepsilon}$*, and that it holds for any* $\varepsilon \in (0, \overline{\varepsilon})$*.*

The interpretation of this theorem is that for any distribution P and a discretized distribution Q, the difference in objective values is bounded by a function of P and Q and the solution is within a ball, $\mathbb{B}$ of the original. In their article on scenario reduction [9] create a formulation and its dual to minimize the value of $d_{f,\rho}(P, Q)$. By minimizing $d_{f,\rho}(P, Q)$, [9] is able to find the discretization that minimizes the change in objective and decisions from the original to the discretized problem. This new formulation is the same as solving a mass transportation problem as in [35].

In order to find the optimal distribution for Q, which only has n points, we must solve a mass transportation problem of a warehouse location problem. The points from the true distribution are the "customers" and the potential points in the discretized distribution are the warehouses. There is a limit of n warehouses, and we must minimize the distance from the customers to the warehouses. From a decision analysis perspective, this is equivalent to placing the CDFs of the true distribution and the CDF of the discretized distribution on the same chart. The distance is the absolute value of the horizontal difference between the two CDF curves. When this distance is zero, it means that the decisions from the discretized model are the same as those coming from the full distribution. For decision analysis, this means that discretizations that match the shape of the true value distribution will result in the same decisions.

2.3 Risk Aversion and Utility Theory

Though calculations may be made using a risk-neutral perspective, in practice, decision makers are likely to be risk averse. With a risk-neutral outlook, to determine the best strategy, a decision maker will need to calculate the mean to choose the best strategy. In a risk neutral environment, discretizations that best match the mean perform the best.

In reality, decision makers are less likely to be risk neutral. An informal study by Ron Howard, a pioneer in decision analysis, found that corporations also have a risk tolerance [14]. In his practice, he used exponential utility functions. To apply the utility functions, he asked his corporate customers what sum of money they were indifferent to investing if there was a $50-50$ probability of winning x or losing $\frac{x}{2}$. These numbers are available in more detail in Table 2 on page 690 of [14]. To summarize, managers are willing to risk 6.4% of sales, 124% of net income, and 15.7% of equity. These numbers serve as a general guideline for the risk tolerance parameter when using exponential utility functions.

The exponential utility function defines utility and the certain equivalent (CE) as:

$$u(x) = \quad -\exp\left(\frac{-x}{\rho}\right) CE = \quad -\rho \cdot \ln\left(-E\left[u(x)\right]\right) \tag{2.7}$$

where x is potential outcome from the strategy's value lottery and ρ is the risk tolerance parameter. The higher this parameter, the closer the decision maker is to being risk neutral. Any investment requiring substantially less than investment than ρ, may also be treated as risk neutral.

The fact that even large corporations are risk averse also follows the findings of the Gambler's Ruin problem first proposed by Huygens [16] and expanded by Coolidge in [8]. If the decision maker is thought of as the gambler, and the rest of the market is thought of as the banker, then it follows that in order to avoid ruin, even when the expected value of any bet is positive, then the best strategy is to reduce the bet size after suffering a loss. In business, this can be seen by the pullback in investment during a major downturn. The application to decision analysis is that decision makers are risk averse, and this will cause them to want to know more about potential outcomes than just the mean.

2.4 Assessment Error and Calibration

When deriving percentiles and probabilities for a discretization, there is usually the assumption of perfectly calibrated assessments. This means that when asking for the 10^{th} percentile, there is only a 10 percent chance that the resulting value will be lower. An assessor is said to be calibrated if when asking for the P_X from an assessor, the true value falls at or below that value X percent of the time [42]. Additional measures of calibration come in terms the interquartile index (II) and the surprise index (SI) [21]. The II is the percentage of true values that fall between the $P25$ and $P75$. This percentage should be 50 percent. The SI is the proportion of true observations that fall outside the P_X and the P_{100-X}. A well-calibrated assessor will have a surprise index of $2X$.

An assessor is said to be overconfident if the proportion of results that are true is greater than the assessed probability. An assessor is said to be under-confident if the proportion of results that are true is lower than the assessed probability. Through various studies, summarized by [21] and [10] and replicated in Table 2.1, we see the observed SI is almost higher in ten of the twelve sets of data. The data from Murphy and Winkler ([27],[28]) comes from meteorologists, and the data from Tomassini et al. The data in ([41]) comes from auditors.

There are a few explanations for why the results from [27], [28], and [41] show relatively accurate surprise index values. In the case of the meteorologists, they have the benefit of regular feedback on their performance, a repeated problem, and training on making assessments. The improvement from training is also visible in [2]. Though the surprise index is still larger, than expected, it is lowered. A second item to consider in the values for the surprise index are the extremes of the percentiles. For those experiments where the tails represent 20 or 25 percent of the area, the value of the surprise index is much closer to the expected value. This is also a recommendation from [41]. This follows the observation from [2] that more extreme percentiles are harder to assess, and will result in larger values for the surprise index relative to the theoretical surprise index.

Lichtenstein provides further evidence of the difficulties in assessing probabilities in [20]. In this article, she shows the calibration from various experiments where the higher the probability assessed, the greater the overconfidence. In this experiment students were given a set of two-answer questions. For each question they had to provide the probability they would get the question correct. These students were divided into three groups, according to their total number of correct responses: best, middling, and worst. As the respondents' confidence in a correct response increased, their probability of being correct increases. But the probability of being correct increases less than the assessed probability of being correct. This suggests the following relationship between the assessed probability, the probability of being correct,

Table 2.1: Assessment Error Summary

Study	N	Interquartile Index	Surprise Index Observed	Surprise Index Expected
Albert and Raiffa (1982) [2]	2270			
Before Training		34	34	2
After Training		44	19	2
Schaefer and Borcherding (1972) [37]	396			
First Day		23	39	2
Fourth Day		38	12	2
Selvidge (1975) [39]				
Five Percentiles	400	56	10	2
Seven Percentiles	520	50	7	2
Murphy and Winkler (1974) [27]	132	45	27	25
Murphy and Winkler (1977) [28]	432	54	21	25
Tomassini et al. (1982) [41]				
First Group	341	71.4	4.2	2
			7.8	20
Second Group	341	54.4	10.8	2
			22.1	20

and overconfidence or under-confidence:

$$PC + UC - OC = PR \tag{2.8}$$

$$\tag{2.9}$$

In Equation (2.9) PC is the proportion of correct answers, UC is the under-confidence, OC is overconfidence, and PR is the probability response, which is the assessed probability of being correct. The plot of PR versus PC is replicated in 2.1. What is surprising is that the worst students were the most overconfident in their probability responses. The worst students are never under-confident, while the middling and best students start off under-confident and then become overconfident as their PR increases.

In the case of assessing the percentiles of a distribution, as described by [2], the assessed value and the true value are different. In [43] they model assessment error as a random variable,

$$x = t + e. \tag{2.10}$$

In Equation (2.10) x is a random variable composed of two elements. The first is t, which is the value that is supposed to be assessed, and the second is e, a random variable for the error in the assessment. This makes the supposition that there is a random variable and that the assessed value is a function of the true value. In their formulation of assessment error [43] assume the following:

1. The expected assessment error is 0, $E(e) = 0$.

2. The error is uncorrelated to the true value.

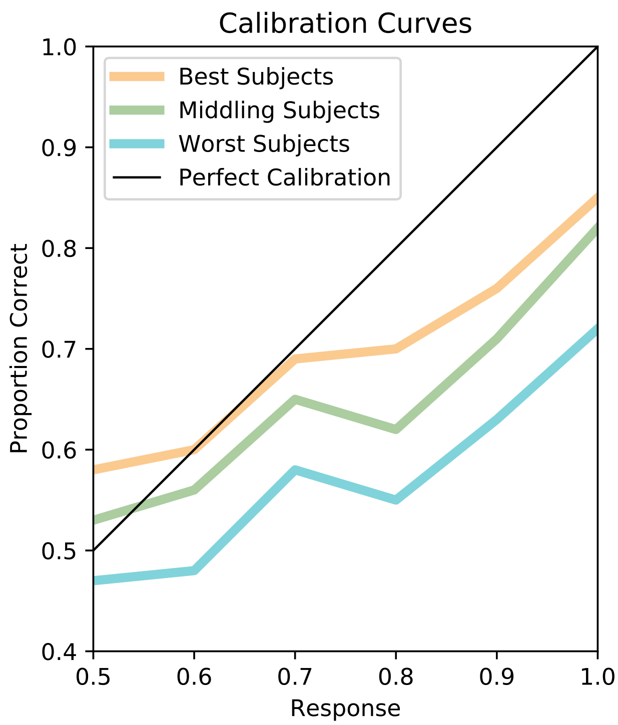

Figure 2.1: Calibration according to knowledge level.

3. Assessment errors are uncorrelated.

We can map the assessed value, t to a percentile , p by using the inverse CDF. This gives $F(t) = p$. To allow for error in the assessment [13] specify the assessed value, x as

$$F(x) = p + \delta, \tag{2.11}$$

where δ is error. They specify a range on the error,

$$|\delta| \leq \Delta. \tag{2.12}$$

Equation (2.12) is scale invariant which allowed [13] to create a set of distributions such that

$$F(x_i^h) \geq q_i - \Delta, i = 1, \ldots, n, F(x_i^h) \leq q_i + \Delta, i = 1, \ldots, n. \tag{2.13}$$

The implication is that the assessor may not be assessing the true distribution, but one of many distributions where the assessed value, x_i has a corresponding percentile that is within Δ of the desired percentile, q_i. This allowed them to compare the performance of ESM, MCS, and EPT under different assumptions for Δ. This analysis also allowed [13] to translate the II and SI found in the literature and provide a value for Δ which matches those II and SI.

In Chapter 5 we revisit the concept of assessment error. We address how assessment error increases with more extreme percentiles. We create a new method to model assessment error. Finally, we address how changes in assessment error affect the accuracy of discretizations.

Chapter 3

Problem-specific Discretizations

3.1 Introduction

In decision analysis there are often problems that come up for the same company repeatedly. These are problems such as how to exploit an oil field or when and how to launch a new drug or consumer product. In these problems the names and types of uncertainties remain the same from problem to problem. What changes are the functional forms of each uncertainty. This chapter introduces problem-specific discretizations. These discretizations define percentiles and probabilities for each uncertainty that minimize the error across a broad range of potential uncertainty combinations.[1]

3.2 General Formulation for Discretization

Problem-specific discretization finds a discretization for the uncertainties of a problem that is going to be revisited frequently. In the problem there are uncertainties whose distributions will change over time. For example, each oil field will have different potential reservoir and recovery ratio. In the consumer

[1]This chapter is based on previously published work in Woodruff, Joshua, and Nedialko B. Dimitrov. "Optimal discretization for decision analysis." Operations Research Perspectives 5 (2018): 288-305. The author's contribution was the conception of the discretization technique, the coding of algorithms to generate the mathematical models, interaction with the publishers, and most revisions. The author did not conceive of the linearization methods and played a smaller role in the organization of this article.

packaged goods industry every new product will have a different potential market share and market size. The realizations of the uncertainties are fed into a value function. Each combination of uncertainty values combines in the decision model to compute the certain equivalent or the net present value.

The general discretization problem assumes independence among the percentile values of the uncertainties. The individual uncertainties may be correlated. The assignment of probabilities is independent. In the independent discretization, the percentiles chosen from one uncertainty are independent from one another. We still allow for dependence between the values of uncertainties. In the examples we use in this dissertation several uncertainties are correlated. We use various methods to determine those correlated values. In an assessment framework, the decision analyst would still elicit dependent (correlated) assessments from the independent percentiles.

To derive our discretizations when the functional forms are unknown, we assume that the true functional form for each uncertainty could come from one of several candidate distributions. The combination of all the potential uncertainty distributions when applied to a value and utility function come to define our set of decision problems, $\mathbb{D}$. We determine the each instance of $\mathbb{D}$ by means of Monte Carlo sampling. This gives us our estimate for the true CE for each instance of $\mathbb{D}$, CE_d. When faced with a client problem, the decision analyst does not know which $d \in \mathbb{D}$ they are addressing. We seek a discretization that works over all cases of $\mathbb{D}$. When the decision analyst believes some potential decision problems are more likely, the decision analyst defines $\mathcal{D}$ as Bayesian prior of the probability distribution over the potential decision problems $\mathbb{D}$. This is a probability assignment on each problem $d \in \mathbb{D}$.

The decision analyst may also wish to only work with specific percentiles, or combinations of percentiles for use with each uncertainty. We define this set as $\mathbb{P}$. We then define $CE_d(p)$ for $p \in \mathbb{P}$ as the equivalent of decision problem d when the distribution p is used for the uncertainties instead of the true distribution. In other words, $CE_d(p)$ is the certain equivalent when we use the discretized distribution instead of the true distribution of the uncertainties. The goal of problem-specific discretizations is to find a $p \in \mathbb{P}$ such that $CE_d(p) \approx CE_d$ for all decision problems $d \in \mathbb{D}$. A discretization with a perfect fit will have $CE_d = CE_d(p)$ for all $d \in \mathbb{D}$.

In order to find $p \in \mathbb{P}$ we formulate the discretization as an optimization problem. This is a novel contribution to the area of discretization, and leads us to the results in the rest of the paper. We formulate the optimization as follows:

$$\arg\min_{p \in \mathbb{P}} \left(\lambda \left[\max_{d \in \mathbb{D}} Err(d,p) \right] + (1-\lambda) \left[E_{d \in \mathcal{D}} Err(d,p) \right] \right), \tag{3.1}$$

where

$$Err(d,p) = \left| \frac{CE_d - CE_d(p)}{CE_d} \right| \text{ or} \tag{3.2}$$

$$Err(d,p) = |CE_d - CE_d(p)| \text{ or} \tag{3.3}$$

$$Err(d,p) = CE_d(p) - CE_d. \tag{3.4}$$

Given a parameter $\lambda \in [0,1]$, optimization (3.1) defines the discretization problem. The result of this optimization is a discretization $p \in \mathbb{P}$, that yields the minimum convex combination of worst case (absolute) error and expected (absolute) error, $E_{d \in \mathcal{D}} Err(d,p)$, with respect to the distribution $\mathcal{D}$. We use $\mathcal{D}$ as the distribution of decision problems to indicate there is a probability associated with each decision problem. Equation (3.2) defines the absolute percentage error in the CE when using the discretized distribution of uncertainties instead of the true distribution. We include (3.3) as an alternative formulation to the error function when CE_d has values that are orders of magnitude different, such as when CE_d may be positive or negative. When the potential values for CE_d are close to 0, their importance will take on an out-sized weight, skewing the results. When λ is one, we seek a discretized distribution that yields the minimum worst case error. When λ is zero, we seek a discretized distribution that yields the minimum average error over the distribution of decision problems $\mathcal{D}$. In the case of $\lambda = 0$, we also include the (3.4). This minimizes the mean error and removes bias from the discretization.

3.3 A Tractable Discretization Instance

Optimal discretization requires a tractable model that the decision analyst can solve during an engagement. This is a model that provides the correct answer and solves quickly (overnight is fast-enough in practice). This section provides a tractable instance of the discretization problem for (3.1). We do this by defining a specific set of discretized probability distributions $\mathbb{P}$, a specific set of problems $\mathbb{D}$, and a probability distribution $\mathcal{D}$ over the problems. The optimal choice of a discretization $p \in \mathbb{P}$ defines the optimal discretization. These definitions allow us to formulate the discretization problem as a tractable non-linear integer program (NLIP).

In our process we have a challenge that prevents us from formulating the model as we envision in 3.2. We discuss how we solve this challenge. Finally, relax some assumptions and provide a second tractable formulation. Solving a tractable discretization instance requires defining the objective value, decisions, and constraints with data such that the computers and engines that solve the model are able to solve it within a few hours to a few days.

3.3.1 NLIP Formulation of Discretization Problem

In order to implement any form of (3.1), we first calculate each value of decision problem. The decision problem is a specific combination of a functional form for each uncertainty in the decision, $d \in \mathbb{D}$. We use a stratified sampling to generate our "true" CE_d for each $d \in \mathbb{D}$. The simulation yields the uncertainty values, a project value distribution, expected utility, and the certain equivalent.

To formulate optimization (3.1) as a tractable NLIP, the key obstacle to overcome is that the objective $Err(d, p)$ is a non-linear function in p as shown in (3.2). In this formula, CE_d is already a constant we obtained from our formulation, but $CE_d(p)$ is our calculated CE. The formula for $CE_d(p)$ is given by

$$\textbf{Certain Equivalent:} \quad CE_d(p) = -\rho_d \cdot ln\left(-\sum_{p \in \mathbb{P}} prob_p \cdot u_d(p)\right), \tag{3.5}$$

$$\textbf{with exponential utility:} \quad u_d(x) = -exp\left(-x/\rho_d\right), \tag{3.6}$$

$$\textbf{and} \quad P(X \leq x) = p \tag{3.7}$$

where ρ_d is the risk tolerance, $prob_p$ is the probability assigned to percentile combination p and $u_d(p)$ is calculated expected utility for decision problem d with percentile combination p. We use the exponential utility function in this example. Different utility functions will change the formulations for both $u_d(p)$ and CE_d. Normally utility is expressed in terms of the value of the project/decision, x. We are searching for the optimal percentiles, so we used (3.7), the definition of the CDF, to relate p to x.

When we apply this non-linear formulation of the CE given by (3.5) to our non-linear solver, Bonmin 1.8.4, it is intractable. To create a tractable formulation we linearize the objective function. We choose to create a Taylor series expansion $Err(d,p)$ around the expected utility, $E[u_d(x)]$. We first substitute the equation for certain equivalent, (3.5), into the definition of $Err(d,p)$ to get

$$Err(d,p) = \left|1 - \frac{-\rho_d \ln\left(-E_p[u_d(x)]\right)}{CE_d}\right|, \tag{3.8}$$

where $E_p[u_d(x)]$ is the expected utility of the decision problem under the new discretized distribution $p \in \mathbb{P}$. Given a $d \in \mathbb{D}$, the only variable in the above formula is $E_p[u_d(x)]$, and everything else is a constant. Though it is possible to expand the Taylor series to an infinite number of terms, we the linear term is sufficient with the test problems we solved. In Figure 3.1 the linearization is close enough for a small range around the mean utility. An quadratic Taylor expansion term can be added to improve the accuracy of the approximation at a cost of additional solve time. For brevity let $T_d = E[u_d(x)]$ be our target utility.

To compute a linearization, we first drop the absolute value sign, assuming the second term of (3.8) is less than one. This gives

$$f(w) = 1 - \frac{-\rho_d \ln\left(-w\right)}{CE_d},$$

which is now a continuous function of w, where w is shorthand for the variable $E_p[u_d(x)]$. We can now do a first order Taylor expansion of this function around T_d to obtain

$$\begin{aligned} f(w) &\approx 0 + f'(T_d)\left(w - T_d\right) \\ &= \frac{-\rho_d}{CE_d \cdot T_d}\left(w - T_d\right). \end{aligned}$$

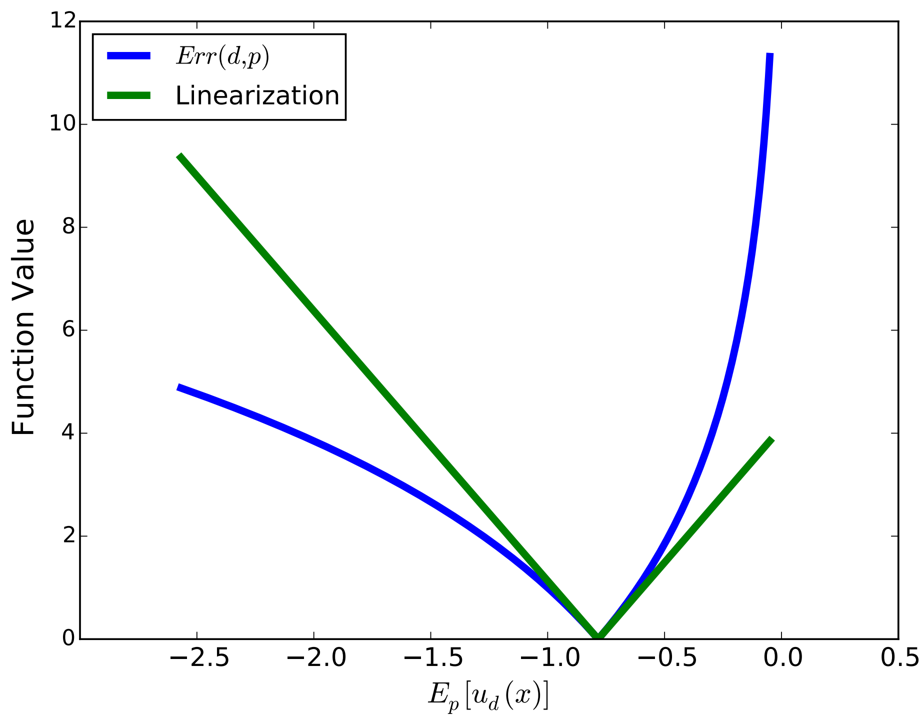

Figure 3.1: This is a sample of a linearization of the absolute percentage error and the true absolute percentage error as a function of the expected utility. If the optimization is not able to find discretizations that closely match T_d, then a quadratic term can be added to improve accuracy.

This approximation is valid when the second term of (3.8) is smaller than one. This happens when w is greater than or equal to T_d. A similar argument, assuming that the second term is greater than one, yields the approximation $\frac{\rho_d}{CE_d \cdot T_d}(w - T_d)$, which is valid when w is smaller than or equal to T_d. Together, these two linearizations are summarized as

$$\delta_d = \frac{-\rho_d}{CE_d \cdot T_d} \tag{3.9}$$

$$Err(d,p) \approx \delta_d \cdot |E_p[u_d(x)] - T_d|, \tag{3.10}$$

which linearizes Equation (3.8). Figure 3.1 plots an example of the true error function and corresponding linearization. In the case where the decision maker is risk neutral, we can skip the calculation of δ_d (3.9) and just use $\delta_d = \frac{1}{CE_d}$.

With this linearized objective function, we can now write an integer program for computing an optimal discretization as follows.

Indices and sets

$i \in I$	:the set of uncertainties
$v^i \in V^i$	:the set of percentile discretization of uncertainty i. These are candidate percentiles fo
$\mathbf{v} \in \otimes V_i$	:a percentile combination for all uncertainties. $\mathbf{v}$ is a vector of length $\lvert I \rvert$.
$d \in \mathbb{D}$	:a finite, discrete set of decision problems
$j \in J$	:the indexes for each of the $\lvert J \rvert$ incompatible sets discretizations

Parameters

λ	:used to compute a convex combination of average and maximum error
T_d	:the true expected utility for decision problem d
δ_d	:a shorthand for $\frac{-\rho_d}{CE_d \cdot T_d}$, a constant used in linearization
N_i	:the maximum number of percentiles per uncertainty for the output discretization
$U_d(\mathbf{v})$	:the utility of the project value for decision problem d and at percentile combination v
δ_j	:the incompatible discretizations, v, in set j
P_d	:the probability assigned to decision problem, d

Decision variables

$p_{\mathbf{v}}$	:the probability assigned to a combination of percentiles $\mathbf{v}$.
o_d	:the over-estimation in approximating T_d with a discretized probability distribution
u_d	:the under-estimation in approximating T_d with a discretized probability distribution
z	:the estimated $max_{d \in \mathbb{D}} Err(d, p)$
x_{v^i}	:the probability assigned to candidate percentile v^i for uncertainty i
y_{v^i}	:1 if percentile v^i is used for uncertainty i and 0 otherwise

Formulation

$$
\begin{aligned}
\min \quad & \lambda \cdot z + (1-\lambda)\, P_d \sum_{d \in \mathcal{D}} P_d \cdot \delta_d \cdot (u_d + o_d) && && (3.11a)\\
\text{s.t.} \quad & \sum_{\mathbf{v} \in \otimes V_i} U_d(\mathbf{v}) p_{\mathbf{v}} - o_d + u_d = T_d && \forall d \in \mathbb{D} && (3.11b)\\
& z \geq \delta_d \cdot (o_d + u_d) && \forall d \in \mathbb{D} && (3.11c)\\
& \sum_{v^i \in V^i} x_{v^i} = 1.0 && \forall i \in I && (3.11d)\\
& \sum_{v^i \in V^i} y_{v^i} \leq N_i && \forall i \in I && (3.11e)\\
& \sum_{v^i \in \delta_j} y_{v^i} \leq 1 && \forall i \in I, \forall j \in J && (3.11f)\\
& x_{v^i} \leq y_{v^i} && \forall i \in I; v^i \in V^i && (3.11g)\\
& p_{\mathbf{v}} = \prod_{v^i \in \mathbf{v}} x_{v^i} && \mathbf{v} \in \otimes V_i && (3.11h)\\
& 0 \leq x_{v_i} \leq 1 && \forall i \in I; v^i \in V^i && (3.11i)\\
& y_{v_i} \in \{0, 1\} && \forall i \in I; v^i \in V^i && (3.11j)\\
& o_d, u_d \geq 0 && \forall d \in \mathbb{D} && (3.11k)
\end{aligned}
$$

The objective (3.11a) of the optimization model is to minimize a convex combination of the largest error z and the average error. In this formulation we show the generalized distribution on $\mathcal{D}$. The second term of the objective function is the average error. This promotes reducing the error In order to compute the linearized error (3.10), we should compute the absolute value of the difference between T_d and $E_p[u_d(x)]$. The formula for T_d is given for formula (3.11b) in Appendix .1. Constraint (3.11b) computes the difference between the target and expected utility. Constraint (3.11c) computes the maximum error, z. Constraint (3.11d) forces the sum of the probabilities for each uncertainty to sum to one. Constraint (3.11e) limits the number of percentiles allowed for each uncertainty. Constraint (3.11f) forces only a single low, a single medium, and a single high percentile in our discretizations. This helps the optimization engine find a solution faster. For example, our low-percentile candidates are $P5$ and $P10$. Only one may be selected for the deiscretization. Constraint (3.11g) forces the assigned probability to zero if the percentile is not used in the discretization. Constraint (3.11h) computes the probability assigned to a percentile combination as a function of the probabilities of each of the uncertainties. This is the only non-linear constraint in the formulation and it enforces that the output distribution $p \in \mathbb{P}$ is independent over the uncertainties. The remaining constraints bound the probability values between 0 and 1, make the indicator variables binary, and make the underage and overage non-negative.

3.3.2 Joint Discretization Problem

Math programming solvers such as CPLEX, or even open source solvers such as CBC tend to solve similarly sized problems much faster than their non-linear engine counterparts. We alter the formulation to create a joint discretization version of the problem and apply CPLEX to solve this problem.

An outcome from the value lottery in a decision problem, $d \in mathbbD$ is a combination of drawing an individual value from each uncertainty and applying each of those values to a formula which determines the net present value. We can call this value $\mathbf{v}$ and is made by applying each $v^i \in \mathbf{v}$ to obtain $U_d(\mathbf{v})$. In joint discretization, have the engine directly apply a probability to each outcome $\mathbf{v}$ and to determine which outcomes are considered by choosing the percentiles of each uncertainty. This relaxation increases the flexibility of the probabilities assigned to a percentile combination and it linearizes the model formulation. Previous discretization techniques only considered uncertainty discretizations independently. Because we consider a set of decision problems and compute the best discretization for that set of problems, it is possible to compute this joint discretization.

The feasible values are $p_{\mathbf{v}} \in [0, 1]$ in both formulations. But in the non-linear formulation, we use Equation (3.11h) to constrain the potential values. The relaxation allows us to find discretizations with less error faster. In this section, we define the formulation for optimal joint discretizations.

We alter Model (3.11) as follows to compute optimal joint discretizations The formulation drops variables x_v^i and any constraints where they appear. These are Constraint (3.11d) and Constraint (3.11h). We also add the following constraints:

$$\sum_{\mathbf{v} \in \otimes V_i} p_{\mathbf{v}} = 1 \tag{3.12a}$$

$$p_{\mathbf{v}} \leq y_{v^i} \qquad \forall \mathbf{v} \in \otimes V_i,\ v^i \in \mathbf{v} \tag{3.12b}$$

$$p_{\mathbf{v}} \geq 0. \tag{3.12c}$$

Constraints (3.12a) and (3.12c) ensure the variables $p_{\mathbf{v}}$ compute a joint probability. Constraint (3.12b) ensures the support of that joint probability is limited to the N_i percentiles for each uncertainty i. The result of Constraint (3.12b) is that experts make the same number of assessments as before.

The full final formulation is as follows:

Indices and sets

$i \in I$	:the set of uncertainties
$v^i \in V^i$	:the set of percentile discretization of uncertainty i. These are candidate percentiles fo
$\mathbf{v} \in \otimes V_i$	:a percentile combination for all uncertainties. $\mathbf{v}$ is a vector of length $\|I\|$.
$d \in \mathbb{D}$	:a finite, discrete set of decision problems
$j \in J$	:the indexes for each of the $\|J\|$ incompatible sets discretizations

Parameters

λ	:used to compute a convex combination of average and maximum error
T_d	:the true expected utility for decision problem d
δ_d	:a shorthand for $\frac{-\rho_d}{CE_d \cdot T_d}$, a constant used in linearization
N_i	:the maximum number of percentiles per uncertainty for the output discretization
$U_d(\mathbf{v})$	:the utility of the project value for decision problem d and at percentile combination
δ_j	:the incompatible discretizations, v, in set j
P_d	:the probability assigned to decision problem, d

Decision variables

$p_{\mathbf{v}}$	:the probability assigned to a combination of percentiles $\mathbf{v}$.
o_d	:the over-estimation in approximating T_d with a discretized probability distribution
u_d	:the under-estimation in approximating T_d with a discretized probability distribution
z	:the estimated $max_{d \in \mathbb{D}} Err(d, p)$
y_{v^i}	:1 if percentile v^i is used for uncertainty i and 0 otherwise

Formulation

$$
\begin{aligned}
\min \quad & \lambda \cdot z + (1-\lambda)\, P_d \sum_{d \in \mathcal{D}} P_d \cdot \delta_d \cdot (u_d + o_d) && && \text{(3.13a)}\\
\text{s.t.} \quad & \sum_{\mathbf{v} \in \otimes V_i} U_d(\mathbf{v}) p_{\mathbf{v}} - o_d + u_d = T_d && \forall d \in \mathbb{D} && \text{(3.13b)}\\
& z \geq \delta_d \cdot (o_d + u_d) && \forall d \in \mathbb{D} && \text{(3.13c)}\\
& \sum_{v^i \in V^i} y_{v^i} \leq N_i && \forall i \in I && \text{(3.13d)}\\
& \sum_{v^i \in \delta_j} y_{v^i} \leq 1 && \forall i \in I, \forall j \in J && \text{(3.13e)}\\
& x_{v^i} \leq y_{v^i} && \forall i \in I; v^i \in V^i && \text{(3.13f)}\\
& 0 \leq x_{v_i} \leq 1 && \forall i \in I; v^i \in V^i && \text{(3.13g)}\\
& y_{v_i} \in \{0, 1\} && \forall i \in I; v^i \in V^i && \text{(3.13h)}\\
& o_d, u_d \geq 0 && \forall d \in \mathbb{D} \sum_{\mathbf{v} \in \otimes V_i} p_{\mathbf{v}} = 1 && \text{(3.13i)}\\
& p_{\mathbf{v}} \leq y_{v^i} && \forall \mathbf{v} \in \otimes V_i,\ v^i \in \mathbf{v} && \text{(3.13j)}\\
& p_{\mathbf{v}} \geq 0. && && \text{(3.13k)}
\end{aligned}
$$

3.4 Analysis

In this section we solve Model (3.11) and also Model (3.13) for a sample problem given by [40]. We briefly describe the example here and more in depth in Appendix .1. We also apply the methodology to a second problem originally given by [6] and expanded by [7] and further described in Appendix .2. We begin with the [40] wildcatter problem.

A wildcatter is a person who drills for oil in an undeveloped field. The amount of oil, the price of oil, the extractable percentage, and the cost are among the uncertainties the wildcatter will face. The functional form of each uncertainty is unknown. Rather than solving the problem with the functional forms used by [40], we use several candidate distributions as shown in Figure 3.2. They are similar in shape and breadth to those in [40], but are not the same. For this analysis, we created nine different "true" distributions per uncertainty. Any one of the candidate distributions could be the true distribution. There are a total of $9^4 = 6,561$ potential decision problems, any of which is equally likely to be the true problem. In this formulation we assume the risk tolerance, ρ, is known at the time of the problem definition by applying estimates from [14]. The optimal discretization will find the discretization for each uncertainty that when combined with the others yields the minimum error.

For each of the $6,651$ decision problems we use Latin hypercube sampling as originally described by [22]. We generate $4,000,000$ values for each uncertainty to generate a set of present values, $\mathbb{X}$. For each $x \in (X)$ we generate a utility and determine CE_d using (3.5) with a risk tolerance value, $\rho = \$16,000,000$. The distribution of the CE_d is found in Figure 3.3. From each CE_d we are also able to obtain a target utility,T_d, using (3.13b). For each decision problem we also calculate δ_d using (3.9).

The percentile combinations are drawn from a Cartesian product of the candidate percentiles for each uncertainty. We define $\otimes V_i$ as the set of potential percentile combinations. We allow each of the four uncertainty percentiles to be in the set $\{5, 10, 45, 50, 55, 90, 95\}$. These seven percentiles encompass common percentiles of $0.05, 0.10, 0.5, 0.9$, and 0.95 which are found in common discretizations such as ESM, MCS, and EPT. The additions of 0.45 and 0.55

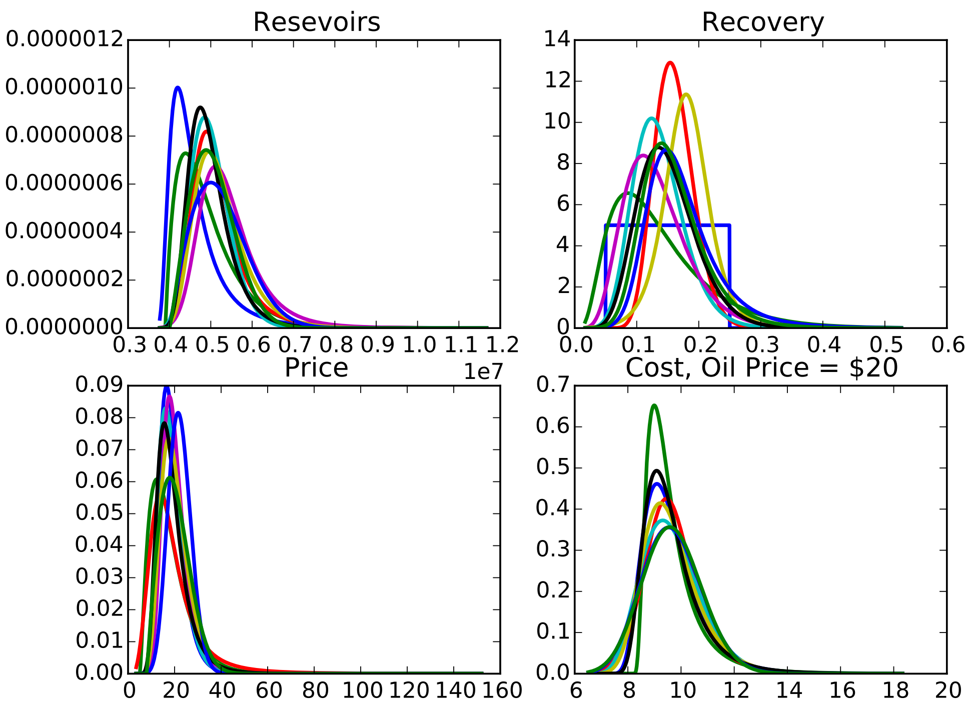

Figure 3.2: Each uncertainty has nine candidate distributions. The decision analyst may include more distributions, perhaps pulled from the Pearson system for ease. The reservoir, price, and cost distributions are bounded from below at zero. The recovery distribution is bounded by 0 and 100 percent. Though most distributions are similar in shape, we also included a uniform distribution in as potential distribution for the fraction of the reserves that may be recovered.

are not commonly assessed percentiles and only serve to illustrate the flexibility of the methodology. The percentile set for each uncertainty represents the set of potential assessment values we might ask an expert to give. A decision analyst may add or remove percentiles. An increase in candidate percentiles may improve accuracy. The down side of increasing the number of candidate percentiles is that it increases the computational complexity and solve time. For each decision problem we have $7^4 = 2,401$ potential percentile combinations. We choose three percentiles for each uncertainty which yields $3^4 = 81$ of those percentile combinations. The result of the optimization assigns each of the 81 outcomes a probability. For this discretization instance, we are defining the distributions in $\otimes V_i$ as independent over the uncertainties. For each of the $2,401 p \in \mathbb{P}$ we calculate the utility for each decision problem $d \in \mathbb{D}$ using (2) to calculate $U_d(\mathbf{v})$ for each $\mathbf{v} \in \otimes V_i$. This provides the data we need to populate our optimization models.

We begin our comparison of optimal discretization to four incumbent discretizations of MCS, ESM, EPT, and HB. With four uncertainties in the problems, this yields 81 potential outcomes for each decision problem. We use the percentile from each discretization to get a value from the decision problem's uncertainty distributions inverse CDF. We compute the project value and utility based on the samples. Finally, we compute the CE using the probabilities assigned to each percentile. This gives us an estimated CE for each decision problem. We compare the estimated CE using the discretization to the CE we obtained by using the simulation for the same problem using the equation

$$100 * \frac{CE_d - CE_d(p)}{CE_d}.. \tag{3.14}$$

This is equivalent to forcing specific values into Model (3.11). We create a distribution of errors for each discretization method and present them in

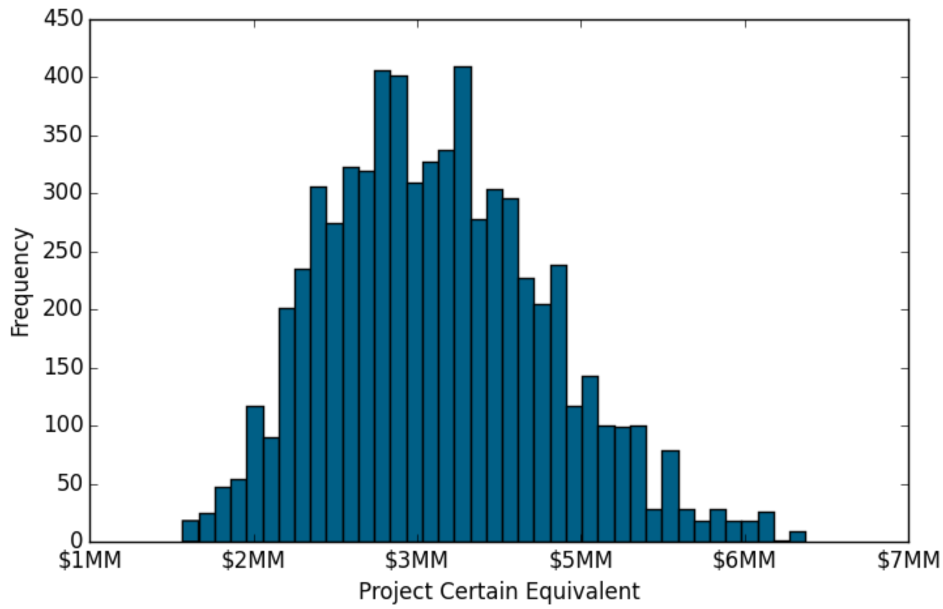

Figure 3.3: The distribution of CE values for the 6,651 decision problems. Though most of the uncertainties seems to have fairly similar distributions, their combinations can have markedly different results.

Figure 3.4. The HB and EPT methods use more extreme percentiles like the 5^{th} and 95^{th} percentiles. The MCS and EPT discretizations use the 10^{th} and 90^{th} percentiles. The accuracy of the discretizations with more extreme values is visible in Figure 3.4. We use two measures of accuracy. The first is the worst-case error. This is the largest absolute value of a percent error from the true CE across all decision problems. The other error metric is the average of the absolute errors. HB has a worst-case of 1.75 percent and EPT has a worst case of 1.47 percent. ESM has an absolute worst case error of 2.02 percent and MCS has a worst case of 6.34 percent. The mean absolute errors of HB and EPT are both 0.25 percent. HB has a slightly better performance in terms of absolute error, but when rounded to the nearest hundredth of a percent, they are the same. MCS and ESM have average absolute errors of 1.30 and 0.41 percent, respectively. In the wildcatter example, the standard deviation of $Err(d, p)$ is larger and the mean CE is further away from 0 when the discretizations using the extreme (5^{th} and 95^{th}) percentiles is used. It is clear that MCS is the worst performer in this group, but only upon examination of the numbers, do we see that HB is the best performer. Another important observation is that the discretizations with the more extreme percentiles of 0.05 and 0.95 tend to perform better than the $P10, P50, P90$ discretizations of ESM and MCS.

In this section, we solve Model (3.11) twice. We use the two extreme values for λ. When $\lambda = 1$ we minimize the worst case error. When $\lambda = 0$, we minimize the average error. We compare the results from the Model (3.11) and Model (3.13) to each other and to the shortcuts.

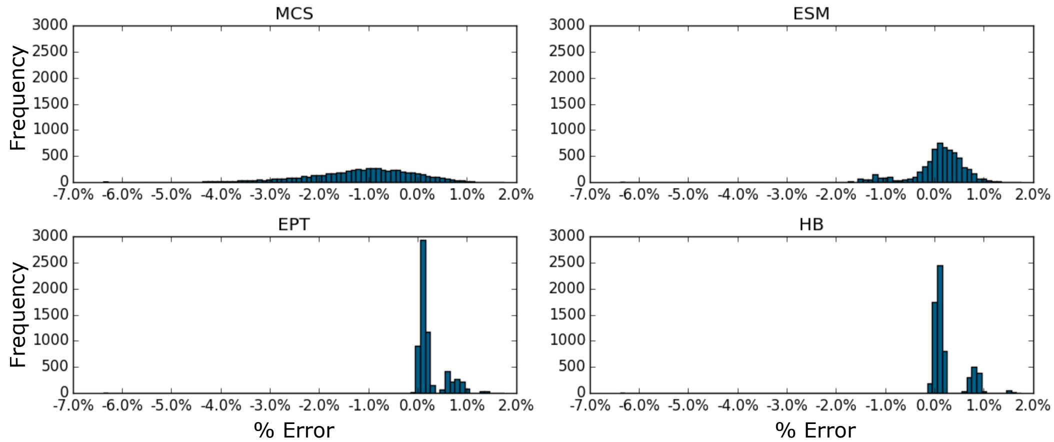

Figure 3.4: The distribution of percent errors for four shortcut methods.

3.4.1 Independent Discretization

In creating optimal discretizations we have two goals in mind. The first goal is to find discretizations that minimize (3.11a). The second goal is to find this solution quickly. We define quickly rather loosely. If this is being done for an ongoing project, we want to be able to generate an optimal discretization for the client before we need to assess percentiles and provide a cumulative distribution function of the value lottery to the client. Otherwise, we want to have the discretizations computed for the next time a decision problem comes up.

We solved the complete model, with all the candidate percentiles for each decision problem. We also solved different versions of problem (3.1) using subsets of the candidate discretizations such as $p5, P50, P95$ and $P10, P50, P90$, or using a sampling of the $6,561$ decision problems. By limiting the candidate discretizations, we are able to reduce the number of variables. Specifically, when we reduce the number of candidate percentiles to three, we are able to solve the model as a continuous problem instead of as a non-linear mixed-integer problem. We try these two sets of three plus the full set. Our second way of reducing the computational time is to reduce the number of decision problems by sampling a percentage of them. We test how the results differ when we chose to minimize the worst-case discretization error and when we try to minimize the average discretization error.

3.4.2 How much benefit do we get from optimizing an independent discretization?

The calculation of the certain equivalent is given by multiplying the probability of each percentile of each uncertainty to determine the probability of an outcome. There may be a covariance among the resulting values, but the percentiles are treated as independent. In the case of the four uncertainties in our sample problem, the probability of any one outcome is the product of the probability of each of the individual uncertainties. The drawback of the non-linear approach is the that there are few available solvers, and large problems generally take too long to solve. For example, in our test problem, solving the full problem with $\lambda = 0.0$ using Bonmin 1.8.4 using an Intel 6-core I7 processor running at 2.6GHz, the average time to generate the model and solve the problem was $129,937.72$ seconds (1.5 days). This problem has $6,651$ decision problems and over $15,000,000$ non-zeros. A larger problem may prove to be intractable without advanced decomposition methods.

The results from of the optimization are shown in Figure 3.5. When comparing to HB, which has the best results in Figure 3.4, independent discretization improves the worst case mean error and the standard deviation of error. As one would expect, the worst case error is lower when optimizing for the worst case error, and the average error is best when optimizing for the average error. The variance of the error larger when optimizing for the worst case error. Either optimization improves upon the results from HB.

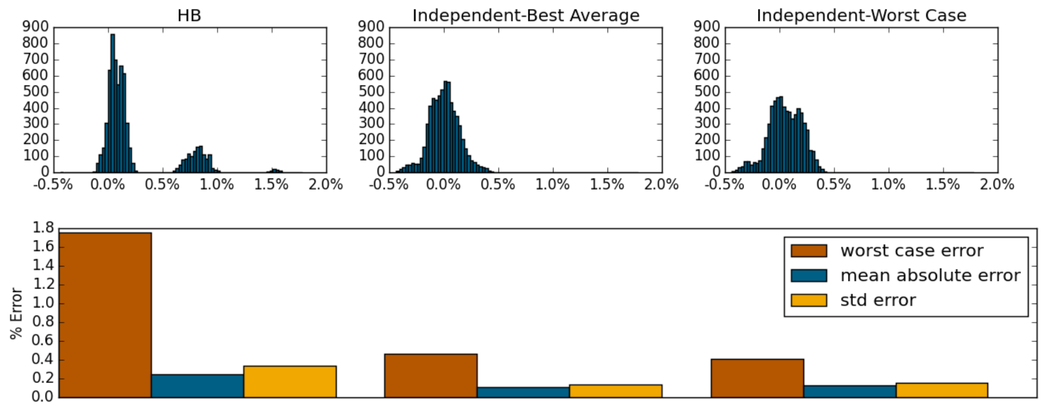

Figure 3.5: The histogram of results compares HB, which has the best average error of the incumbent methods with the optimized discretizations using both the optimal average and optimal worst-case preferences. Below each histogram is a bar chart for the discretization method which shows the worst case error, the mean absolute error, and the standard deviation of error. The optimized results show a reduction in average absolute error of 56 percent and a reduction of worst-case error of 74 percent.

We present the results of all discretizations in 3.5.1 at the end of this chapter. Both discretizations use more extreme percentiles of $P5$ and $P95$, and also use some of the $P45$ or $P55$ percentiles.

3.4.3 How much do we lose by solving a smaller sample of decision problems?

Given the 1.5 day time frame for solving for $6,651$ decision problems with $2,401$ possible combinations of percentiles, we tested the effects of sampling the decision problems to reduce the problem size. In sampling the decision problems, we select a uniformly random subset of the decision problems and then applied the optimal discretization for that subset to the entire set of problems. We display the results in Figure 3.6. We test the sampling with $1, 10$, and 20 percent of the $6,651$ decision problems using both worst case and best average objectives. The solve time is linear with the number of decision problems that we sample. Sampling with 1 percent took 24 minutes, sampling with 10 percent took just under 3 hours, and sampling with 20 percent took just under 6 hours. Solution quality, as measured as the increase in objective value from the optimal value with 100 percent sampling improves with the number of samples. A 1 percent sample results in a 34 percent increase in the average error. A 10 percent sample results in an increase of 1 percent in the average error. Sampling with 20 percent results in and increase of 1.4 percent in the average error. The increase in average error in the sampling is likely due to the randomness of the sampling. When we looked at the solution quality, there is a noticeable difference between choosing $\lambda = 1$ and $\lambda = 0$. For the smaller samples ($<$ 20 percent), minimizing the worst case led to varying degrees of over fitting, with increases in worst case error of 25, 15.7, and 6 percent for the 1, 10, and 20 percent samples respectively. Sampling the decision problems results in roughly linear speedups in performance with a small loss of accuracy.

3.4.4 How much do we lose by restricting the candidate percentiles?

Some of the most common discretizations use either $P10, P50, P90$, like MCS or ESM, or $P5, P50, P95$, like EPT. In comparing both the shortcut methods and the discretization results, it seems the most accurate discretizations come from using the more extreme percentiles. If $P5, P50, P95$ discretizations are more accurate, it can save processing time to restrict the per-

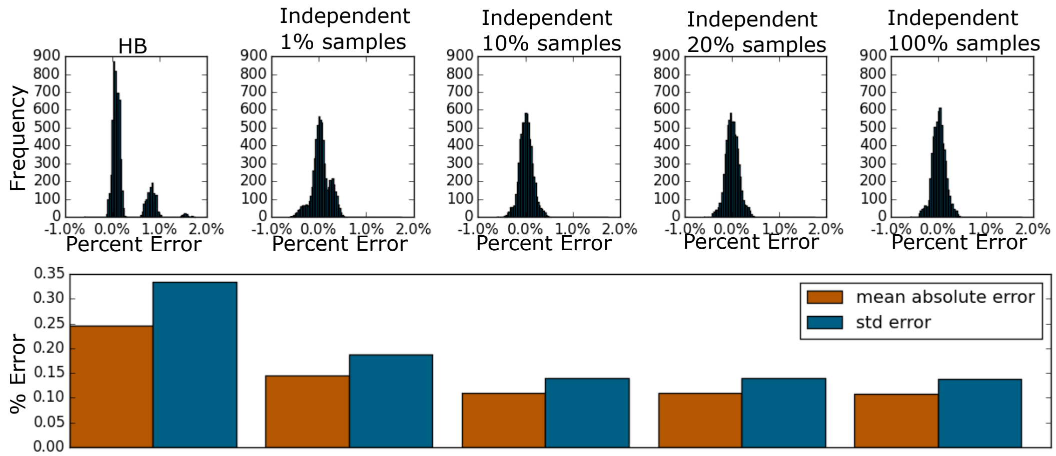

Figure 3.6: As the number of samples increases in percentage, the overall accuracy of the discretization improves. After 10 percent of the samples, the average error is 1 percent worse than the optimum using the entire set of decision problems.

centiles. Given the $P10, P50, P90$ discretizations are also popular, we also want to know what improvement in accuracy we can expect when considering the more extreme percentiles. We solve the problem using either the maximum error or the average error objectives. The first improvement is the rapid speedup in solution time. The range of reduction is from 99.5 percent to 99.9 percent reduction in the time required to generate a discretization. The solution times were in the 100 to 300 second range, reducing the solve time by more than 99 percent. When limiting the candidate discretizations to P10, P50, P90, the mean absolute error is 4.8 percent lower than the mean absolute error using the HB shortcut. It should be pointed out this slight improvement comes using less-extreme values than those required by HB. In comparison to using all the candidate percentiles from a full optimization, the mean absolute error is still 117 percent worse when using the $P10, P50, P90$ percentiles of ESM or MCS. These results are shown in Figure 3.7. Using the P5, P50, P95 percentiles improves the accuracy of the optimal discretization while solving quickly. The optimized discretization increases worst case error by just 0.25 percent over the optimal results obtained from considering all the percentiles. This result is shown in Figure 3.8.

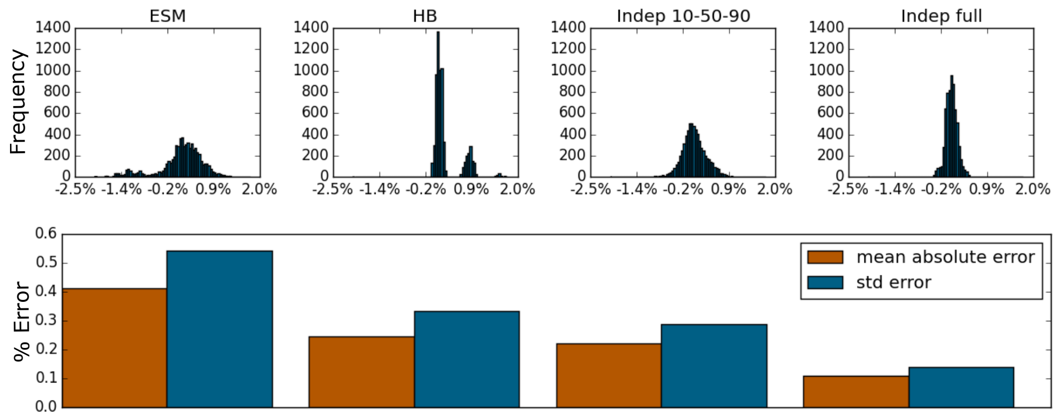

Figure 3.7: Using only the $10 - 50 - 90$ percentiles reduces the error in comparison to the shortcut methods. This subset has about twice the error of the full set of candidate percentiles.

3.4.5 What benefit do we derive when we remove the independence of uncertainties?

Solving with a non-linear solver has mixed results. The improvement in accuracy is substantial, but some instances take days to solve. In a large business problem with 12 to 15 uncertainties, the size of the problem becomes intractable. Previous discretization methods focused on individual uncertainties, which were combined to create a distribution of the decision problem values. We propose a new approach which relaxes the independence of uncertainty percentiles and creates a joint distribution.

Joint discretization improves both performance time and the accuracy

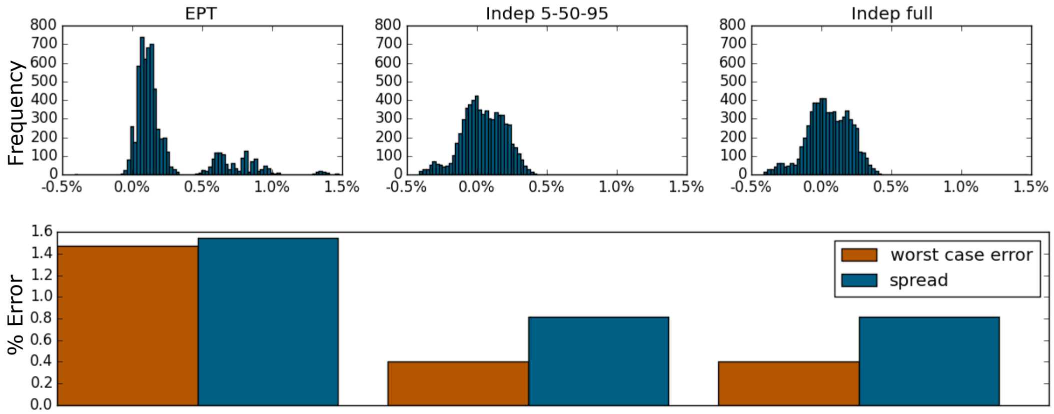

Figure 3.8: Limiting the candidate percentiles to $5-50-95$ reduces the error in comparison to the shortcut methods, and is only slightly worse that when considering a larger assortment of candidate percentiles.

of the discretizations. The solution time using CPLEX 12.5 is just under 2 hours for the mean absolute error, and about 1 hour and 40 minutes for the worst case error. This compares favorably to the 1.5 and 1.2 day solution times for the independent discretizations. The joint discretization reduces the mean absolute error by 34 percent over the independent discretization. In comparison to the shortcut methods, this is a 71 percent reduction in mean absolute error of the best-performing shortcut (HB). For the worst case error, the joint discretization reduces the error by 41 percent when compared to the independent discretization, and it reduces the worst case error by 86 percent when compared to the best shortcut method (EPT). These results are visible in Figures 3.9 and 3.10.

Joint discretization has another benefit over independent discretization. As seen in Section 3.5.1 a joint discretization does not use every possible percentile combination. While there could typically be 81 values when using a three-point discretization for four uncertainties, the number of outcomes is reduced to 31 for $\lambda = 0$, which requires more scenarios than the best worst case. For both a practitioner and a client, this means there may be fewer assessments required if certain percentiles are omitted.

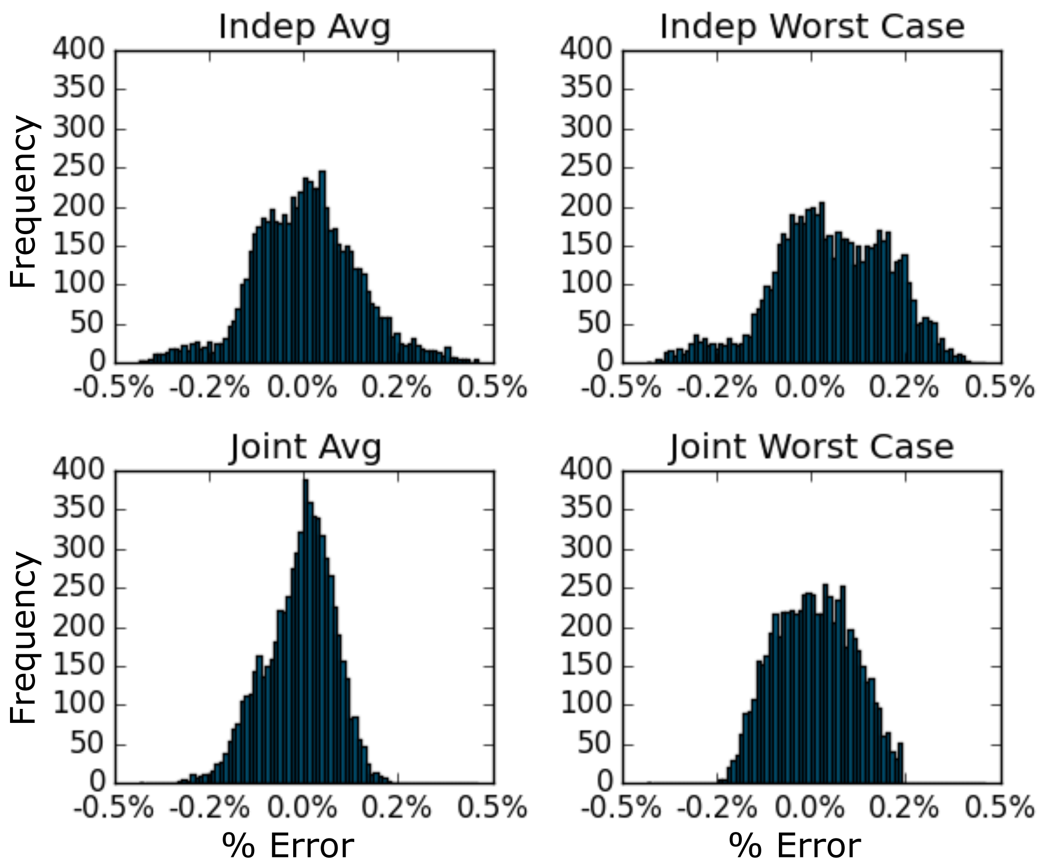

Figure 3.9: A comparison of the independent and joint discretization method results.

3.4.6 What is the value provided by optimal discretization?

In order to determine the effectiveness of optimal discretization, we determine how much of a boost in CE do we expect to get from using optimal

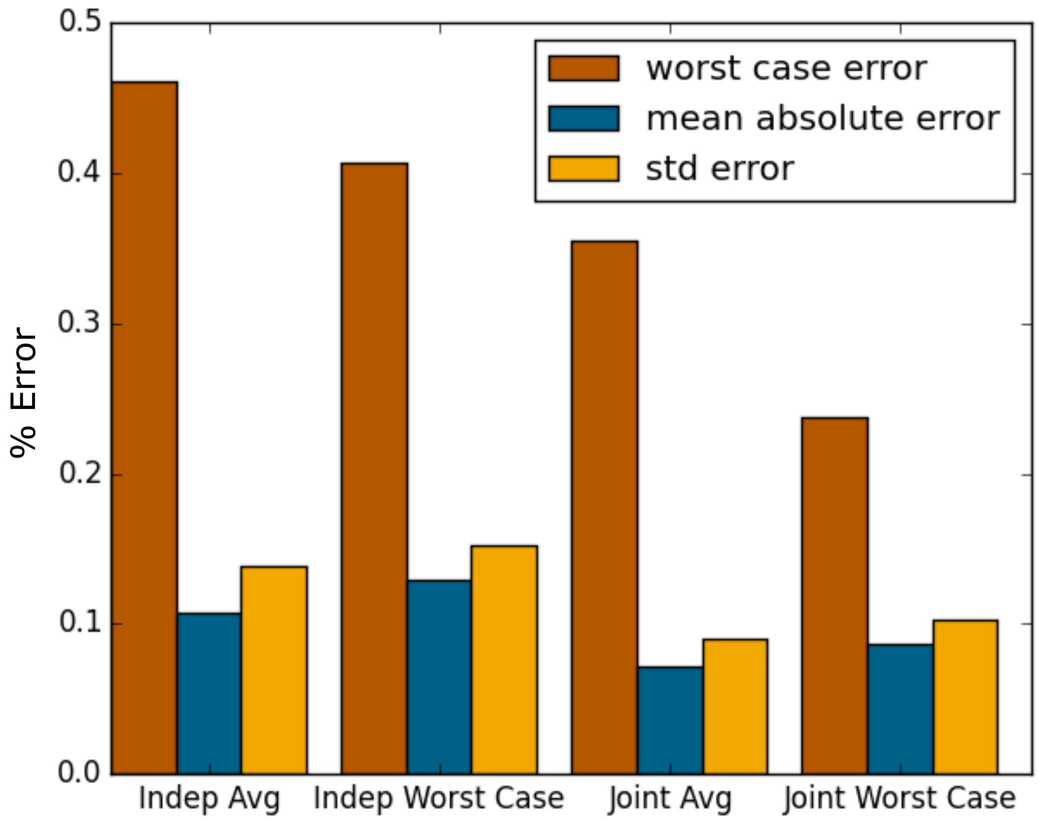

Figure 3.10: A comparison of the independent and joint discretization method results.

discretization instead of shortcut discretizations. We define our value based on whether the decision changes based on the results of the discretization. If the results of two discretizations both indicate that the company should initiate a project, there is no change in value because the value is the same. If the decision is to correctly initiate the project when originally the discretization would not have recommended the project, then the present value of the project is accrued to the new discretization. In the different conditions where either discretization correctly or incorrectly accepts or rejects a project and the other one does the opposite, we accrue or decrement that value of the change in decision accordingly. In this section, we modify the problem in order to induce an increase in different decisions and compare the results.

We begin by adjusting the initial capital required in Equation (1) so that the median CE is now zero. In half the decision problems, the best decision is now to pass on the project, and in half, the decision is to accept the project. The histogram of the project values is the same as in Figure 3.3 but shifted lower by a total of \$3.50MM. With several decision problems having CEs near zero, we modify the equation for $Err(d,p)$ to be Equation (3.3). This changes the formula for the error approximation equation, Equation (3.10), to

$$Err(d,p) \approx \frac{-\rho_d}{T_d} \left| E_p[u_d(x)] - T_d \right| . \tag{3.15}$$

Using a new values for δ_d in Model (3.11), we solve the same set of models again to obtain new optimal discretizations. These discretizations are different due to the increased importance of negative results. For each discretization we determine the additional value derived from knowing the true distributions of the uncertainties as opposed to using the discretizations of the uncertainties.

From our initial Monte Carlo integration, we determine the CE_d of each decision problem. We compare CE_d to the $CE_d(p)$ given by the discretization. In our sample problem the two strategic options are to initiate the project, or to not initiate the project. The outcomes from the discretizations are to correctly initiate or pass on the project, or to incorrectly initiate or pass on the project. We define relative cost (RC) as the expected additional cost of using a discretization instead of knowing the functional form of the uncertainties. For each decision problem $d \in \mathbb{D}$, RC_d is the mean absolute value of the CE_d when the wrong decision is made due to the discretization and zero otherwise. For example, when the true CE is 100, and the discretized CE is negative, the value of having the true CE is 100. When the true CE is $10,000$, and the discretized CE is 1, both CE values will recommend initiating the project. In this case, the value of knowing the true CE is 0 because the decision is the same, even if the accuracy was off by almost $10,000$. The relative cost of the discretization for a decision problem, d is as follows:

$$RC_d = \begin{cases} CE_d & \text{if } CE_d > 0 \text{ and } CE_d(p) < 0 \\ -CE_d & \text{if } CE_d < 0 \text{ and } CE_d(p) > 0 \\ 0 & \text{otherwise.} \end{cases} \tag{3.16}$$

over all the decision problems. The discretization with the lowest relative cost is the discretization where the decision from using the discretization matches the decision that would come from knowing the functional forms of the uncertainties and the true CE the most. The higher the RC, the worse a discretization is in terms of value. We can compare the average RC for the different discretizations to determine how much additional value one method has over another.

We begin by comparing the RC for the shortcuts. Figure 3.11 shows the results of the relative cost calculations. The histograms show how often each discretization has a an added cost in the $6,561$ decision problems. Those cases where the additional cost is zero are omitted, as their frequency is much greater than the others. Figure 3.11 indicates the MCS shortcut tends to have the most instances of RC and the largest RC values. Among the shortcuts, this produces the largest mean RC. EPT and HB perform better than MCS and ESM. The average RC for ESM is only 35.28 percent worse than EPT. This compares to the average error being about 67.08 percent worse than HB. In absolute terms, the additional value provided by EPT over ESM is \$35.48, which for a project with an average CE of \$52,642.89 is only 0.07 percent. Problems with a more strategic options and a larger range of project values will likely result in larger RC differences.

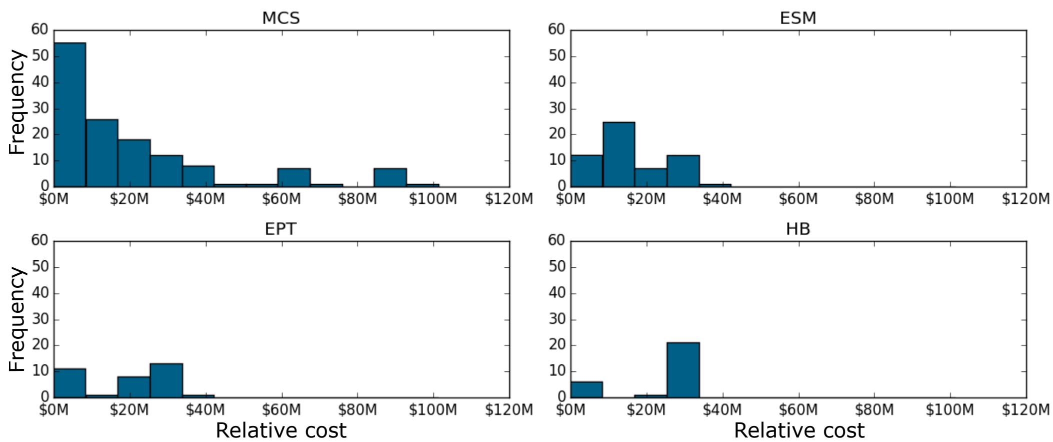

Figure 3.11: The distribution of the relative cost (of not knowing the true distributions of the uncertainties) for four shortcut methods. The value of knowing the true distribution for most of the decision problems is \$0. This means most of the time, the discretization is on the right side of 0. In some cases, as with MCS, the relative cost can be as high as \$100,000. Note: there were a large number of observations at zero, which were removed to better visualize the remaining observations.

Next we calculate RC for the optimized discretizations. We compare the joint discretizations best average, the independent best average, the independent worst case, and the EPT discretization. The optimized discretizations had a wide range of RC as seen in Figure 3.12. At one extreme, the optimizations using average error had RC values of \$1.62 and \$4.04 for the joint discretization and independent discretization respectively. This means knowing the functional forms of the uncertainty distributions provides almost no value above using a discretization (as long as the assessments are accurate). At the other extreme, the optimizations using worst case error performed substantially worse than any of the shortcuts. The RC for worst case errors were \$695.30 and \$201.09 for the joint discretization (not shown) and independent discretization respectively. The reason behind this complete flip in performance is that minimizing worst case error tends to focus on the most extreme-valued decision problems. None of the other results influence the discretization. For the joint discretization, the true CEs of the decision problems where the optimal discretization leads to the wrong decision, has a range between $-\$72,903$ and $\$79,812$. The independent discretization has a range between $-\$72,903$ and $\$5,884$.

Sampling the decision problems and limiting the percentiles yields similar results as compared to the original decision problems and error function. That is that they had a lower RC in comparison to the shortcuts. The general exception is that worst-case optimization underperformed its best average counterpart. In only six out of 30 runs minimizing the worst case had a lower RC than minimizing the average error. The best-performing methods used the more extreme percentiles. Using more samples typically results in better alower RC, but not always. For instance, the best RC came from solving the joint discretization optimization using 20 percent of the decision problems and the best average. It yields a RC of only \$0.52. This is likely a result of serendipitous sampling. The worst result comes from optimizing for the worst case, maintaining independence of uncertainties, and using 10^{th}, 50^{th}, and 90^{th} percentiles. This discretization had a RC of \$840.59.

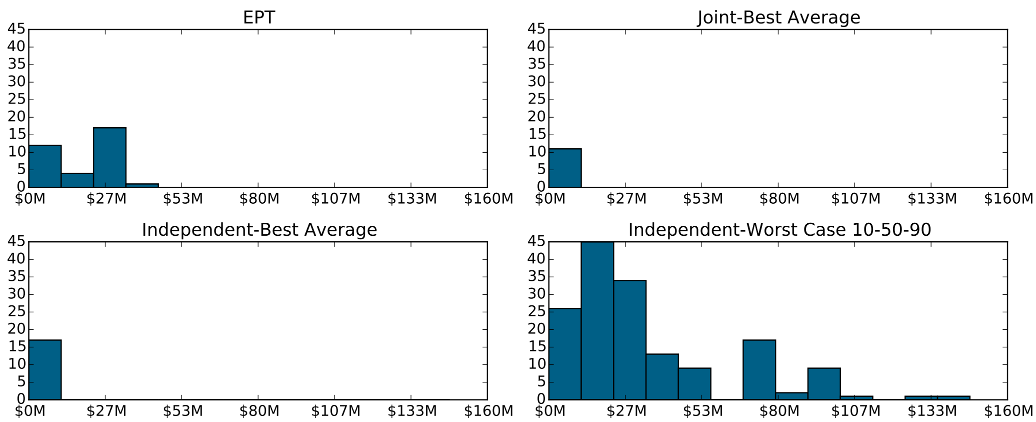

Figure 3.12: The distribution of the relative cost comparing EPT with the results from optimal average error for joint and independent discretizations and optimal worst-case independent discretization using only the 10^{th}, 50^{th}, and 90^{th} percentiles. The worst case optimization has the most decision problems and highest RC of any discretization we test. For this discretization, the RC of one of the decision problems is over $\$140,000$. Note: Each distribution has a large frequency of values at zero that we have removed to better show the scale of the non-zeros.

3.4.7 How well do the discretizations work with new uncertainty distributions when applied to the original problem?

So far this method has performed extremely well when optimized against a training set of distributions. We use the term "training set" in the same way it is used in machine learning and forecasting. In predictive analytics we use a set of data to generate model parameters; in our case these are the discretizations. The results of the first model are tested against another sample set of data in order to determine if the model works for the entire set of data. It can also be noted that if the problem to be solved is from one of a potential set of distributions, the decision analyst can estimate the CE of every uncertainty distribution combination and come up with a distribution of the CE. In a situation like this, the process of optimization does not help the decision-making process. In practice, all potential distributions for every uncertainty should be used in the optimization model, as it is important to include as much information as possible into the results.

To test the performance of optimal discretization we change the functional form of all the uncertainties in the Wildcatter model from [40]. We begin by using the historical pricing of the West Texas Intermediate benchmark. We downloaded the prices from the United States Energy Information Administration for the front month Cushing, OK Crude Oil Future Contract on their web site [1]. We used the reservoir and cost data distributions from the original [40] paper, and we used a beta(3,27) distribution for the recoverable oil percentage. We chose this number to have a mean of 10 percent and would range between 1.5 percent and 26 percent. When comparing to the distributions in Figure 3.2, this tends to be on the low side, but within the realm of the feasible.

Examining the price distribution in the original [40] paper and in Figure 3.2, we determined the oil price was somewhere between \$10 and \$50. The WTI price data begins on April 4, 1983, with a price of 29.44 and remains below \$50 until October 5, 2004. We use he daily closing price to populate our price distribution in our first example.

In a second test, we wanted to see if the methodology might also be applicable to shale drillers. In this test case, we used recent prices. We used the two years of price history, from September 14, 2015 until September 12, 2017. We also doubled the capital cost of drilling a well, and we doubled the production rate. Because we used historical data, our distributions as seen in Figure 3.13 have their own shapes. The data pulled from a 20 year span between 1984 and 2004 is multi-modal positively skewed. The two year span between 2015 and 2017 is negatively skewed.

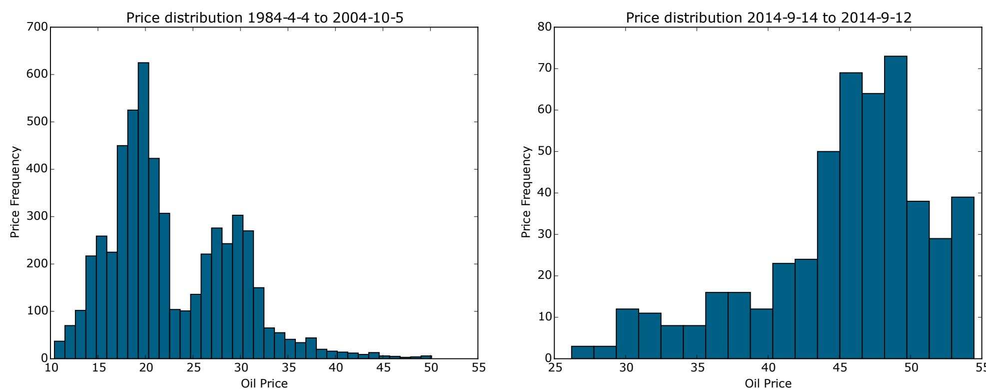

Figure 3.13: The oil price distributions, when drawn from historical data, do not resemble any of the distributions we have used to train the model.

In both examples, we estimate the CE using the Latin hypercube technique. We applied the discretization percentiles and probabilities that we generated previously. These are available for reference in Sppendix 3.5.1. We chose the best average and worst case discretizations for all candidate percentiles and the 5, 50, 95, and 10,50, 90 optimized discretizations. It should be noted none of the uncertainty distributions in our new problem (the test set) were any of the distributions used to calculate the optimal discretizations (the training set). We find that without having the new distributions in the training set, some of the very best performing optimal discretizations from subsection 3.4.2 and subsection 3.4.5 underperformed the shortcuts. We also find that the consistently best-performing discretization is still an optimized discretization.

The results from this example indicate that simplicity is may be the most robust. The results are shown in Figure 3.14. The best-performing discretization is the independent discretization that discretizes using the $10-50-90$ percentiles. In general, the optimized $10-50-90$ shortcuts performed better using the new distributions in the example problems, while in the training sets, the optimized $5-50-95$ discretizations performed better. In the first example, the mean is much further away from zero, so differences in percent error tend to be closer. In the second example, the mean is much closer to zero, and differences are greater. It should be noted that just as with the optimal discretizations, the shortcuts also vary in their performance between the two examples. In the first example, ESM has the best performance of all the shortcuts we test. MCS, which is also a $10-50-90$ shortcut performs better than HB and EPT, which use more extreme values.

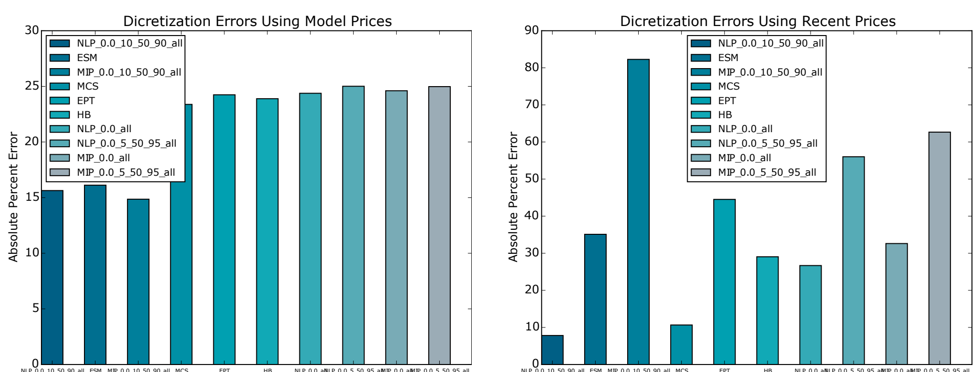

Figure 3.14: West Texas Intermediate oil prices representing a twenty year history and oil prices representative of the oil prices during the fracking boom in the united states.

3.4.8 How well do the discretizations work with other problems?

So far the numerical analysis has focused on the Wildcatter problem introduced by [40]. We now present a shorter analysis of Eagle Airlines, first introduced by [6] and further refined by [7]. A short description of Eagle Airlines is given in Appendix .2. For this problem we also have four important correlated uncertainties, price, hours, capacity, and operational cost that affect the value of purchasing an airplane by a company for the purpose of providing charter flights. For each of these uncertainties we created a set of potential uncertainties. These are shown in Figure 3.15. With the Cartesian combination of each of these uncertainties we determined the expected value (risk neutral) of the purchase decision. The distribution of the expected value of the purchase is given by Figure 3.16.

We solve for the independent discretizations using $P10-P50-P90$ and $P5-P50-P95$ percentiles across all the Cartesian of decision problems. We apply the resulting discretizations to the correlated uncertainties of the true distributions to determine the error of the optimized discretizations and the shortcut methods. These results are shown in Figure 3.17, and we present the discretizations in Section 3.5.1.

In this example, the best discretization for the training set that uses some potential distributions to generate the discretization uses $P5-P50-P95$ for each uncertainty, with values similar to EPT. When we determine the error using various discretizations and using the true distributions given by [26]. The discretization using the $P10-P50-P90$ percentiles has the least absolute error from the true expected value. Though this example does not provide absolute proof, the Eagle Airlines example shows that a less extreme set of percentiles is robust for determining the CE and expected value of a project

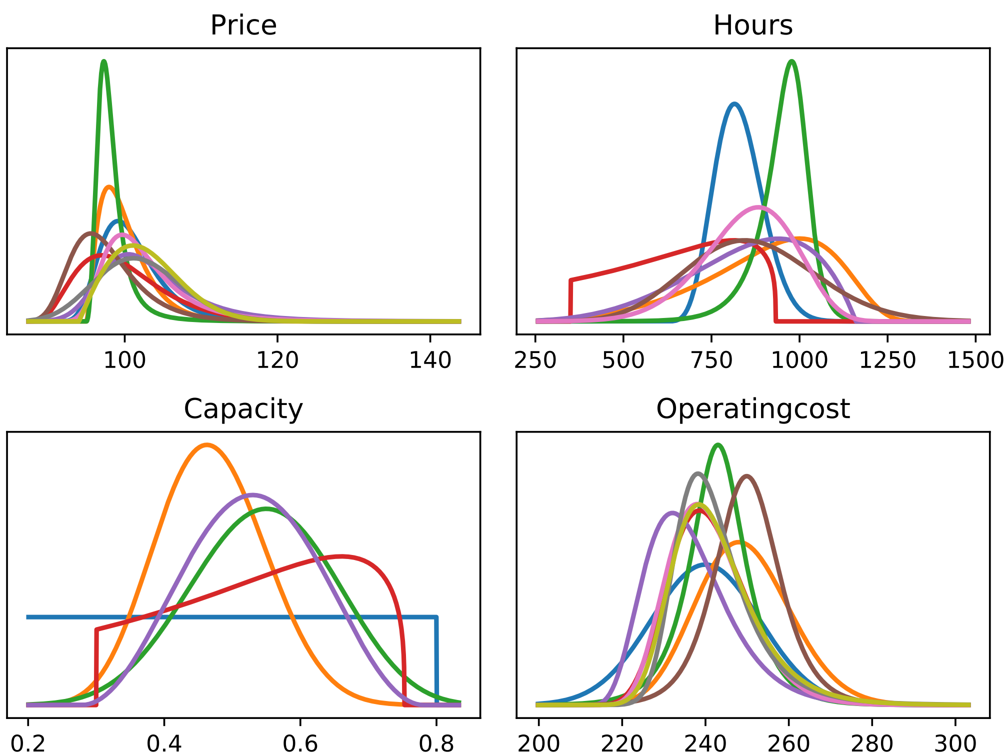

Figure 3.15: The potential distributions for the four uncertainties of Eagle Airlines. None of these distributions is the true distribution of the given problem.

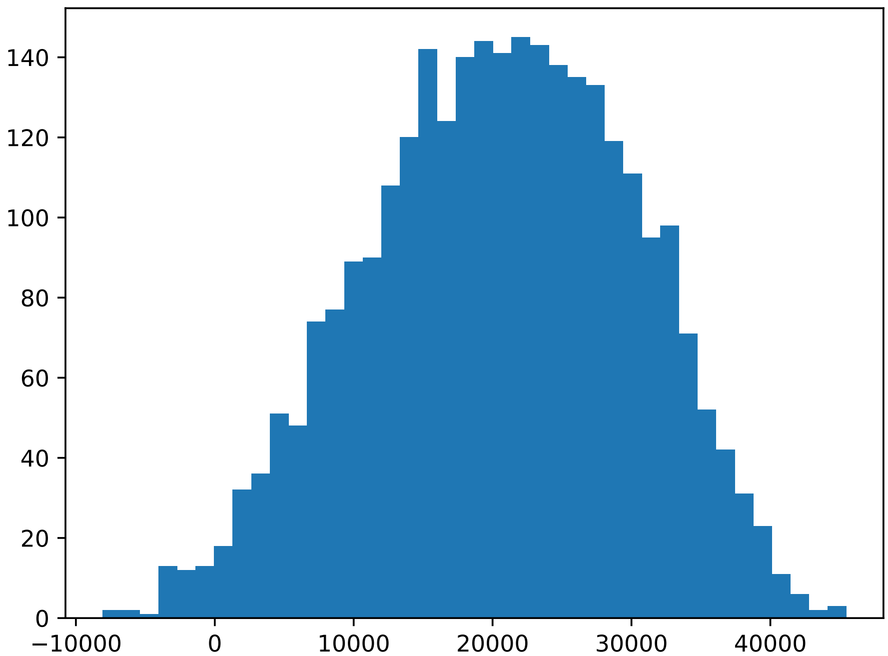

Figure 3.16: The histogram of the expected value of the various uncertainty distribution combinations.

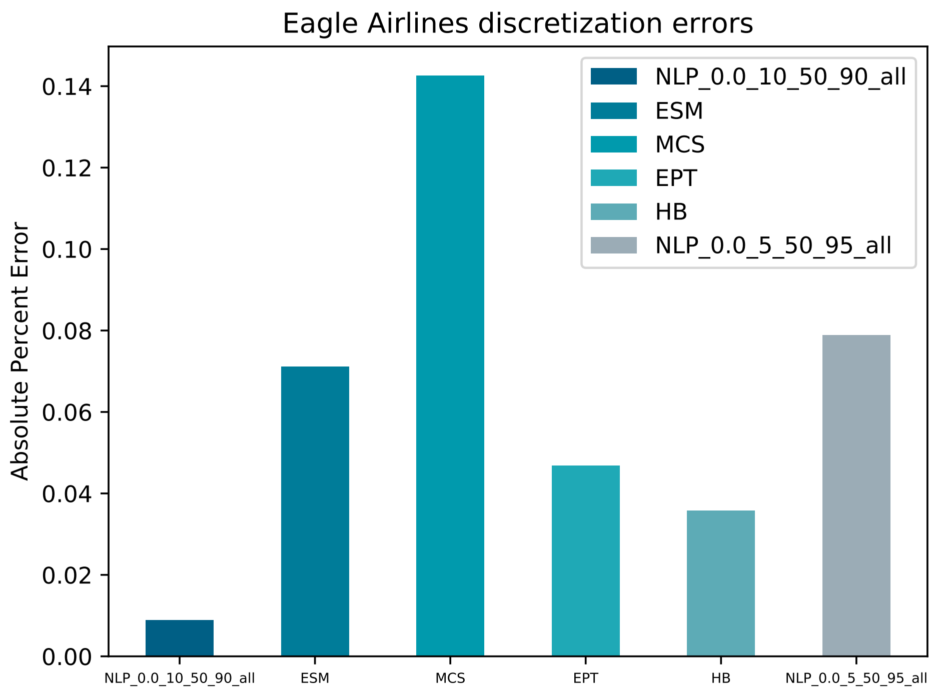

Figure 3.17: A summary of selected discretizations using the example of Eagle Airlines given by [7]. All errors are less than 0.14% with the $P10-P50-P90$ turning out the best.

when the true distributions are unknown and not part of the training set.

These examples should not be taken as conclusive. They illustrate that the improved performance of an optimized discretization or a shortcut is dependent on the distributions of the uncertainties. The results show optimal discretizations can have robust results for a specific type of decision problem that is repeatable. A result we do not show in Figure 3.14 is that worst-case optimization consistently under-performs the average-case optimization. We also found independent discretizations outperform joint discretizations. Finally, we find that discretizations that only use a sample of the data still perform within a few percentage points of the best one. A ten percent sample performs the best over the examples we test. We believe the degradation in performance in both the shortcut and optimized discretizations in comparison to the $10-50-90$ discretizations is due to over-fitting and the use of extreme results to provide an initially better fit.

3.5 Discussion and Recommendations

In the computational experiments we perform, optimized discretization of Model (3.1) improves on existing discretization methods. This improvement can be over worst-case $Err(d, p)$, average $Err(d, p)$, or a convex combination. The methodology provides a large amount of flexibility. While we use the absolute percentage error for much of our analysis, we also switched to the absolute CE error when we calculated the relative cost of using discretizations in Subsection 3.4.6. Additionally, our error functions are linear, and may be expanded to quadratic when the discretizations stray too far from the minimum to provide a good estimate. The methodology is able to compute both independent and joint discretizations – a novel approach over past discretization methods that focus solely on independent discretizations.

Based on our findings, we make recommendations to the practitioner who would like to improve the accuracy of their discretizations and value of their recommendations. We believe more testing is necessary before choosing between joint and independent discretization methods. While a joint discretization generally provides more accurate discretizations over the training problems, joint discretizations seem to over-fit. When using a joint discretization, it is important to have a large number of training problems.

In our tests, the 10 percent sample size results offer significant error reduction over shortcuts (70 percent) and reduce the time for the non-linear optimization by 90%. We do not know if this improvement in performance while maintaining and edge in accuracy will hold with other problems. The time required for non-linear optimization solvers to generate solutions can take days, and it is worth experimenting with sampling to generate results that are better than shortcuts in a reasonable amount of time.

We recommend using the average error method over using the worst-case error method. The analysis of the relative cost of the worst-case analysis tends to show that optimizing to the worst case provides the least value of any discretization method. Optimizing over the average error provided the highest value discretizations. The results when using the recommended problem size and discretization method are shown in Figure 3.18.

Practically, the decision problem set over which the optimized discretization is computed can make a significant difference in the output. If a practitioner knows relatively little about the client and problem, the practitioner should select a decision problem set $\mathbb{D}$ that includes large ranges of uncertainty distributions and value functions. This would result in an optimized discretization that works reasonably well across this large range of problems. However, if the practitioner knows more about the client or industry, the practitioner should select a decision problem set $\mathbb{D}$ that still has many instances in it, but focuses on the ranges of parameters present in the industry. This would result in optimized discretizations that yield small errors on that small parameter range. The practitioner can include optimized discretization in the decision analysis process and determine how much reducing the variability of an uncertainty will go towards reducing the distribution of errors of the discretization.

From our observations, the computation time required for finding an optimized discretization increases linearly in $|\mathbb{D}|$ due to increases in the number of constraints. Computing optimized joint discretizations depends on solving a mixed integer linear program which is generally faster than computing optimized independent discretizations. In both independent and joint discretization the computation time increases exponentially with the number of uncertainties, and the number of candidate percentiles. A reduction in the number of candidate percentiles will reduce computation time.

We found optimized discretizations make a greater use of the 5^{th} and 95^{th} percentiles relative to the use of the 10^{th} and 90^{th} percentiles. In their research, [2] noted that assessing more extreme values is also more prone to error, and the results from [11] and [12] also make use of more extreme percentiles. An expert that has twice the experience is likely to have seen twice the number of extreme events, and is likely to be able to better assess the value of those extreme events. The result is that someone who is assessing the 95^{th} percentile, may only be assessing a value at the 90^{th} percentile. In addition to being more robust, $P10 - P50 - P90$ discretizations may also be less susceptible

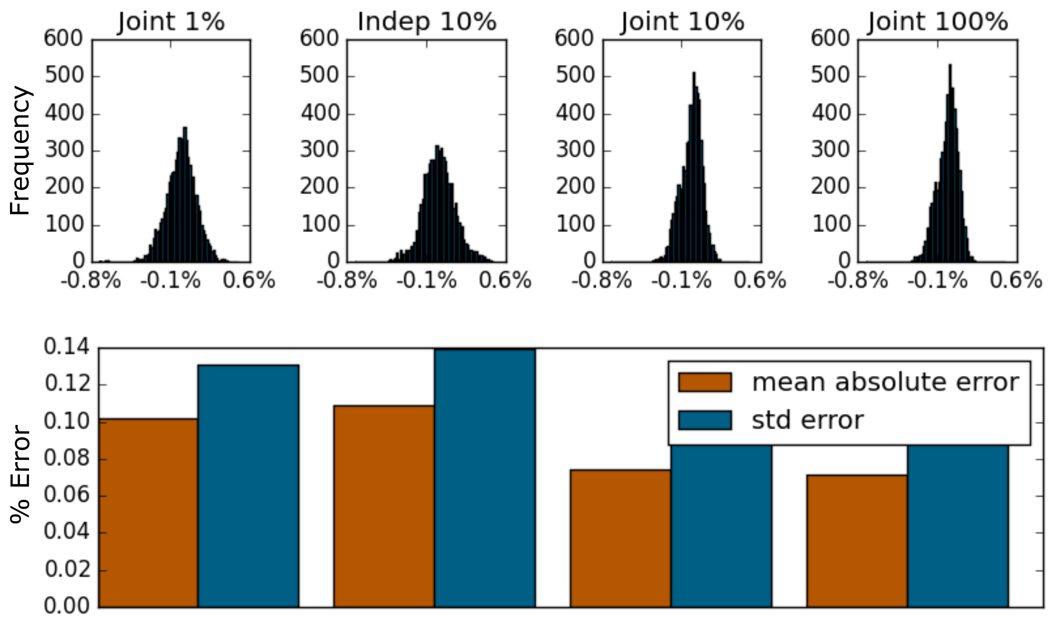

Figure 3.18: A joint discretization that samples 10 percent of the decision problems yields results that are better than shortcuts, solve quickly, and are close in terms of resulting error to the use of 100 percent sampling.

to assessment error than are $P5 - P50 - P95$ discretizations. This adds an uncertainty to the set of decision problems.

In our analysis we used a linearization of absolute percentage error. Optimal discretization is flexible in its ability to use multiple objective functions. Other objectives we have considered are measuring deviation from expected value or adding additional terms to the Taylor expansion of the error function. It is our recommendation that the Taylor expansion of the objective function be linear if possible so as to keep solution times as short as possible. In conclusion, optimized discretization can help decision analysis practitioners create discretizations that are specific to their current projects that are likely to be more accurate than shortcut methods. Intuitively, the key difference between optimized discretizations and other discretization methods is that optimized discretizations take as input an entire decision problem set $\mathbb{D}$ and a valuation function like (1). This allows optimized discretizations to focus on producing lower CE errors than using traditional discretization. Figure 3.18 shows how the errors change when switching between different sampling percentages and between Model (3.11) and Model (3.13). The difference is less than 0.04 percent between the 10 percent sample using Model (3.11) and the 100 percent sample using Model (3.13). The gain in robustness favors the independent discretization with a 10 percent sampling of the decision problems.

3.5.1 Discretization Values

We present selected joint and independent discretization values for the Wildcatter problem and then Eagle Airlines. The shortcut names are the same as used in the article. The optimized discretization names are coded. The first code is either “NLP” or “MIP”. Independent discretizations are solved with a non-linear programming solver and hence have the code "NLP". Joint discretizations are solved with a mixed-integer programming solver and hence have the code "MIP". The next code is either a zero or a one. Zero indicates the discretization is solved to minimize the average error. A one indicates the discretization is solved to minimize the worst case error. The next three numbers are optional. These numbers indicate whether specific percentiles are used. For example, "5_50_95" indicates the 5^{th}, 50^{th}, and 95^{th} were the only percentiles allowed in the discretization. The final code indicates how many sample decision problems are used to create the discretization.

This table shows the percentiles and probabilities of the shortcuts plus the results of Model (3.11) with $\lambda = 1$ and the percentiles forced to $P5, P50, P95$.

Table 3.1: Wildcatter Independent Discretizations

		Percentiles			Probabilities		
Discretization	Uncertainty	Q1	Q2	Q3	P1	P2	P3
MCS	Reservoir	0.10	0.50	0.90	0.25	0.50	0.25
MCS	Recovery	0.10	0.50	0.90	0.25	0.50	0.25
MCS	Price	0.10	0.50	0.90	0.25	0.50	0.25
MCS	Cost	0.10	0.50	0.90	0.25	0.50	0.25
ESM	Reservoir	0.10	0.50	0.90	0.30	0.40	0.30
ESM	Recovery	0.10	0.50	0.90	0.30	0.40	0.30
ESM	Price	0.10	0.50	0.90	0.30	0.40	0.30
ESM	Cost	0.10	0.50	0.90	0.30	0.40	0.30
HB	Reservoir	0.04	0.50	0.96	0.16	0.67	0.16
HB	Recovery	0.05	0.50	0.95	0.18	0.63	0.18
HB	Price	0.04	0.50	0.96	0.16	0.67	0.16
HB	Cost	0.04	0.50	0.96	0.16	0.67	0.16
EPT	Reservoir	0.05	0.50	0.95	0.18	0.63	0.18
EPT	Recovery	0.05	0.50	0.95	0.18	0.63	0.18
EPT	Price	0.05	0.50	0.95	0.18	0.63	0.18
EPT	Cost	0.05	0.50	0.95	0.18	0.63	0.18
NLP_1.0_5_50_95_all	Reservoir	0.05	0.50	0.95	0.25	0.61	0.14
NLP_1.0_5_50_95_all	Recovery	0.05	0.50	0.95	0.27	0.50	0.23
NLP_1.0_5_50_95_all	Price	0.05	0.50	0.95	0.03	0.86	0.11
NLP_1.0_5_50_95_all	Cost	0.05	0.50	0.95	0.21	0.63	0.16

Table 3.2: Wildcatter Independent Discretizations, cont.

		Percentiles			Probabilities		
Discretization	Uncertainty	Q1	Q2	Q3	P1	P2	P3
NLP_0.0_5_50_95_all	Reservoir	0.05	0.50	0.95	0.15	0.66	0.18
NLP_0.0_5_50_95_all	Recovery	0.05	0.50	0.95	0.20	0.60	0.20
NLP_0.0_5_50_95_all	Price	0.05	0.50	0.95	0.19	0.63	0.18
NLP_0.0_5_50_95_all	Cost	0.05	0.50	0.95	0.19	0.62	0.19
NLP_0.0_10_50_90_all	Reservoir	0.10	0.50	0.90	0.35	0.34	0.31
NLP_0.0_10_50_90_all	Recovery	0.10	0.50	0.90	0.27	0.46	0.27
NLP_0.0_10_50_90_all	Price	0.10	0.50	0.90	0.16	0.62	0.22
NLP_0.0_10_50_90_all	Cost	0.10	0.50	0.90	0.35	0.41	0.24
NLP_0.0_all	Reservoir	0.05	0.50	0.95	0.20	0.61	0.19
NLP_0.0_all	Recovery	0.10	0.55	0.95	0.26	0.57	0.17
NLP_0.0_all	Price	0.05	0.50	0.95	0.19	0.63	0.18
NLP_0.0_all	Cost	0.10	0.55	0.95	0.29	0.53	0.18
NLP_1.0_all	Reservoir	0.05	0.55	0.90	0.22	0.52	0.27
NLP_1.0_all	Recovery	0.05	0.55	0.90	0.32	0.33	0.36
NLP_1.0_all	Price	0.05	0.50	0.90	0.25	0.44	0.31
NLP_1.0_all	Cost	0.10	0.55	0.95	0.28	0.52	0.19

This table shows the percentiles and probabilities for various runs of Model (3.11). The first three sets of discretizations, are for $\lambda = 0$. The last set has $\lambda = 1$. The first set forces the percentiles to be $P5, P50, P95$. The second set forces the percentiles to be $P10, P50, P90$. The third and fourth set allow all seven percentiles.

Table 3.3: Wildcatter Independent Discretizations, cont. (2)

		Percentiles			Probabilities		
Discretization	Uncertainty	Q1	Q2	Q3	P1	P2	P3
NLP_0.0_66	Reservoir	0.05	0.45	0.95	0.13	0.67	0.20
NLP_0.0_66	Recovery	0.05	0.50	0.95	0.20	0.61	0.19
NLP_0.0_66	Price	0.05	0.50	0.95	0.18	0.64	0.18
NLP_0.0_66	Cost	0.05	0.50	0.95	0.19	0.62	0.19
NLP_0.0_328	Reservoir	0.10	0.50	0.95	0.18	0.64	0.19
NLP_0.0_328	Recovery	0.05	0.50	0.95	0.20	0.60	0.20
NLP_0.0_328	Price	0.05	0.50	0.95	0.18	0.64	0.18
NLP_0.0_328	Cost	0.05	0.45	0.95	0.15	0.64	0.20
NLP_0.0_656	Reservoir	0.10	0.50	0.95	0.20	0.61	0.19
NLP_0.0_656	Recovery	0.05	0.50	0.95	0.20	0.61	0.19
NLP_0.0_656	Price	0.05	0.50	0.95	0.18	0.64	0.18
NLP_0.0_656	Cost	0.10	0.55	0.95	0.29	0.52	0.19
NLP_0.0_1312	Reservoir	0.10	0.55	0.95	0.24	0.59	0.18
NLP_0.0_1312	Recovery	0.05	0.50	0.95	0.20	0.60	0.20
NLP_0.0_1312	Price	0.05	0.50	0.95	0.19	0.63	0.18
NLP_0.0_1312	Cost	0.10	0.55	0.95	0.29	0.53	0.18
NLP_0.0_all	Reservoir	0.05	0.50	0.95	0.20	0.61	0.19
NLP_0.0_all	Recovery	0.10	0.55	0.95	0.26	0.57	0.17
NLP_0.0_all	Price	0.05	0.50	0.95	0.19	0.63	0.18
NLP_0.0_all	Cost	0.10	0.55	0.95	0.29	0.53	0.18

The discretizations for $\lambda = 0$ for Model (3.11) with 66, 328, 1312, and all decision problems. The

The next joint discretization is for the average error minimization. The number of non-zero percentile combinations is much larger here, which gives a more robust answer when computing out-of-sample percent errors.

Table 3.4: Wildcatter Joint Discretizations

Reservoir Quantile	*Recovery Quantile*	*Price Quantile*	*Cost Quantile*	*MIP_1.0_10_50_90_all*	*MIP_0.0_10_50_90_all*
0.10	0.10	0.90	0.90		0.088
0.10	0.50	0.10	0.10	0.086	
0.10	0.50	0.50	0.10	0.133	0.026
0.10	0.50	0.50	0.90	0.047	
0.10	0.50	0.90	0.10		0.156
0.10	0.90	0.50	0.50	0.065	
0.10	0.90	0.90	0.10	0.049	
0.10	0.90	0.90	0.50	0.023	
0.50	0.10	0.10	0.90		0.135
0.50	0.10	0.50	0.90	0.254	0.109
0.50	0.50	0.50	0.10		0.048
0.50	0.50	0.50	0.50	0.052	
0.50	0.50	0.90	0.50		0.051
0.50	0.90	0.50	0.90		0.030
0.50	0.90	0.90	0.50	0.045	0.022
0.90	0.10	0.10	0.50	0.031	
0.90	0.10	0.10	0.90		0.001
0.90	0.10	0.50	0.50	0.057	
0.90	0.50	0.10	0.10	0.057	0.102
0.90	0.90	0.10	0.50		0.061
0.90	0.90	0.50	0.50		0.172
0.90	0.90	0.90	0.50	0.100	

Table 3.5: Wildcatter Joint Discretizations, cont.

Reservoir Quantile	*Recovery Quantile*	*Price Quantile*	*Cost Quantile*	*MIP_1.0_all*
0.10	0.05	0.55	0.90	0.033
0.10	0.50	0.55	0.45	0.064
0.10	0.50	0.55	0.90	0.176
0.10	0.95	0.55	0.45	0.060
0.45	0.05	0.55	0.45	0.040
0.45	0.05	0.55	0.90	0.100
0.45	0.50	0.05	0.10	0.147
0.45	0.50	0.55	0.10	0.035
0.45	0.50	0.55	0.45	0.158
0.45	0.95	0.55	0.45	0.006
0.90	0.05	0.55	0.10	0.008
0.90	0.05	0.55	0.45	0.047
0.90	0.95	0.95	0.10	0.111
0.90	0.95	0.95	0.45	0.016

Table 3.6: Wildcatter Joint Discretizations, cont. (2)

Reservoir Quantile	Recovery Quantile	Price Quantile	Cost Quantile	MIP_0.0_all
0.05	0.10	0.05	0.10	0.045
0.05	0.10	0.50	0.10	0.010
0.05	0.10	0.50	0.55	0.018
0.05	0.55	0.05	0.10	0.001
0.05	0.55	0.05	0.95	0.013
0.05	0.55	0.50	0.10	0.049
0.05	0.55	0.50	0.95	0.035
0.05	0.55	0.95	0.10	0.004
0.05	0.90	0.05	0.55	0.013
0.05	0.90	0.05	0.95	0.001
0.05	0.90	0.95	0.10	0.026
0.50	0.10	0.05	0.95	0.020
0.50	0.10	0.50	0.55	0.111
0.50	0.55	0.50	0.10	0.046
0.50	0.55	0.50	0.55	0.210
0.50	0.55	0.50	0.95	0.060
0.50	0.55	0.95	0.55	0.007
0.50	0.90	0.50	0.10	0.060
0.50	0.90	0.95	0.55	0.047
0.50	0.90	0.95	0.95	0.028
0.95	0.10	0.05	0.95	0.007
0.95	0.10	0.50	0.55	0.028
0.95	0.10	0.95	0.10	0.060
0.95	0.55	0.50	0.55	0.002
0.95	0.55	0.50	0.95	0.015
0.95	0.55	0.95	0.95	0.003
0.95	0.90	0.05	0.55	0.074
0.95	0.90	0.50	0.10	0.000
0.95	0.90	0.50	0.55	0.001
0.95	0.90	0.50	0.95	0.004

Chapter 4

Shape-matching Discretizations

4.1 Introduction

In decision analysis, the objective is to gain clarity of action for strategic, high-value decisions. When comparing different strategies, the risk-neutral decision maker should choose the strategy that has the best mean value. All decisions have risk and if the answer were known there would be no need for analysis. Part of this risk is that the decision will not lead to a good outcome. We define "good", as being better than the next alternative, which could be to do nothing, or to undertake a safe strategy. Interpreting the meaning of CE, where the value lottery is transformed by a utility function, may not be intuitive for a decision maker. Instead the decision maker might prefer a more intuitive approach and make a decision based on the value lottery at various percentiles. Figure 4.1 shows the CDF of the value of the aircraft purchase from the Eagle Airlines problem described briefly in the Appendix in Section .2. The true mean of the project is \$11847. The mean value given by the EPT discretization is \$11865, which is gives an error of 17, or an error of 0.14 percent.

A positive mean value may be enough to approve the purchase. If the decision maker is concerned about the performance at different percentiles, then the decision maker can look up the desired percentile on the cumulative probability axis and move horizontally to the right to determine what the

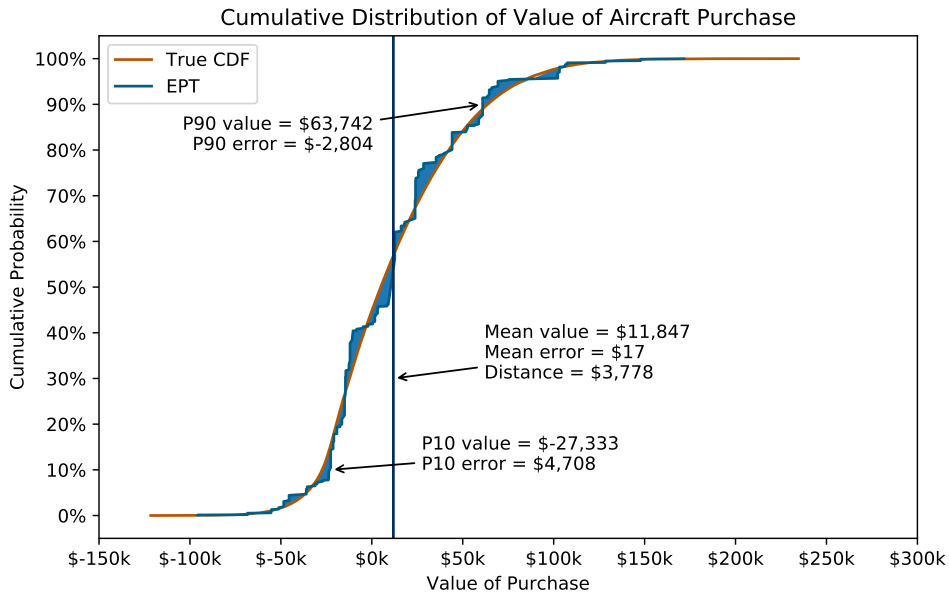

Figure 4.1: EPT distance comparison.

value for the discretization at that percentile. The blue area between the true distribution and the discretization in Figure 4.1 is the error obtained by looking up the value of the decision at each percentile and comparing it to the true value. Discretizations that have no error between their CDF and the true CDF match the shape. To track how well a discretization matches the shape of the true CDF, we introduce the distance metric, D. The distance metric differs from the Kolmogorov-Smirnov (KS) test in that it measures a mean absolute horizontal distance rather than a maximum vertical distance.

A mean horizontal distance tells a decision maker on average how far off is the discretized CDF from the true CDF. The KS distance tells the user what the difference in percentile is for any specific value. In the example in Figure 4.1 at the 10^{th} percentile, the true value is $-\$27,333$. The discretization gives a value of $-\$22,625$. The true value at the 10^{th} percentile is $\$4,708$ worse than the value given by the discretization. If a decision maker is going to use values at different percentiles to inform his/her decision, it is important to match the shape when choosing a discretization. When matching the shape, the error between the discretized value lottery and the true value lottery at each p is minimized, allowing for a more accurate assessment of risk.

The rest of this chapter is organized as follows. We begin by defining the distance metric and specify the conditions and define a closed form to calculate distance in Section 4.2. In Section 4.3 we test various combinations of distributions, correlations, and operations (sum,the sum of products) and how often they meet the conditions to apply our closed-form estimate for distance. In Section 4.4 we compare the closed form estimation of distance to the actual. We do this for conditions that do and do not meet the necessary criteria for the closed form. Finally, in Section 4.5 we analyze how different metrics affect the distance, and we analyze the errors at specific percentiles.

4.2 The Distance Metric

In this section we define the formula, create a closed form calculation for distance, and determine the necessary conditions required to match the shape.

We define distance as the absolute value of the difference of two cumulative distribution functions when integrated from zero to one:

Definition 4.1. *Given two distributions, 1 and 2, where $F_i^{-1}(p)$ is the inverse of the CDF of distribution i, Distance, D is defined as:*

$$Dist = \int_{p=0}^{1} \left| F_1^{-1}(p) - F_2^{-1}(p) \right| dp \tag{4.1}$$

Definition 4.2. *Given two distributions, 1 and 2, where $F_i^{-1}(p)$ is the inverse of the CDF of distribution i, the percentile, p_0 is the value of p such that:*

$$F_1^{-1}(p_0) = F_2^{-1}(p_0) \tag{4.2}$$

Theorem 4.1 (Distance is only zero when mean and variance match)**.** *Given two normal distributions $\mathcal{N}(\mu_1, \sigma_1^2)$ and $\mathcal{N}(\mu_2, \sigma_2^2)$ with $\mu_1, \mu_2 \in \mathbb{R}$ and $\sigma_1, \sigma_2 > 0$, and $\sigma_2 \geq \sigma_1$, the distance between two normal distributions is only zero when $\mu_1 = \mu_2$ and $\sigma_1 = \sigma_2$*

Proof. $F_2^{-1}(0) \leq F_1^{-1}(0)$ because $\sigma_2 \geq \sigma_1$. Therefore distance can be re-written as $Dist = \int_{p=0}^{p_0} \left(F_1^{-1}(p) - F_2^{-1}(p)\right) dp + \int_{p=p_0}^{1} \left(F_2^{-1}(p) - F_1^{-1}(p)\right) dp$. Because distributions 1 and 2 are normal distributions, their inverse CDF functions may also be re-written as $F_i^{-1}(p) = \mu_i + \sigma_i \cdot \Phi^{-1}(p)$, where Φ^{-1} is the inverse of the CDF of the standard normal distribution. Substituting,

$$\begin{aligned} Dist = & \int_{p=0}^{p_0} \left(\mu_1 + \sigma_1 \cdot \Phi^{-1}(p) - \mu_2 - \sigma_2 \cdot \Phi^{-1}(p)\right) dp \\ & + \int_{p=p_0}^{1} \left(\mu_2 + \sigma_2 \cdot \Phi^{-1}(p) - \mu_1 - \sigma_1 \cdot \Phi^{-1}(p)\right). \\ = & (\mu_1 - \mu_2) \cdot p_0 + (\sigma_1 - \sigma_2) \cdot \int_{p=0}^{p_0} \Phi^{-1}(p) dp \\ & + (\mu_2 - \mu_1) * (1 - p_0) + (\sigma_2 - \sigma_1) \int_{p=p_0}^{1} \Phi^{-1}(p) dp. \end{aligned} \tag{4.3}$$

Additionally, $\int_{p=0}^{1} \Phi(p) dp = 0$. And, $\int_{p=0}^{p_0} \Phi^{-1}(p) dp + \int_{p=p_0}^{1} \Phi^{-1}(p) dp = 0$ therefore, $\int_{p=0}^{p_0} \Phi^{-1}(p) dp = -\int_{p=p_0}^{1} \Phi^{-1}(p) dp$.

$$Dist = (\mu_1 - \mu_2) \cdot (2p_0 - 1) + 2(\sigma_1 - \sigma_2) \int_{p=0}^{p_0} \Phi^{-1}(p) dp \tag{4.4}$$

The closed form for $\int_{p=0}^{p_0} \Phi^{-1}(p)dp$ is $-\varphi\left(\Phi^{-1}(p_0)\right)$.

$$Dist = \qquad (\mu_1 - \mu_2) \cdot (2p_0 - 1) - 2(\sigma_1 - \sigma_2)\varphi\left(\Phi^{-1}(p_0)\right) \tag{4.5}$$

$$\tag{4.6}$$

$\varphi \geq 0$ because it is the probability density function of the standard normal. $\sigma_1 - \sigma_2 \leq 0$. $2(\sigma_1 - \sigma_2) - \varphi\left(\Phi^{-1}(p_0)\right) >= 0$ and is only $= 0$ when $\sigma_1 = \sigma_2$. Additionally, $p_0 \geq 0.5$ only when $\mu_1 \geq \mu_2$, and $p_0 \leq 0.5$ only when $\mu_1 \leq \mu_2$. $(\mu_1 - \mu_2) \cdot (2p_0 - 1) >= 0$ and $(\mu_1 - \mu_2) \cdot (2p_0 - 1) = 0$ only when $\mu_1 = \mu_2$. Therefore, $Dist = 0$ if and only if $\mu_1 = \mu_2$ and $\sigma_1 = \sigma_2$. This completes the proof. $\square$

Theorem 4.1 establishes the conditions that for two normal distributions to match shapes, they must also have the same mean and standard deviation. Equation (4.6) provides a closed form estimate of the distance when we have the mean and standard deviation of two distributions. From a discretization standpoint, the discretizations that best match the mean and the standard deviation will also match the shape.

4.3 Under What Conditions May We Expect Normality?

The Central Limit Theorem (CLT) states that the mean of independent identically distributed random variables will converge to a normal distribution. There are several variants of the CLT, such as the Lyapunov CLT, which allows for the sum of independent, but not identically distributed random variables to converge to a normal. There is also a variant where the sum of weakly correlated random variables may converge to a normal. In all versions of the

CLT, the number of random variables approaches infinity. In decision analysis, there is never the assumption that there are an infinite number of random variables. There are a finite number of correlated, non-identically distributed random variables that are either summed, multiplied, or both. In this section we determine under which conditions, are the sums, and sums of products of random variables "close enough".

We begin by choosing anywhere between 4 and 20 distributions randomly from the Pearson system shown in Section 1.2. We test with samples drawn from various regions and sub-regions of the Pearson system. The regions are

- The entire region shown in Figure 1.2,
- The sub-region of the Pearson system shown that except the Pearson IV distributions,
- The sub-region of the Pearson system that defines the bell-shaped beta distributions,
- The sub-region of the Pearson system that defines the j-shaped beta distributions,
- The sub-region of the Pearson system that defines the u-shaped beta distributions.

For each distribution we randomly determine whether is has a positive or negative skewness. For each set of randomly selected distributions, we test with covariance values of $\{0, 0.25, 0.50, 0.75, 1\}$. From each distribution we draw $10,000$ uniform random variables. We correlate those percentiles and apply them to the inverse CDF of each distribution. We sum the values of the

$10,000$ samples of each variable. In addition to aggregating the variables by summing them, we also multiply pairs of random variables and then sum the resulting values. Each pairwise multiplication creates a new random variable. This sum is now represents a sum of half the number of uncertainties we started with. For example, if there are four uncertainties, $X_1 \cdots X_4$, we create new random variables $Y_1 = X_1 \cdot X_2$ and $Y_2 = X_3 \cdot X_4$. Finally, our value lottery is the sum of Y_1 and Y_2. We call this version of the aggregation as "combined". From the value lotteries we compute the mean and variance. We generate these values with random variables that have a variable mean and variance, and also with uncertainties that have a mean and variance of 1.0. We generate $10,000$ point distribution for each combination of number of uncertainties, correlation, aggregation type and fixed or variable values for mean and variance $1,000$ times. The $1,000$ tests allows us to test the frequency that a certain set of conditions results in a normal distribution.

To determine if the samples create a normal distribution, we turn to the Kolmogrov-Smirnov goodness of fit test (KS test) for the normal distribution with estimated parameters. We begin by estimating the parameters from the $10,000$ points from the distribution for the mean of the value lottery, X as $\bar{X}$ and the variance as S^2. We sort the $10,000$ points to obtain $X_1, X_2 \cdots X_{10,000}$. If $\hat{F}$ is the CDF of the $\mathbf{N}(\bar{X}, S^2)$ and $F(x) = \frac{\sum_{i=1}^{10,000}(X_i \leq x)}{10,000}$, we define

$$D = \sup_x \left\{ \left| F(x) - \hat{F}(x) \right| \right\}. \tag{4.7}$$

If

$$\left(\sqrt{n} - 0.01 + \frac{0.85}{\sqrt{n}} \right) D_n > c'_{1-\alpha} \tag{4.8}$$

then we can reject H_0 and say that the $10,000$ samples come from a distribution that is not normal. For our calculations, we use $\alpha = 0.05$ and $c_{1-\alpha} = 0.895$.

Since we always use $n = 10,000$ samples our test for each of the $1,000$ iterations is $99.9985D > 0.895$ to test whether the $10,000$ points do not come from a normal distribution.

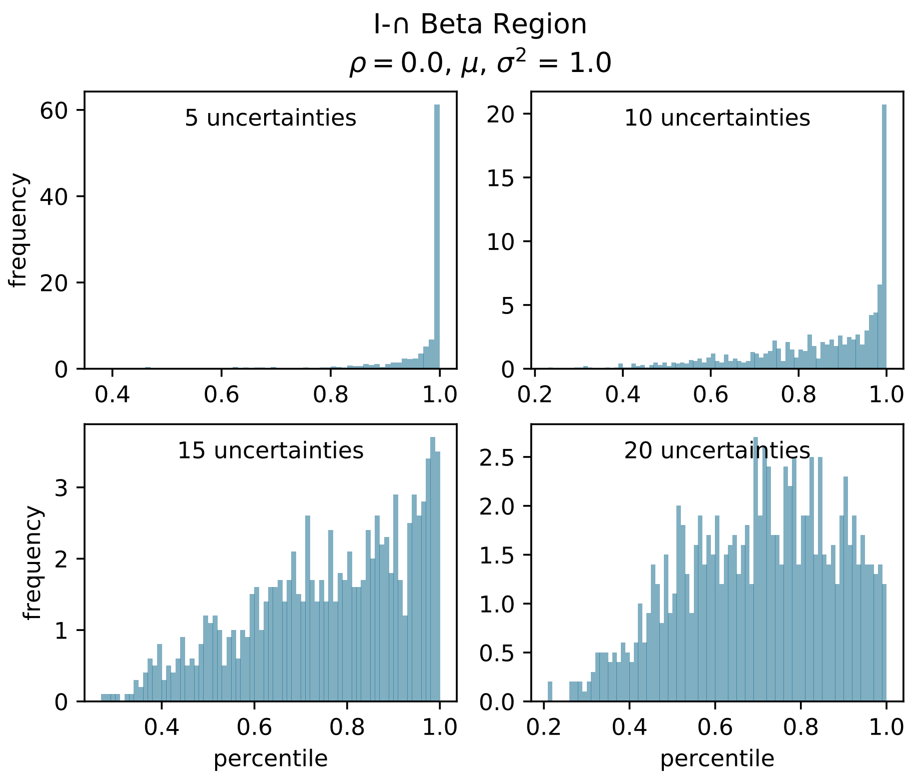

Figure 4.2: Each histogram shows the value of the CDF function for the KS1 distribution with a shape parameter of $10,000$ using the results from Equation (4.7).

As the number of uncertainties increases, the probability of accepting the null hypothesis increases. This happens earlier when the shapes of the source distributions are already closer to normal, such as the bell-shaped beta distributions. When the shape of the source distributions is something like the j-shaped betas, the probability is lower. As the correlation increases, the probability of accepting the null hypothesis decreases. Within conditions where we use the same correlation, but vary the number of uncertainties, the probability of accepting the null hypothesis increases with the number of uncertainties, just not as quickly. We also found that even if the source uncertainties were not independent and identically distributed (IID), but did share the same mean and variance, they tended to have a higher probability of null acceptance. The combined aggregation reduces the probability of null acceptance.

Figure 4.2 shows the histogram of the CDF values for the KS1 distribution. This figure is for the bell-shaped beta region with $5, 10, 15$, and 20 summed uncertainties that each have a mean and variance of 1. Values at the 95^{th} percentile or lower correspond to $D = 0.00895$ which is the largest value of D in Equation (4.8) for which we do not reject normality. The uncorrelated bell-shaped beta distributions that share the same mean and variance are the random variables most likely whose sum is a normal distribution. They have a 66.5 percent chance of summing to a normal when there are 20 uncertainties.

In Figure 4.3 we sum 20 bell-shaped betas with a mean and variance of 1. When uncorrelated, these uncertainties have the largest probability of all our parameter combinations of having their sums be a normal distribution. As the correlation increases, the probability of the sum having the null hypothesis accepted decreases from 0.665 to $0.359, 0.272$, and 0.202 for correlations of $0, 0.25, 0.50$, and 0.75. These values are presented in Section .3 in the Appendix. At $\rho = 1.0$ the probability drops to 0.155.

Not all source distributions are created alike. The skew and kurtosis combinations differ by region. The Pearson IV region is unbounded and has a higher kurtosis than all Pearson distributions with the same skewness. The Gamma (Pearson III), Beta Prime (Pearson VI), and Inverse Gamma (Pearson

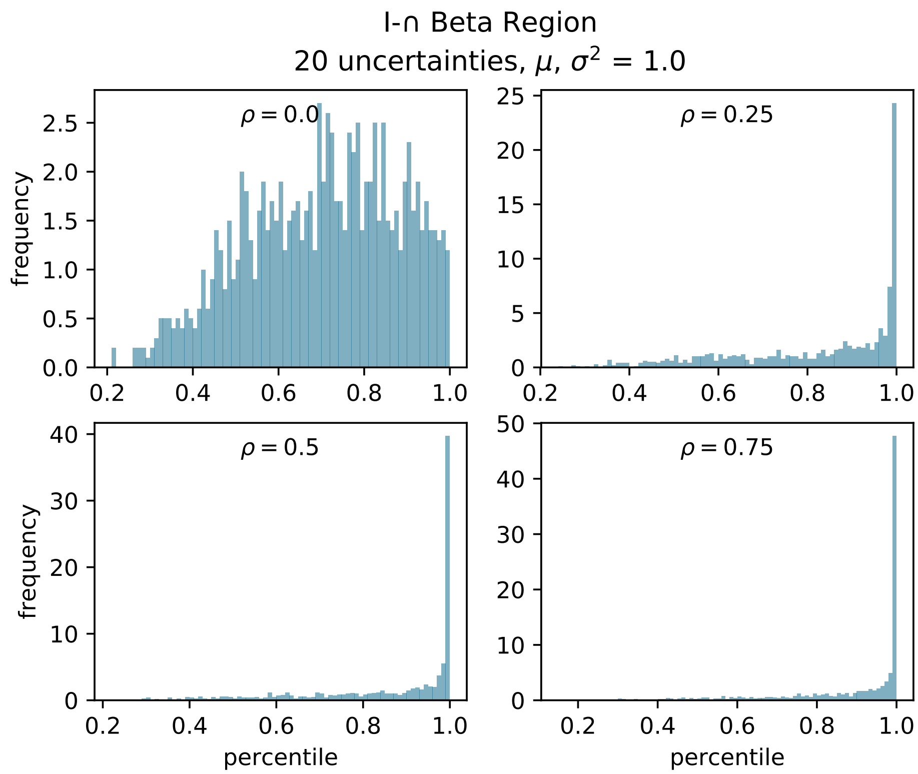

Figure 4.3: Each histogram shows the value of the CDF function for the KS1 distribution with a shape parameter of $10,000$ using the results from Equation (4.7) as the correlation increases.

V) distributions are semi-bounded distributions. They have less kurtosis that Pearson IV distributions, but more kurtosis than Pearson I (Beta) distributions. The Beta distributions are bounded on both sides. They are divided into the U-shaped, which have a high probability density near the extreme values. The J-shaped region has a high probability at only one of the extreme values. The bell-shaped betas have the highest probability as some point between the extremes. Each of these types of distributions contributes to the normality of the sum.

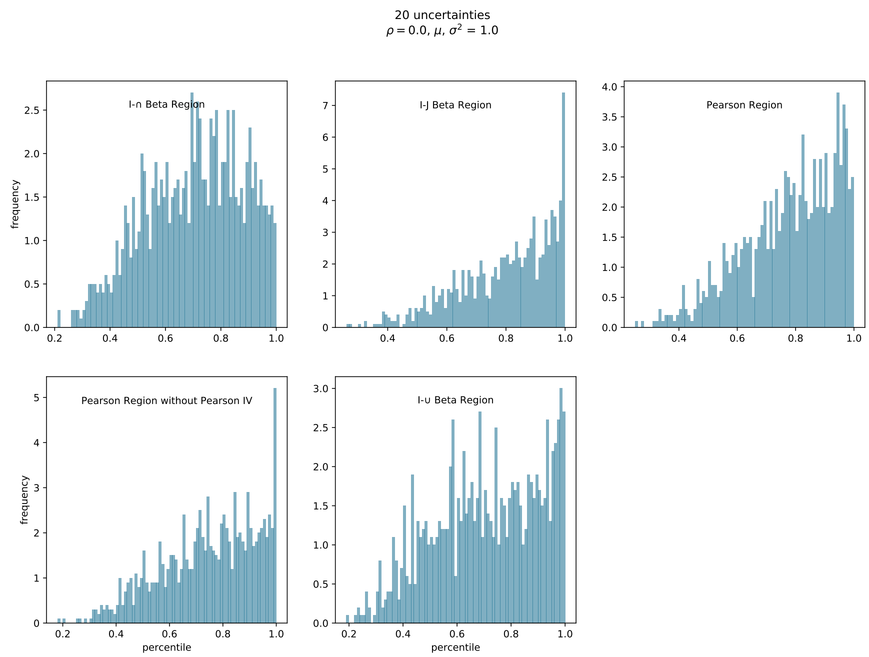

Figure 4.4: Each histogram shows the value of the CDF function for the KS1 distribution with a shape parameter of 10,000 for the different regions.

Figure 4.4 sums 20 uncertainties the are drawn from the different regions given in each sub-plot. The combination least likely to yield a normal sum is the Pearson $I - J$ region with a probability of 42.5 percent. The entire

Pearson region is next with a probability of 49.4 percent. When the distribution sampling excludes the Pearson IV distributions, the probability jumps to 55.8 percent. This is the effect of removing the heavy tails from the Leptokurtic distributions found in the Pearson IV region. Surprisingly, the $I - \cup$ region has the second highest probability of accepting the null hypothesis at 62.3 percent. At its extreme, a distribution drawn from the $I - \cup$ region can be thought of as having two values, one at each bound. This is similar to a Bernoulli distribution. When combined, these form a binomial distribution which can be approximated by a normal distribution when the number of uncertainties is large enough and the skew is small enough. The $I - \cap$ region is the most likely to produce a sum of uncertainties whose distribution is normal. Though this region has some level of skew and kurtosis, 50 percent of distributions randomly drawn from this region have a skewness less than 1.08 and 50 percent of sampled distributions will have an excess kurtosis of 1.34 or less. A normal distribution has a skewness of 0 and an excess kurtosis of 0. It is likely this relative similarity in terms of shape and skew and kurtosis measures contributes to the greater likelihood that sums of bell-shaped betas will be normal distributions.

Figure 4.5 presents the case where the conditions on the mean and variance of the uncertainties change. In the top row, we present the base case, where $\mu = \sigma^2 = 1$. We choose the $I - \cap$ region for the first two columns, and the Pearson region without the Pearson IV region for the third column. The first row uses fixed μ and σ^2, and the second row uses variable μ and σ^2. The difference between the first and second columns is that in the first column, there is no correlation, and in the second column $\rho = 0.25$. The third column has no correlation. These combinations provide a cross-section of regions that

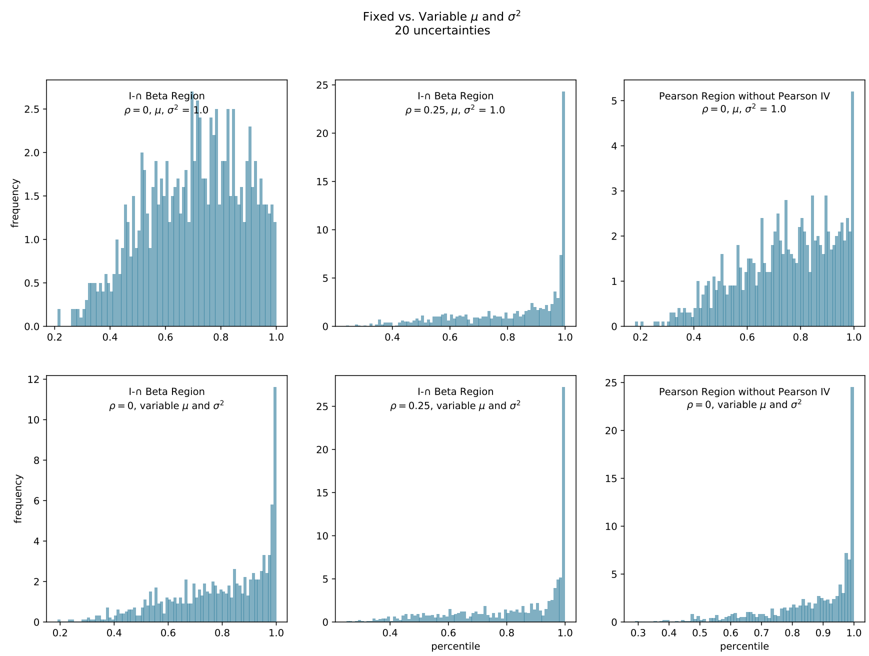

Figure 4.5: Each histogram shows the value of the CDF function for the KS1 distribution with a shape parameter of $10,000$ for the different regions with either fixed μ and σ^2 or variable μ and σ^2.

have relatively high probabilities of normality with a fixed μ and σ^2 and shows what happens under various perturbations.

When we allow the uncertainties to vary in the third column, the probability of accepting the null hypothesis decreases. For the $I - \cap$ region with 20 uncertainties and $\rho = 20$, the probability decreases from 66.5 percent to 45.3 percent. For the $I - \cap$ region with 20 uncertainties and $\rho = 0.25$ (second column), the fixed μ and σ^2 probability is lower than with no correlation at 35.9 percent. This probability only drops slightly to 34.8 percent when using a variable μ and σ^2. The probability of accepting the null hypothesis for 20 uncertainties and $\rho = 0$ for the sum of uncertainties drawn from the Pearson region without the Pearson IV with $\mu = \sigma^2 = 1$ is 55.8 percent. The probability drops to 23.6 percent when μ and σ^2 are allowed to vary. The tables in the Appendix in Section .3 only show the probability increasing in $\frac{25}{165}$ cases when switching between fixed and variable μ and σ^2. These increases are usually only less than 1%. The largest increase in the probability of accepting the null hypothesis is 1.3 percent. This uses the combined aggregation for 20 uncertainties drawn from the $I - \cup$ region with $\rho = 0.25$.

Figure 4.6 shows the effects the combined aggregation. We compare the CDF values from the $I - \cup$ region with 20 base uncertainties. This has one of the best probabilities of normality, which is only 1.3 percent. For the top row, we set $\rho = 0$ and we set $\mu = \sigma^2 = 1$. In the second row, we set $\rho = 0.25$ and we let μ and σ^2 vary. Across the columns we switch from a sum of 20 uncertainties, to a sum of 10 uncertainties. The combined uncertainties will be the sum of 10 values. The third column is a combined aggregation of 20 uncertainties. In all cases, the highest probability of accepting the null hypothesis comes from summing 20 uncertainties, with probabilities of 62.3 percent for $\rho = 0$ and 12.0

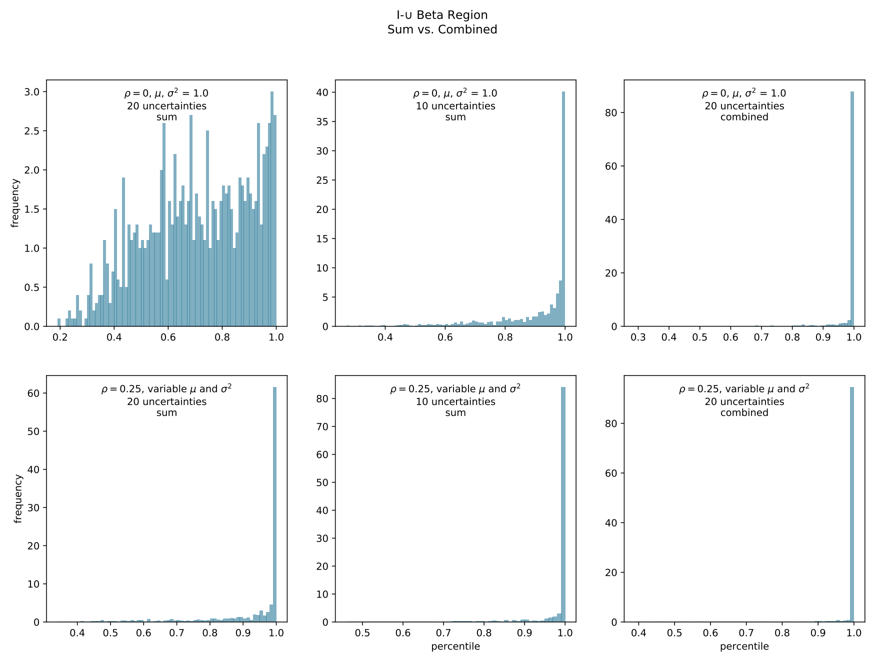

Figure 4.6: Each histogram shows the value of the CDF function for the KS1 distribution with a shape parameter of $10,000$ for the $I - \cup$ region with either fixed μ and σ^2 or variable μ and σ^2.

percent for $\rho = 0.25$. The respective probabilities decrease to 17.2 percent and 2.7 when reducing the uncertainties to 10. Combining uncertainties reduces the probability of accepting the null hypothesis further. This is likely due to the odd distributions resulting from taking the product of two uncertainties many of whose domain of values cross zero. In general, [38] noted the product of two normal variables is not a normal variable. If Figure 4.4 we see that the original shape and properties of the uncertainties help determine the number of uncertainties required to create a normal distribution through summation. The PDF of these distributions, especially when the distribution straddles 0, is a spike, like placing two exponential distributions back to back. This lack of normality affects the probability of accepting the null hypothesis of the resulting sum.

4.4 Accuracy of the Closed Form Solution

In Section 4.3 we find that it is possible to have a normal distribution under conditions seen in a decision analysis problem. In a decision analysis problem we may have 20 uncertainties which have a correlation of $\rho = 0.25$ whos values we multiply and then sum. We view this is something typical in a practical problem, and this only has a 0.2% probability of accepting the null hypothesis per Table 6. Given the probabilities seen in the tables in the Appendix in Section .3, it is also likely that almost all decision analysis problems will have a distribution of the value lottery that is not normal due to a finite number of uncertainties, the use of products of uncertainties, and correlations, and non independent and identical distribution of the uncertainties.

In this section we analyze the distance metric and its relationship to the accuracy of the mean and variance of discretizations. First we compare the theoretical distance from Equation (4.6) to the computational distance derived from simulating the discretizations. For each discretization in HB, EPT, MCS, and ESM, we use the same percentile sampled for the complete distribution and determine the corresponding percentile from using the discretization. For example, MCS assigns a probability of 30 percent to the $P10$. If in the simulation using the true distribution the percentile value we sample a percentile value less than 30, we use the $P10$ for the value from the MCS discretization. This has the effect of reducing the variability between the discretization results and the "true" results. For each discretization and "true" simulation combination, we determine the mean and variance of each along with whether or not the "true" distribution is normal. With these sets of points and the statistics of those points, we are able to determine both the theoretical and the actual distance.

A first observation is that as the theoretical distance increases, the actual distance increases as well. This is the case for both normal and non-normal distributions. In both cases, there is a line that emanates from the origin. On the independent axis is the theoretical distance. On the dependent axis is the actual distance. There is a clustering of error around a zero theoretical distance. This indicates that even when the mean and variance derived from the discretization are zero and closely match the simulated distribution, there are still some discrepancies in the shape. In Figure 4.1 the discretization crosses the "true" distribution several times, but the mean and variance are close to the original. In this case, the distance is still be off by a few orders of magnitude. In Figure 4.1 the mean is off by \$17 or 0.1 percent, and the variance is off by 1.3 percent. This yields a theoretical distance of \$192. The actual distance is $\$3,779$. This discrepancy can be attributed to the large jumps in the probabilities of events. In Figure 4.1 the value where all four discretizations assume the median value is 15.75 percent.

The theoretical provides an estimate for the lower bound of $Dist$. For the distributions where the sum or sum of products is a statistically normal, that lower bound takes the equation of:

$$\lfloor Dist \rfloor = 1.015 * Dist(\mu_1, \sigma_1, \mu_2, \sigma_2) - 1.096. \tag{4.9}$$

We determine the slope and intercept by clustering the theoretical values using the Python K-means algorithm in the Python sklearn clustering package. We first generate the clusters from the theoretical distance values. We use the predictions of the algorithm to assign the value of the closest center to each theoretical distance. For each cluster center for the theoretical distance we determine the minimum value of the actual distance. We apply linear regression to get the estimate for the lower bound of the error. We apply this same methodology to the non-normal distributions as well. For those distributions, the lower bound of the error is estimated to be:

$$\lfloor Dist \rfloor = 0.513 * Dist(\mu_1, \sigma_1, \mu_2, \sigma_2) - 3.129. \tag{4.10}$$

We present the scatter plots of the actual distance versus the theoretical distance in Figure 4.7. The left plot shows the scatter plot when the source distribution is statistically normal. The right plot shows when the source distribution is not normal. One observation is that within the scatter plot for the normal source distributions there are distinct lines. We label the source

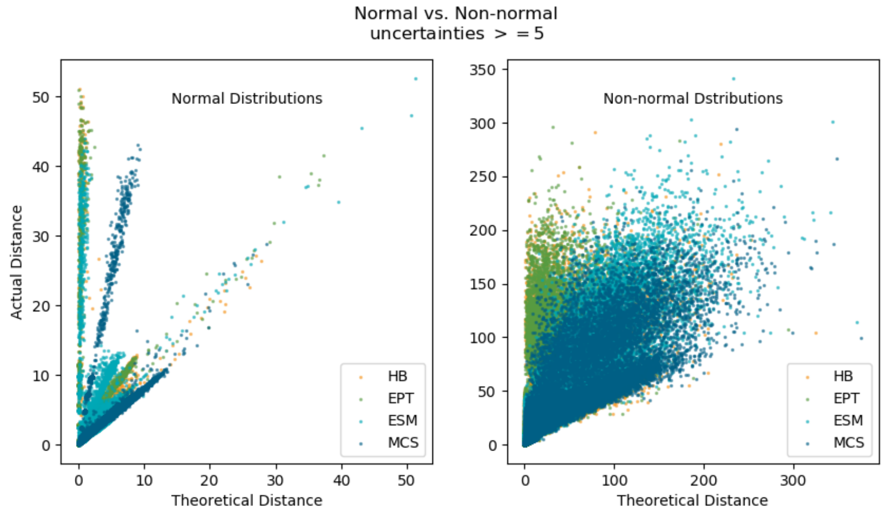

Figure 4.7: The scatter plot of the theoretical distance to the actual distance.

values from each discretization and find that the discretizations have their own relationships between the bounds of the true error and the theoretical distance. In general the HB and EPT have many of the smallest theoretical distance values. This is due to their ability to match the mean an variance as shown in [12]. ESM performs better than MCS when estimating μ and σ^2, but it too has a steeper slope for its lines, meaning its distance is higher while MCS may not be as accurate for μ and σ^2, but has a lower actual distance.

When evaluating the theoretical and actual distances for the discretizations for both normal and non-normal "true" distributions, we see that is in Figure 4.7 HB and EPT have the lowest theoretical distances for normal and non-normal distributions. While the actual distance increases from the theoretical, MCS remains the same, as seen in Table 4.4. In general, HB has the best actual distance, followed by EPT. MCS and ESM reverse their order when moving from theoretical to actual. The general stability of the discretization

Table 4.1: Theoretical vs. Actual Distances

Is Normal?	Theoretical or Actual?	HB	EPT	ESM	MCS
Normal	Theoretical	3.046	3.043	3.824	5.447
	Actual	4.320	4.538	4.875	5.159
Non-Normal	Theoretical	4.917	4.316	6.253	7.532
	Actual	6.679	6.979	8.081	7.544

could be attributed to the fact that its extreme values are not as extreme as HB and EPT, and its weighting of the P50 is higher than that of ESM.

In order to explore this further, we plot the scatter for individual discretizations. We add a legend for the number of uncertainties and create a different axes for each sub-region. We limit the discretizations to the distributions that are non-normal, as they represent 93.38 percent of the distributions that use five or more uncertainties and have uncertainties with variable μ and σ^2 and $\rho = 0.25$. Each combination of Pearson region, discretization, number of uncertainties, variable versus fixed μ and σ^2, ρ, and aggregation type leads to a different clustering of data points.

In Figure 4.8 and Figure 4.9 we see the scatter plots for HB and MCS. Each axis within the plot represents a region and we plot the values by the number of uncertainties and the type of aggregation. In general, the fewer the number of uncertainties, the lower the theoretical and actual distance metrics. We also see that in all the plots, the combined uncertainties have the most theoretical and actual distance, and all follow a linear pattern, with the combined uncertainties showing the largest variability. We also see that for the HB discretization, the maximum actual value is at or below the actual maximum value for MCS. In all plots, including the ones not shown, we find that the theoretical distance forms a lower bound. For distributions that are

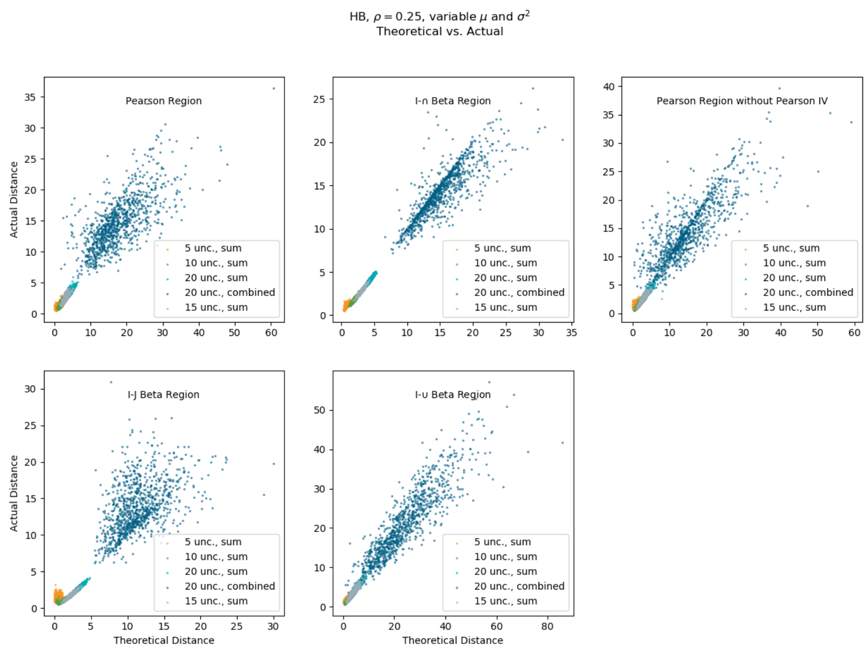

Figure 4.8: The scatter plot of the theoretical distance to the actual distance for HB.

normal, the upper bound is not well-defined.

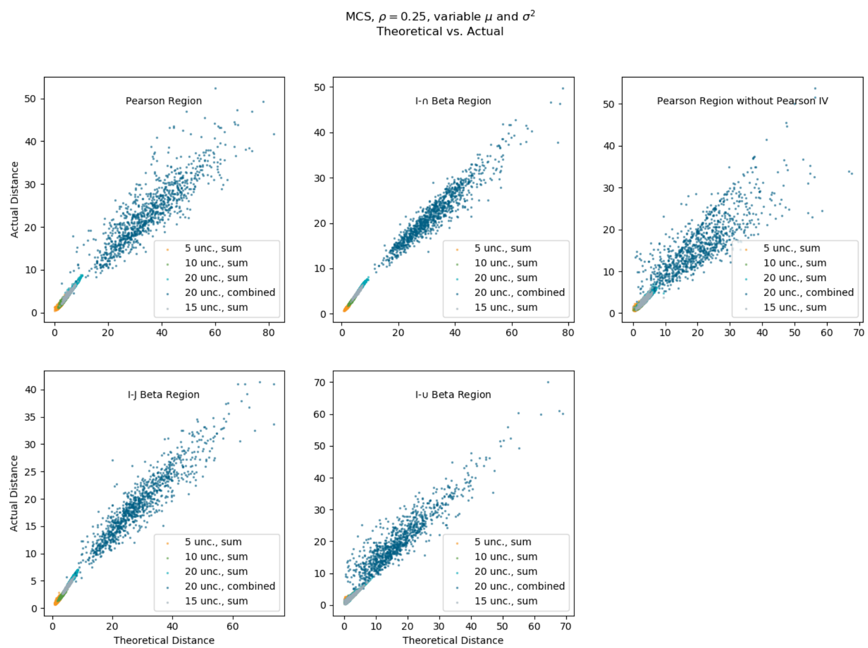

Figure 4.9: The scatter plot of the theoretical distance to the actual distance for MCS.

For each combination of discretization, region, uncertainties, normality, etc., we determine how well the theoretical distance approximates the true distances. We do this by solving linear regressions for both the floor and the ceiling of the distance.

$$\lfloor Dist \rfloor = M_{floor} \cdot Dist(\mu_1, \sigma_1, \mu_2, \sigma_2) + B_{floor} \tag{4.11}$$

$$\lceil Dist \rceil = M_{ceiling} \cdot Dist(\mu_1, \sigma_1, \mu_2, \sigma_2) + B_{ceiling} \tag{4.12}$$

If the theoretical distance is exact, we have $slope_{floor} = slope_{ceiling} = 1$ and both intercepts as zero. This is the base for estimation. In the case of MCS in the Pearson region with 20 uncorrelated uncertainties whose sum is a normal distribution. Here, the lower bound is $1.009 * Dist(\mu_1, \sigma_1, \mu_2, \sigma_2) - 0.278$ and the upper bound on error is $1.009 * Dist(\mu_1, \sigma_1, \mu_2, \sigma_2) + 0.054$. Figure 4.10 shows a comparison of several scatter plots for different discretizations. In general, it shows the theoretical distance provides a good bound for the MCS discretization. It also provides a good bound for most cases of ESM as shown in the tables in the Appendix in Section .4. EPT and HB have better accuracy for the mean and variance as shown in [12]. This improved accuracy translates to the aggregated sums, which result in lower theoretical error shown below. With a low theoretical error, we often see EPT and HB distance values with little relation to their theoretical distance values. This is shown when the slope and intercept of the upper bound for the true distance is much higher than the lower bound for the true distance and is an indicator of the difference from being a normal distribution and how well the theoretical distance formula will work. An example is provided in Appendix .4

The bounding functions represent the lower bound and upper bound between the theoretical distance and the maximum distance. When the slopes are equal, there is a constant deviation. In other times, the slopes have opposite signs, which indicate that the resulting distribution is not normal and that the Equation (4.6) will not give a good estimate. This means that it is possible for discretization that have low errors for μ and σ^2 to do a worse job in matching the shape than discretizations with larger errors in μ and σ

To better illustrate how this is possible, we return to the Eagle Airlines problem and show the results from Figure 4.11 when we apply the ESM discretization. This discretization is less accurate for determining the mean and the variance and will theoretically have a larger distance error. The ESM dis-

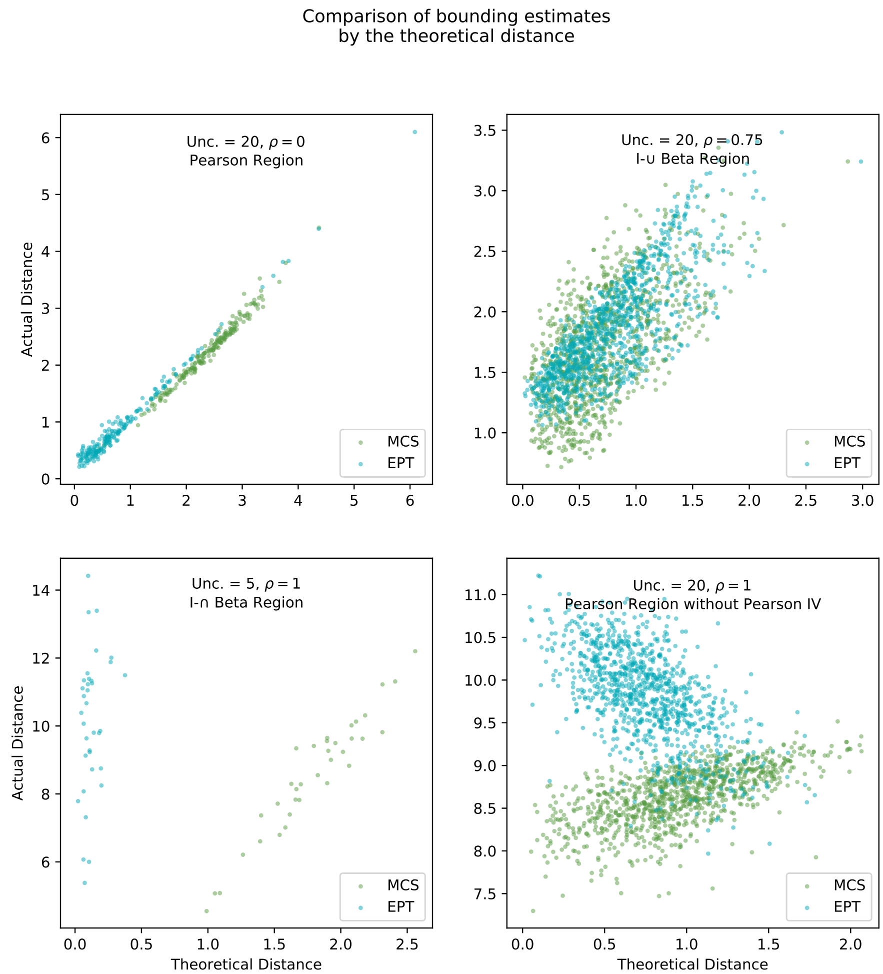

Figure 4.10: The scatter plot of the theoretical distance to the actual distance for several cases.

cretization applies a probability of 0.40 to the $P50$, resulting in that scenario only accounting for 2.56 percent of all values, which is decidedly smaller than the jump of 15.75 percent from EPT. Using ESM, the theoretical distance increases to $\$1,532$, but its actual distance is $\$2,839$. This means on average, the ESM discretization will have \$940 less in error when looking at a random percentile. The mean error is 0.22 percent and the variance error is 10.57 percent. The variance error for EPT was only -1.28 percent. At first glance, it seems that ESM matches the shape better than EPT. In analyzing the shape between the $P15$ and $P75$, the jumps for ESM are smaller, and the amount in blue is significantly lower. EPT uses the $P5$ and $P95$ values while ESM uses the $P10$ and $P90$ values. In Chapter 3 the discretizations that use the more extreme percentiles were more accurate in calculating the CE. This is that case with this problem as well.

When looking at values outside the $p15$ to $p75$ range in Figure 4.11 and comparing it to Figure 4.1, there are some important pieces of data to consider. The more extreme percentiles of EPT yield a wider range of values. For ESM the range is between $-\$72,957$ and $\$139,110$. For EPT the range is between $-\$95,773$ and $\$171,682$. The simulation of $1,000,000$ values based on the functional form of the uncertainties has a range between $-\$128,261$ and $\$238,656$. The use of the extreme values for EPT also yields better estimates at the $P10$ and $P90$ for EPT over ESM. ESM under-estimates the $P10$ and $P90$ by$\$5,417$ and $\$6,749$ respectively. These errors are smaller for EPT where the errors are an over-estimate of $\$4,708$ at the $P10$ and an under-estimate of $\$2,804$ at the $P90$. The case with Eagle Airlines and the results of discretizing using EPT and ESM show there are many factors in play when selecting a discretization. In Section 4.5 we further analyze the distance error

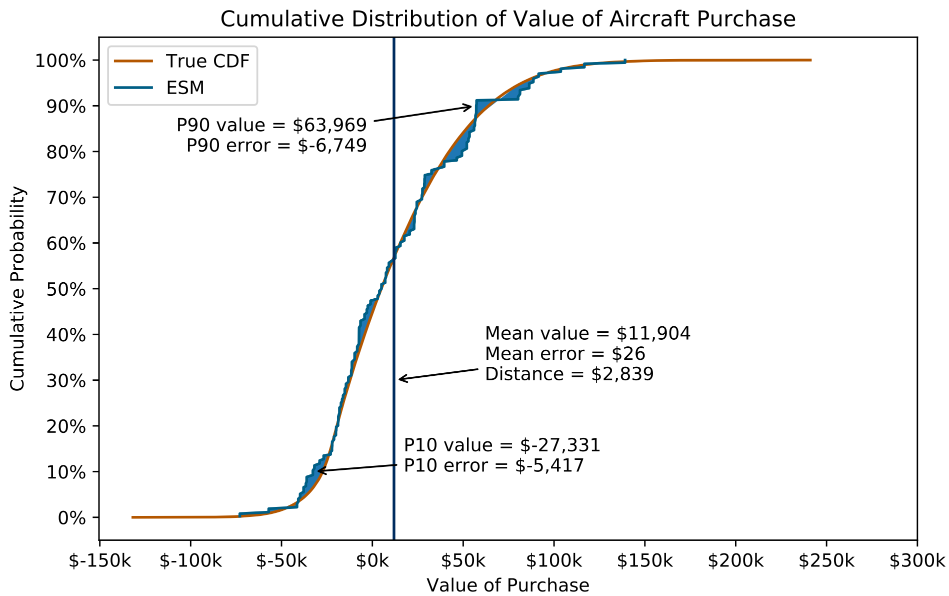

Figure 4.11: The blue area between the two curves shows the distance now using the ESM discretization.

for the discretization in comparison to their errors for μ and σ^2.

4.5 Distance, μ, and σ^2 Accuracy

To analyze the effect of the error of the discretized mean to the distance, we plot error of the mean against the distance. We assign a different color to each discretization. An overview of these plots is in Figure 4.12. Overall there is a direct link between the minimum distance and the absolute value of the mean error. Each discretization has a different distribution of distances conditioned on the absolute value of the mean error. If we apply Equation (4.6), if $\sigma_1 == \sigma_2$, and if $\mu_1 > \mu_2$, then $p_0 = 1$ and $Dist = \mu_1 - \mu_2$. Following the same methodology, if $\mu_2 > \mu_1$, $Dist = \mu_2 - \mu_1$. This explains the lower bound visible in Figure 4.12.

The next step is to determine which discretization yields the lowest distance. Due to the volume of data it is difficult to determine if MCS has the lowest error per mean error, or if it shows as the lowest due to its order in plotting. To determine the relationship between distance and the mean error, we filter the data by region, the values of μ and σ^2, and ρ. We also superimpose the least squares regression of the absolute mean error to the distance. We plot from 0 to the maximum mean error. This provides a scale of the error along with a visual representation of the fit. Figure 4.13 shows the Pearson region without the Pearson IV uncertainties, a variable μ and σ^2, and $\rho = 0.25$. We choose these filters as they draw from uncertainties that decision analysts are likely to see (few decision analysis problems have uncertainties that are completely unbounded), there will be some correlation, and each uncertainty has a distinct μ and σ^2.

We find that the best performing discretization varies from setting to set-

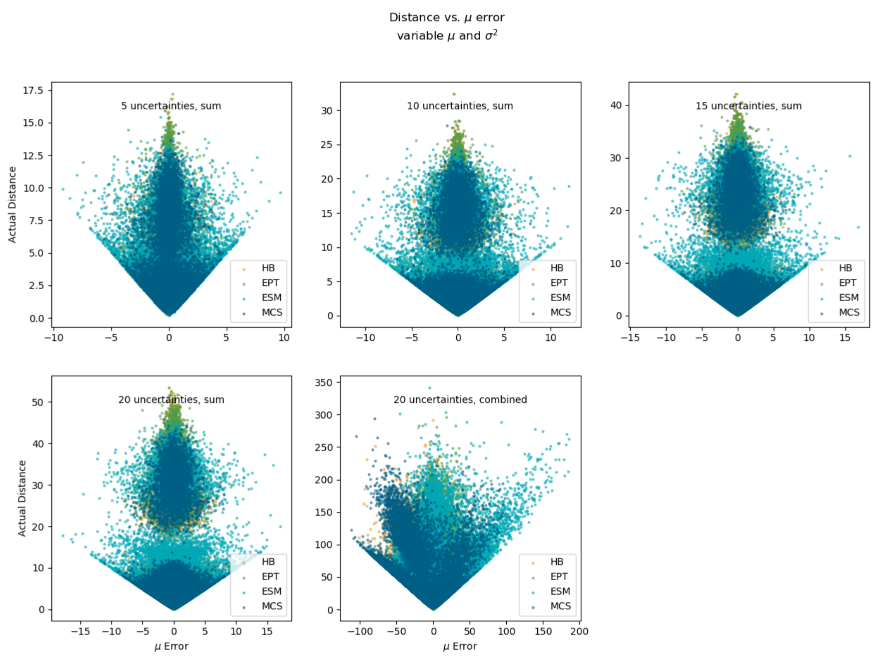

Figure 4.12: The mean error versus the distance.

ting, even controlling for the region, and independence. The best performer in Figure 4.13 is hard to ascertain based only of the distribution of the error in μ and the distance. A pattern that does present itself is the relationship between the error in μ and the minimum distance error increases linearly with the difference in the μ values. With 20 uncertainties combined into pairs of products and summed, all the discretizations perform well. In order to better visualize the distribution, we apply a least squares regression for each discretization. These are shown in the dashed lines of Figure 4.13. A discretization with only an error in μ and no error in σ and where the source distribution is a normal would have an intercept at zero. The discretizations with the lowest intercept values will have the least error in σ. For the 20 multiplied and summed (combined) distributions in Figure 4.13 the intercepts are 6.21 (HB), 6.53 (MCS), 8.98 (EPT), and 13.32 (ESM). This order switches with the when viewing the 20 summed uncertainties, we see almost the opposite. In this case, the intercepts are at 1.77 (EPT), 1.84 (ESM), 3.39 (HB), and 3.79 (MCS). In this case, the difference in error is not as large as with the combined scenario.

The differences in performance are more easy to see when the source distributions are more likely to combine to create normal distributions. This is the case where there is no correlation and all the source distributions come from the bell-shaped beta region. This is visible in Figure 4.14. Though not shown, the results are similar when μ and σ are variable versus fixed at 1. In this figure, we can see that HB and EPT have some of the lowest error. Their least squares fit lines only extend a short distance because due to a low deviation from the true μ. ESM, which is slightly worse, has a greater range for the μ and the larger range of σ errors shows in the larger values of distance metrics. Finally, MCS has the largest breadth in μ errors and the most error

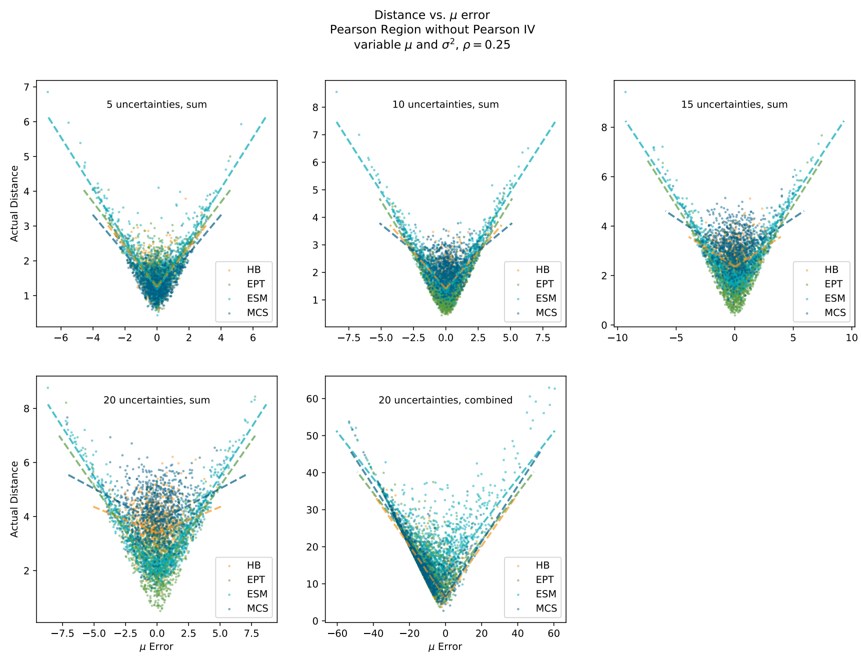

Figure 4.13: The mean error versus the distance.

in σ. The intercepts for these discretizations are 0.27 (HB), 0.28 (EPT), 0.48 (ESM), and 1.84 (MCS). The analytical formula for the distance in equation (4.6) explains why there is a lower bound on the distance for each value of μ. When we set $\sigma_1 = \sigma_2$, this means the two cumulative distribution functions never intersect. When $\mu_1 > \mu_2$, then $p_0 = 1$ and the distance increases with a slope of 1 as μ_1 increases. When $\mu_2 > \mu_1$, $p_0 = 0$ and as μ_1 decreases by 1, the distance increases by 1.

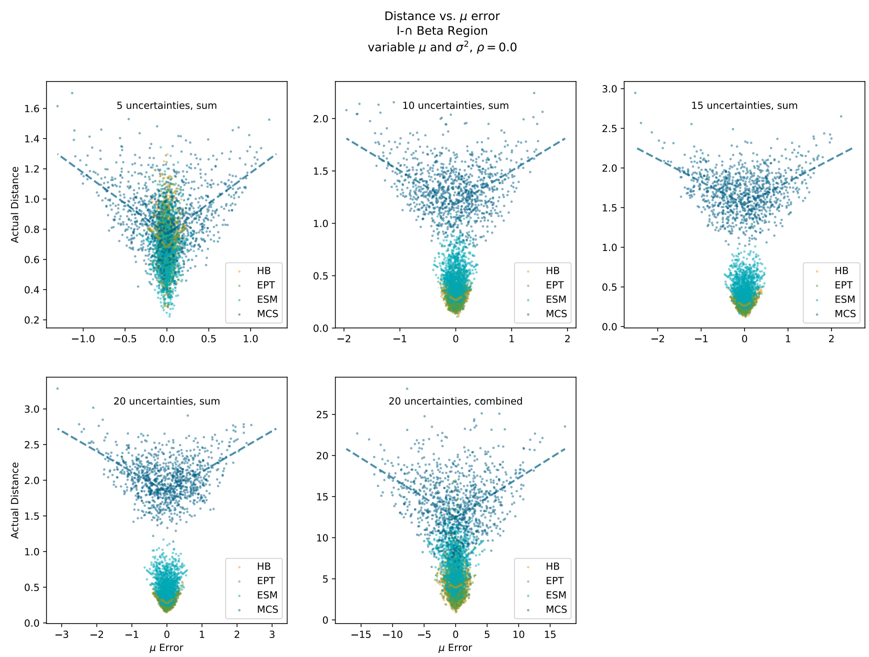

Figure 4.14: The mean error versus the distance.

When we compare the error of σ to the distance, the pattern changes. For continuity we present the distance versus σ scatter plots using the same conditions of Pearson region, variability in μ and σ, and correlation as described for Figures 4.13 and 4.14. One difference is that most of the errors in σ tend to be below the true σ.

We obtain similar results when we plot the distance against the error for σ^2. In Figure 4.15 the minimum distance error also increases with the absolute increase in σ^2. This follows the Equation (4.6) which shows a linear increase of the theoretical distance with the increasing difference in the values of σ and which are also affected by p_0. This figure is different in that most of the error for σ^2 is negative. The notable different is that when we use the combined aggregation, the error in σ^2 is more balanced between positive and negative.

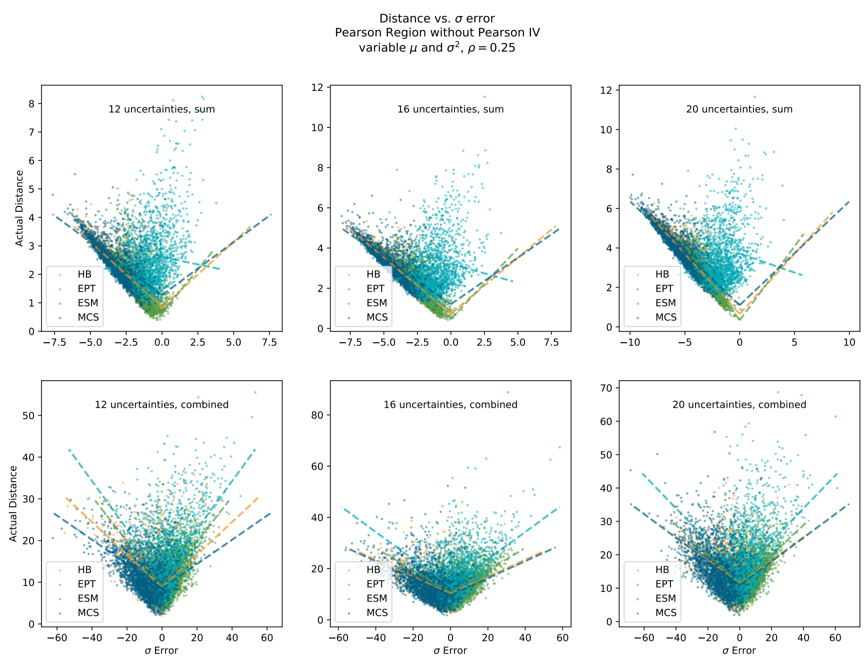

Figure 4.15: The variance error versus the distance.

The analysis shows that as the error for μ and σ^2 increases, so does the distance. Additionally, we find that as the theoretical distance increases, so does the actual distance, though it usually serves as a lower bound. The plots in Figure 4.7 show that different discretizations have theoretical and actual distances that are clustered in different regions. The various other figures in this chapter also show that errors are clustered and vary depending on the factors used in the simulations such as the number of uncertainties, the Pearson sub-region, the discretization, the rank correlation, and the method of aggregation. In order to determine more clearly the situations when one discretization may yield better results than another, we look at the discretizations by region and aggregation method and compare the mean absolute errors at different percentiles.

To compare percentiles, we compare the value of the CDF of the aggregated values when using the "true" values and when we compare them to the discretized values. We determine the error for the following percentiles: $P5$, $P10$, $P50$, $P90$, and $P95$. The distance metric would include these values and combines them in one single metric. This analysis shows where the different discretization methods perform at different percentiles of the CDF.

For this analysis we show the percentile errors for a specific region and number of uncertainties in a single figure. We show the correlations of 0.0, 0.25, 0.5, and 0.75 in each chart. Each chart shows the errors for each discretization method and method of aggregation.

We begin with a figure where the aggregated values are most likely to be normally distributed. This is in the $\cap$-beta region of the Pearson distribution with 20 uncertainties that all have $\mu = \sigma = 1.0$. This is seen in Figure 4.16. It shows some items that are common in our analysis. The first is that the least amount of error is at the $P50$ and increases as the percentiles become more extreme. They show the ESM discretization generally having the least error, EPT and HB, which have similar discretization percentiles and probabilities

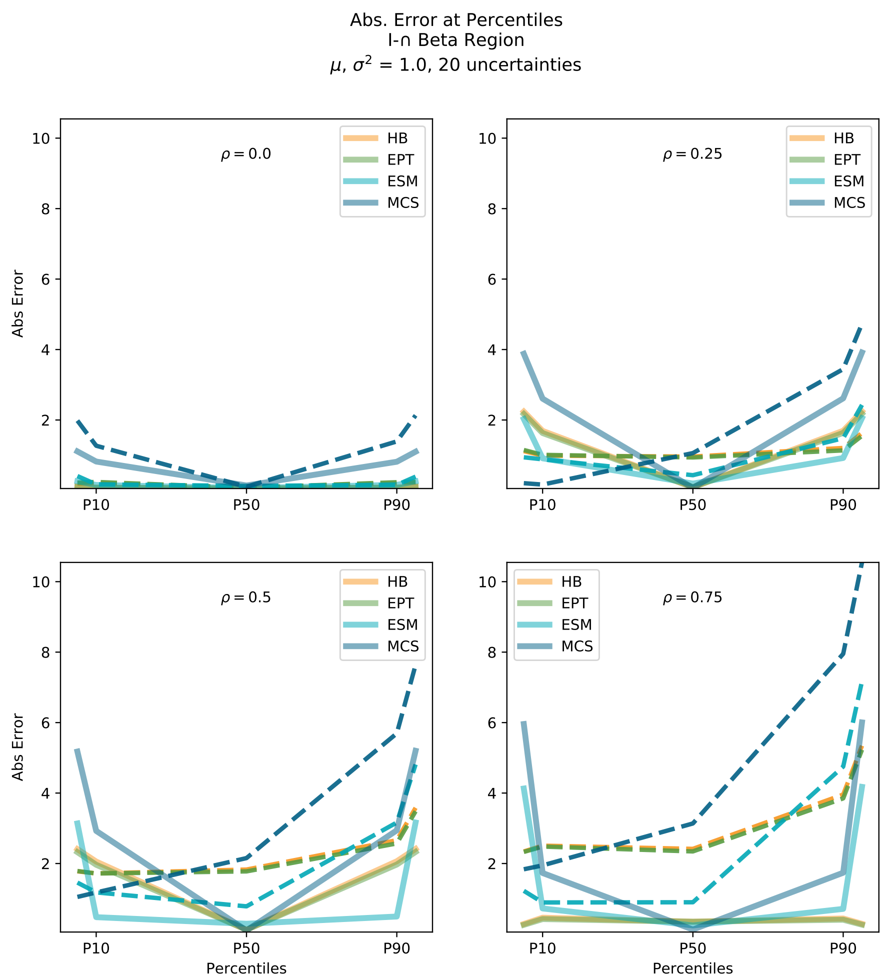

Figure 4.16: The solid line represents the absolute error at each percentile when summed, the dashed line represents the error when combined.

in the region are almost exactly the same, and MCS tends to have the highest error.

In Figure 4.17 we expand the region, allow μ and σ to vary, and reduce the number of uncertainties to 12. Under these conditions, the average errors reverse themselves. We find that MCS typically has the lowest error at each of the percentiles and ESM usually has the most. We also find that HB now differentiates itself from EPT because HB uses different discretizations for different regions of the Pearson system. If it is possible to assess more extreme percentiles, the HB discretization is recommended. If not, the MCS discretization is the next best alternative.

4.6 Conclusions

In this chapter we discuss the shape-matching ability of different discretizations and the conditions that improve shape matching for all discretizations. To measure how well the discretized distribution and the true distribution match, we use the distance metric which sums the absolute difference between the two cumulative distribution functions. We derive an analytical formula for the distance when the two distributions are normal. From this, we show an estimated frequency of a normal distribution when the following were considered:

- The Pearson sub-region
- The number of uncertainties
- The variability in the mean and variance of the uncertainties
- The aggregation method of the uncertainties

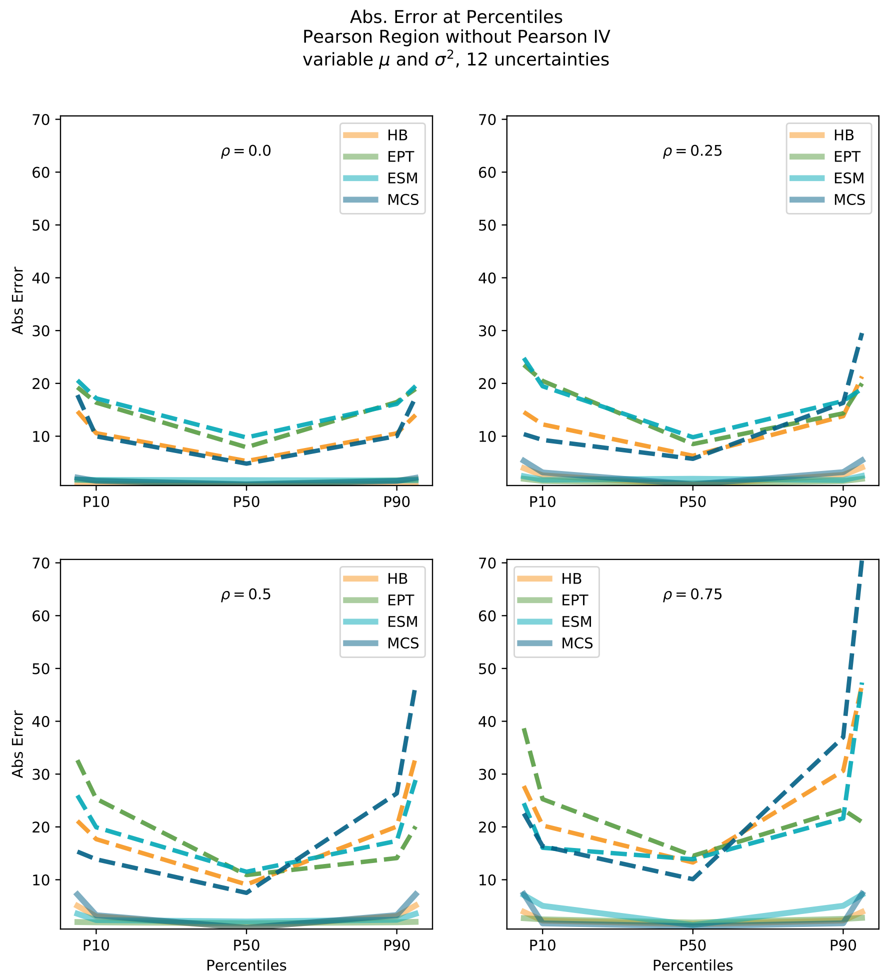

Figure 4.17: The solid line represents the absolute error at each percentile when summed, the dashed line represents the error when combined.

- The correlation of the uncertainties

Though the conditions for normality are unlikely in a decision analysis problem (a large number of uncorrelated uncertainties with a fixed mean and variance from a single sub-region of the Pearson system), the formula for distance (4.6) provides a lower bound on the true distance. The scatter plots in Figures 4.8 and 4.8 show this.

An initial path we explored was to see if we are able to create individual discretizations that can match the shape using the techniques described by [9]. We found these techniques created discretizations that matched the shape better than all the other discretizations at the single uncertainty level. These discretizations have a lower variance than the other discretizations, so the discretized uncertainties were aggregated, their lower variance was projected either proportionally for the sums, or geometrically for the combined uncertainties. This lead to discretizations that have more error with the increase in the number of uncertainties and were therefore not presented.

We further found that when comparing the error in μ or the error in σ, the distance formula accurately predicted the lower bound for the distance as seen in Figures 4.12, 4.13 , 4.14, and 4.15. We also saw that the HB and ESM discretizations had the least error for μ and σ^2, but their actual distance metrics were higher than predicted. The recommendations from this analysis are to use HB as overall, its error for μ and σ^2 are the best, and so it its distance calculation. When using the $P10$ and $P90$ as the assessed extreme values, the MCS discretization is worse than ESM for μ and σ^2, but not by much. MCS's actual distance is lower on average than from ESM. If more information is available, we refer the reader to the bounding tables in the Appendix in Section .4.

Chapter 5

The Role of Assessment Error in Discretization Accuracy

5.1 Introduction

In Chapters 3 and 4 we see the use of more extreme percentiles in discretizations improve the accuracy of those discretizations. In Chapter 3 the discretizations with more extreme percentiles better matched the true CE of the training distributions. In Chapter 4 the HB and EPT discretizations match the mean and variance of the underlying uncertainties better, and they have a lower average distance from the true CDF of the value lottery. These comparisons make the assumption that the assessment is accurate. In this chapter we analyze the effects of assessment error on the accuracy of discretizations and determine the robustness of the accuracy under different assumptions for the assessment error.

From the literature we know the following and are summarized in [21]:

- Assessors that are trained are better calibrated than those who are not.
- Assessors that receive regular feedback regarding their results are better calibrated. Training seems to provide a one-time boost, but reinforcement leads to long-term calibration.
- Most assessors suffer from overconfidence.

- More extreme percentiles are more difficult to assess correctly and have relatively larger surprise index scores.

In this chapter we propose a novel methodology for expressing assessment error. This new methodology allows us to express the following:

- bias
- correlation among assessment errors
- dependence on the percentile being assessed

Each of these items is consistent with the observations of [21]. Based on the existence of bias, correlation, and percentile dependence, the accuracy of various discretizations when assumptions of perfect calibration are relaxed. In the rest of this chapter we measure the effects of assessment error on various accuracy metrics in order to determine how the HB, EPT, ESM, and MCS perform with respect to μ and σ^2 absolute error, and determine under different conditions which discretization provides the best accuracy.

5.2 Assessment Error Definition

In discretization, we assess the percentile, p. But if the assessment is not exact, then the expert is assessing a different percentile which we call q_p because it is different than p, but also dependent on p. The difference between p and q_p is the assessment error, e. We have seen from [2] that more extreme percentiles are more difficult to assess. We can expand our definition of e so that it is parameterized by the percentile for which the assessor is trying to assess, e_p. This creates the relationship

$$q_p = p + e_p \tag{5.1}$$

In order to measure the accuracy of a discretization under the assumption there will be assessment errors, we can compare the statistics defined in chapter 4 with and without assessment error. For example, if measuring the accuracy of the MCS distribution for a $\beta(2,5)$ distribution, we can assess the $P10$, $P50$, and $P90$ to obtain values of 0.0926, 0.2644, and 0.5103 respectively. Applying the probabilities of 0.25, 0.50, and 0.25, this gives a mean value of 0.2829. The true mean of a $\beta(2,5)$ distribution is 0.2857, $\frac{2}{7}$, and the mean percent error is -0.97 percent. If instead of providing the $P10$, $P50$, and $P90$, the expert instead provides the $P12$, $P49$, and $P85$, whose respective values are 0.1029, 0.2602 and 0.4613, then the mean obtained with this specific assessment error is 0.2711, yielding a mean percent error of -5.12 percent. By introducing assessment error, the accuracy of the discretization changes.

The drawback of the methodology in equation (5.1) when compared to that proposed by [13] is that all assessed values still must be possible within the true distribution. The methodology proposed by [13] transforms the assessment error from assessing the incorrect percentiles for the true distribution to making the correct assessments for the incorrect distribution. This allows for more flexibility, but does not allow for the effects of bias, correlation, and the dependence of errors on the assessed percentile.

In order to model the differing assessments of experts we model e_p as a distribution. In order to determine the effect of assessment error, we sample across each e_p to obtain a distribution of the assessed values which we can compare to the true value of the original distribution. In order to do this, we need a distribution for each e_p such that $q_p \in \{0, 1\}$.

The assumptions we make about e_p differ from those in [43]. In Wallsten's article he makes the following assumptions

1. The expected assessment error is 0, $E(e) = 0$.
2. The error is uncorrelated to the true value.
3. Assessment errors are uncorrelated.

We make some changes to those assumptions based on findings in the literature. From the summarized findings in [21] and Table 2.1 in Chapter 2 we see the surprise index is usually much larger than the expected value. This indicates that most of the error should be skewed towards the $P50$. For assessed percentiles below 50 percent, the true percentile assessment will be higher. For assessed percentiles above 50 percent, the true percentile assessment will be lower. We also see in Table 2.1 that the surprise index is lower when the percentiles are further from the extremes, however, it is unclear if the better calibration is due to the use of less-extreme percentiles or if they are due to regular feedback on assessments. We also allow for correlation. In our analysis we use a rank correlation between $CDF(Q_p)$ and $CDF(q_{100-p})$.

5.3 Methodology

We assume that the assessed percentile q_p takes the form of a beta distribution. We can create a wide range of shapes, variances, and biases by changing the α and β parameters, the location parameter, and the scale. For assessments at the 50^{th} percentile, we use $\alpha = \beta = 4$. When the percentile is less than 50 we use $\beta = 5$, and when the percentile is greater than 50, we use $\alpha = 5$. To calculate the other parameter, we specify that the mode, m, is at the cumulative probability of 0.25 for percentiles less than 50, and a mode at a cumulative probability of 0.75 when the percentile is greater than 50 and given by the following formulas:

$$\alpha = \frac{1 + m \cdot (\beta - 2)}{1 - m} = 2.33 \tag{5.2}$$

$$\beta = \frac{\alpha - 1 + (2 - \alpha) \cdot m}{m} = 2.33 \tag{5.3}$$

The result is a bell-shaped beta with a skew towards the middle for the extreme percentiles. The beta distribution has a range from 0 to 1. If its probability density function is $f(x, \alpha, \beta)$, then we can reduce the domain by using the *scale* parameter and we can change the minimum value by using the *location* parameter. This transforms the variable so that $y = \frac{x - location}{scale}$ and $f(x, \alpha, \beta, location, scale) = \frac{f(y,\alpha,\beta)}{scale}$. For our analysis, we use scale values of 0 (no assessment error), $0.05, 0.1$, and 0.2. We also set the mode to be exactly at the desired percentile as long as it does not force the location to start at a percentile of less than 0. In the case of the lower percentiles with an assessment error, the probability that the assessor is under-confident is always 25 percent, and the probability of being overconfident is 75 percent. The change in scale does not change the ratio of under-confidence to overconfidence, but changes the probability of selecting values. When the scale increases, it is possible to assess percentiles that are further away from the desired percentile. An example with a Bernoulli distribution for assessing the $P95$ could be that 0.25 of the time the assessed value is the $P96$ and 0.75 of the time the assessed value is the $P94$. The accuracy would be different than if 0.25 of the time, the assessed value is the $P98$ and 0.75 of the time the assessed value is the $P92$. In both cases, the surprise index is the same, but the scale of the errors is larger in the second, which we show yields different accuracy values than the first Bernoulli distribution.

In order to represent correlation between assessments of the extreme values, we rank correlate the two extreme assessments. We maintain the middle assessment as independent. The rank correlations we use are -1.0, -0.75, -0.50, -0.25, 0.0, 0.25, 0.5, 0.75, and 1.0. This allows us to test when the assessments are independent, when the surprise index values are symmetrical, and when the assessments are biased upwards or downwards.

5.4 Analysis

In Chapter 4 and in [12] we see the HB and EPT are discretizations that create the least error for both the μ and σ^2. The ESM and MCS discretizations have higher error metrics. We begin by comparing the the errors of the mean and variance for the discretizations over the Pearson region. These are the similar to the results presented by [12]. Figure 5.1 shows the absolute error for μ for all the discretizations as being fairly accurate, but with HB and EPT outperforming. The errors for each region and are presented in the Appendix in Section .5. In every region HB had the lowest mean absolute μ error except in the Beta Prime region. This is due to the objective function chosen by Hammond and Bickel in [12] that minimizes the error of both μ and σ^2 in combination. We see this in Figure 5.2 where in the Beta Prime region, the mean absolute error for σ^2 is higher for EPT than for HB. In combination HB is lower. The data also shows that MCS usually performs the worst in most areas for both μ and σ^2. The only exception is the Pearson $I - \cup$ area, where

MCS has the lowest μ error and the second smallest σ^2 error.

The results in the Pearson system show that overall, the discretizations with the more extreme percentiles (HB and EPT) perform better than the ones with less extreme percentiles (ESM and MCS). The observations from [21], [2], [37], [41], and [27], summarized in Table 2.1 show that more extreme percentiles result in more of a surprise index. We examine the effect of a scale of $5\%, 10\%$, and 20% error in the assessment error e_p. That is to say, when the scale is 20%, then $\max(e_p) - \min(e_p) = 0.2$. We simulate values for e_p where we permute both the scale and the rank correlation PX and $P(100 - X)$, where $p \neq 50$ and measure the average absolute errors for μ and σ^2 at each point used by [12]. For each discretization, scale, correlation we generate 5000 points for each position in the Pearson system for each discretization.

We use the PearsonDS library in R in order to determine the values for a given percentile. In order to minimize variability we determine the three correlated percentiles we will use in each sample. We then use these percentiles to get the appropriate assessed percentile based on the desired percentile, p, and the scale from the Beta distribution we are applying. We use these three percentiles to determine the assessed values from the true distribution. This is similar to what might happen in a project. The experts give three values based on their assessments, and the decision analysts determine the valuation of the strategy based on the probabilities they apply to these assessed values.

When comparing the results for each discretization as the scale increases, we see that the absolute error in both μ and σ^2 also increases. This is irrespective of the rank correlation between the extreme assessments. Figure 5.3 shows the increase in error as the scale of the assessment error increases. MCS without assessment error has a mean absolute error for μ of 3.48%. When the

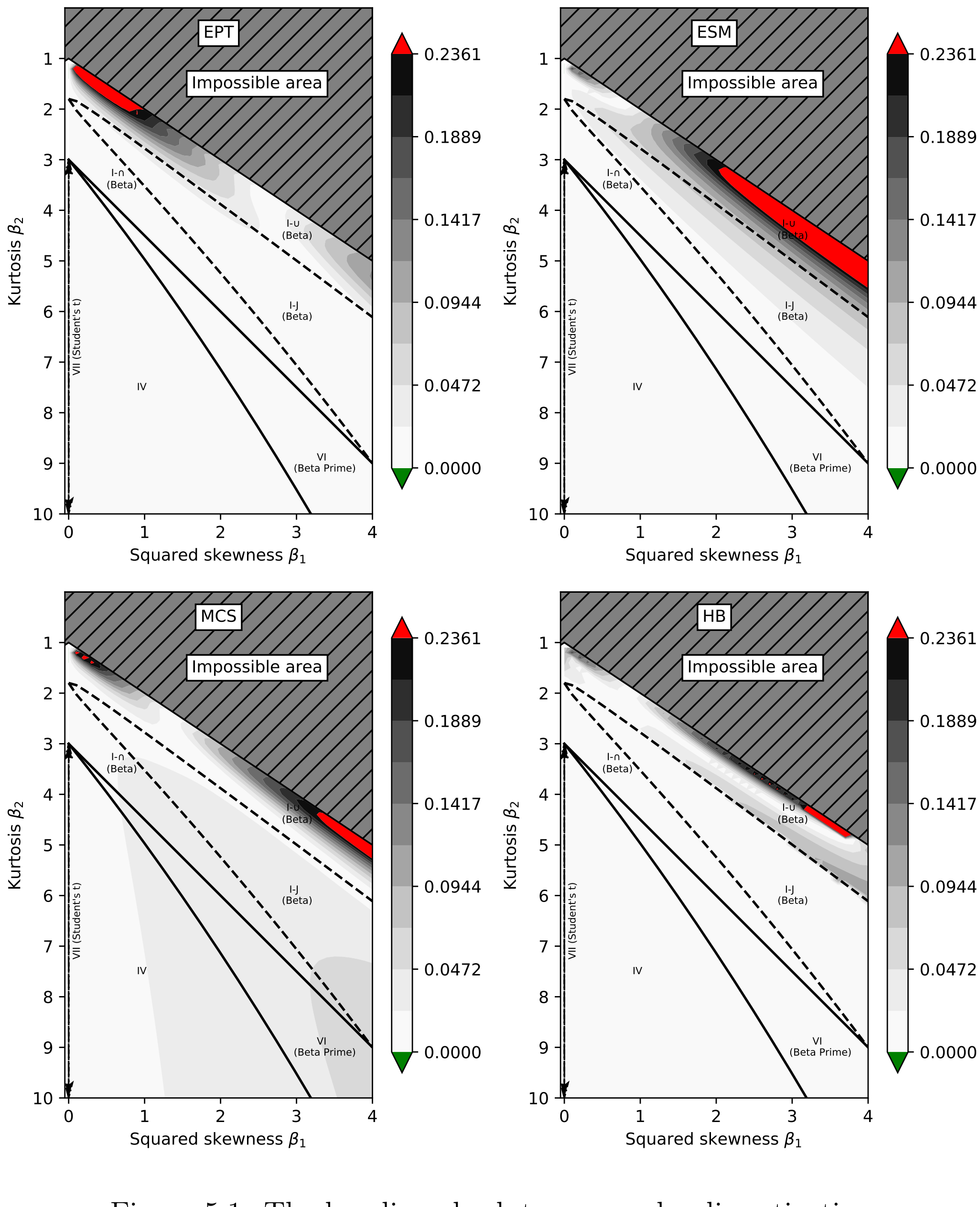

Figure 5.1: The baseline absolute μ error by discretization

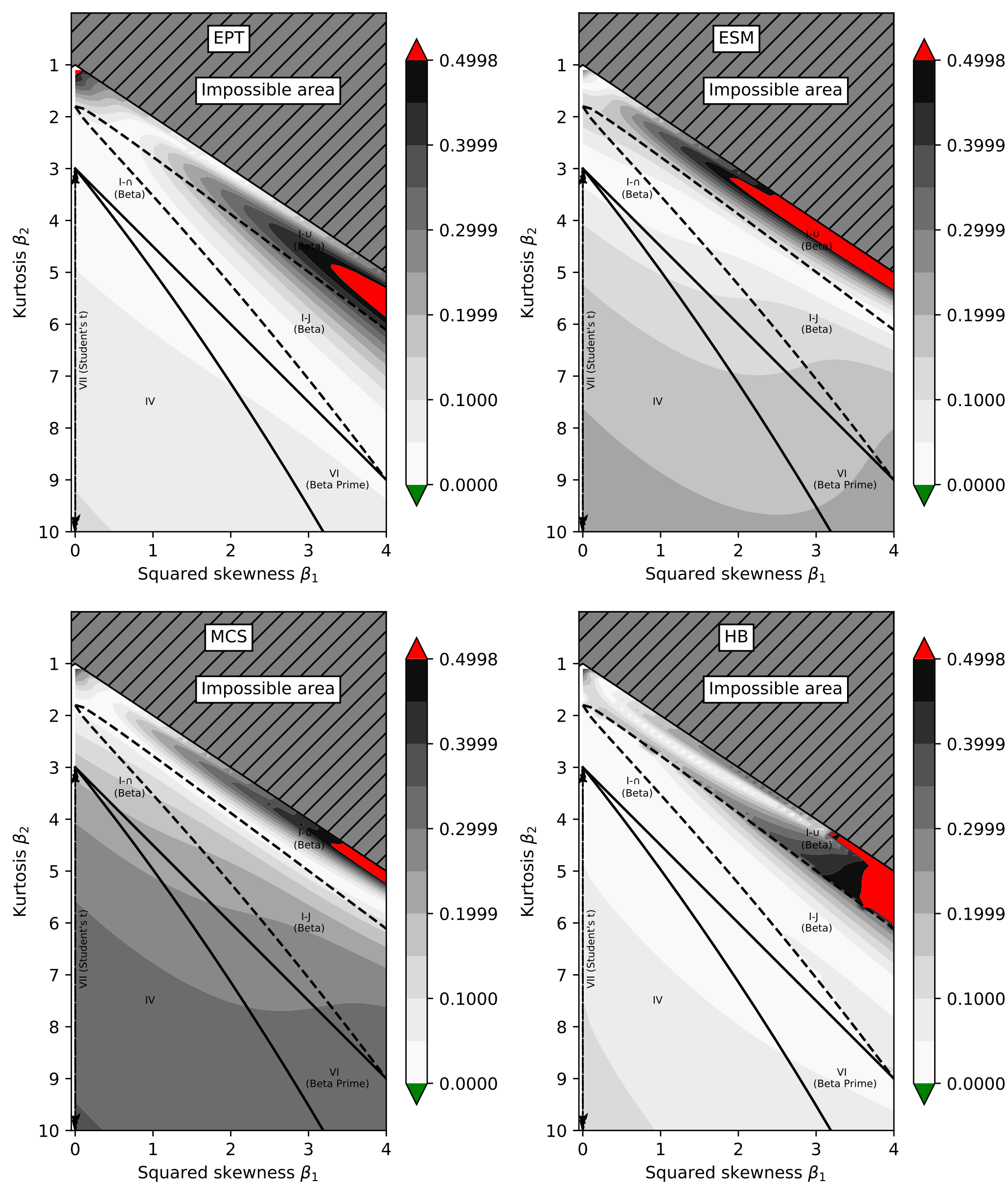

Figure 5.2: The baseline absolute σ^2 error by discretization

scale increases to $0.05, 0.10$, and 0.20, the error increases to $4.02\%, 4.98\%$, and 7.56% respectively.

For the HB discretization we can visually see the increase in error is more dramatic. Figure 5.4 shows the majority of the Pearson zone for no assessment error as being the lightest color. As the scale increases to 0.20, the darker colors predominate, signaling that under most conditions, the increase in assessment error is more pronounced. In comparison, the Pearson zone for MCS with a scale of 0.20 has more lighter colors. When taking the mean error of the absolute value of the μ errors, the results confirm the conclusions from the visual inspection. The mean absolute μ error increases from 0.96% for the HB discretization with no assessment error to 2.78% for scale $= 0.05$ and finally to 4.72% and 8.72% for scales 0.10 and 0.20 respectively. With scale $= 0.10$ the HB discretization still outperforms the MCS discretization, but the roles reverse as the scale increases to 0.20. This pattern is similar for ESM where the mean absolute μ error is lower than MCS's error for the zero assessment error and for 0.05, but the ESM error is larger for scale $= 0.10$ and scale$= 0.20$. ESM also outperforms HB with scale $= 0.20$. To compare all discretizations with all the correlations and all the scale errors, we refer the reader to the summary tables in the Appendix in Section .4.

The same pattern repeats with the mean absolute σ^2 error. In Figure 5.5 the error for σ^2 increases with the scale of the assessment error. For ESM the mean absolute σ^2 error increases from 16.48% for the true discretization to 26.62% for the assessment error with scale $= 0.20$. In the case of variance, ESM outperforms MCS for all assessment error scales. And HB outperforms ESM for scale ≤ 0.10. The data show that as the scale of the assessment error increases, so does the error of μ and σ^2. The data also shows that the EPT and

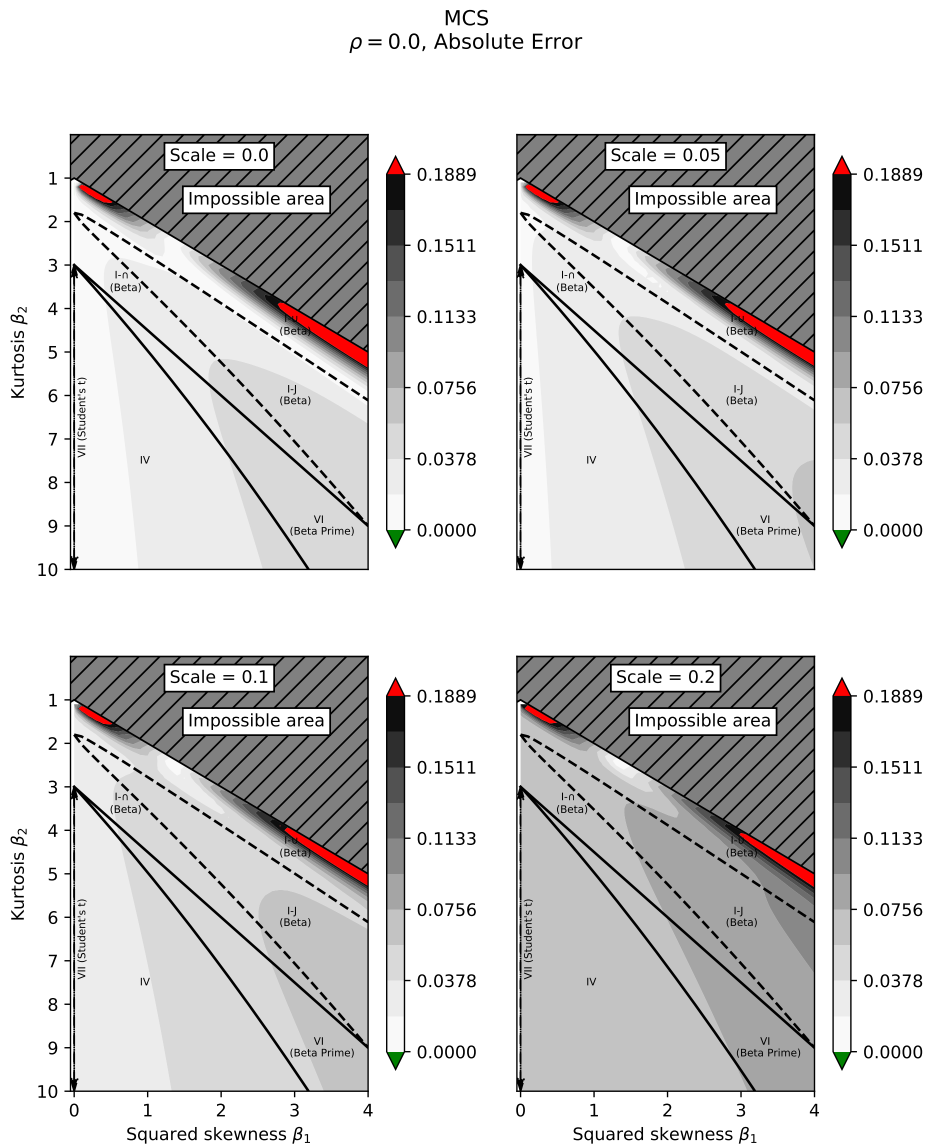

Figure 5.3: The absolute error in μ for the MCS discretization as the scale of the assessment error increases.

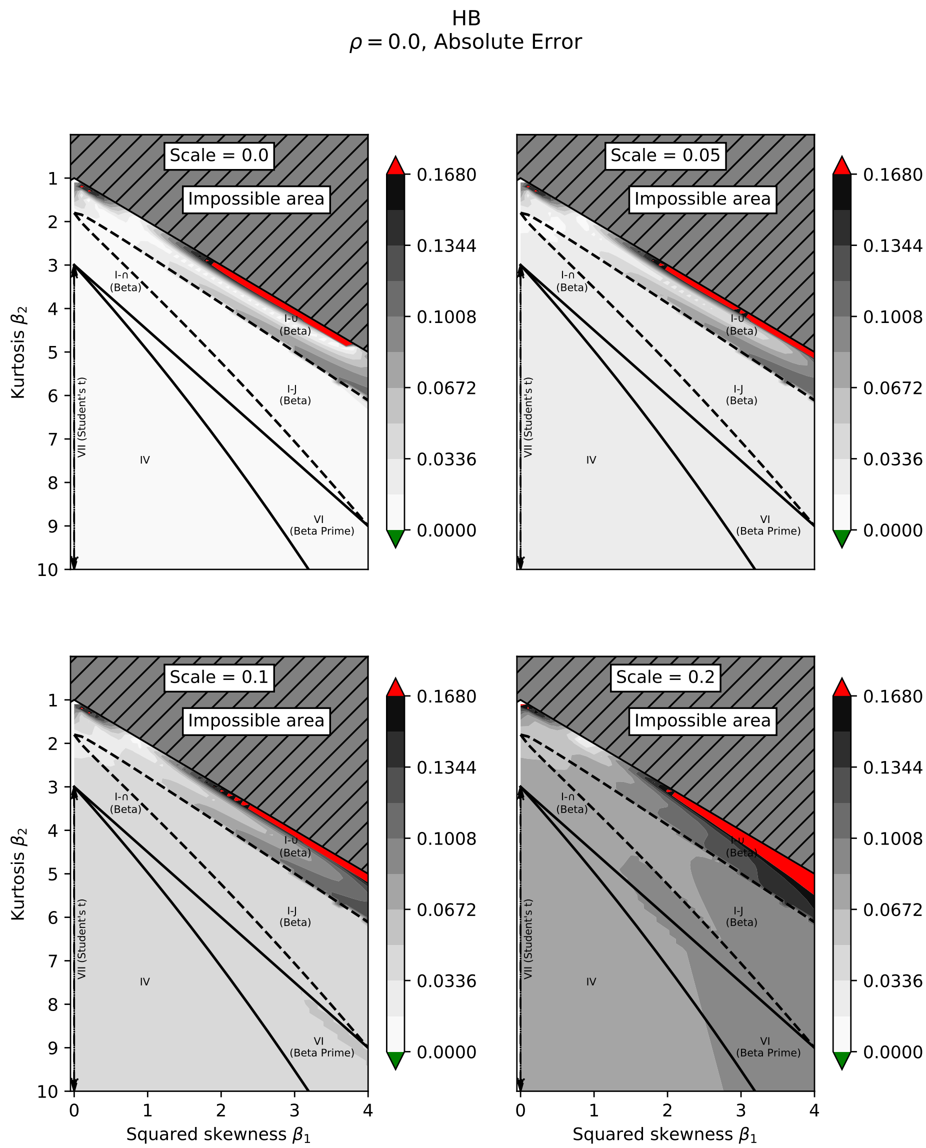

Figure 5.4: The absolute error in μ for the HB discretization as the scale of the assessment error increases.

HB discretizations perform best when the scale of the assessment error ≤ 0.10 for both μ and σ^2. When there is high assessment error, such as when scale = 20, the choice between MCS and ESM depends on the region from which the uncertainties come from, and whether it is more important to estimate the μ or σ^2.

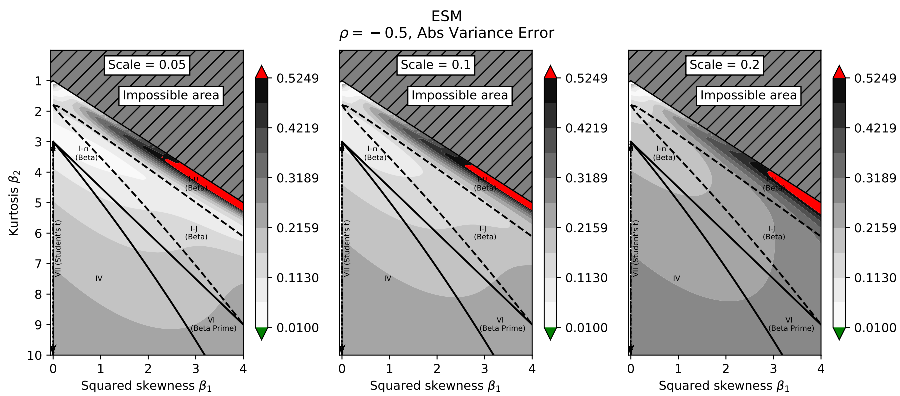

Figure 5.5: The absolute error in σ^2 for the HB discretization as the scale of the assessment error increases.

The effect of the correlation of the two extreme values also plays a role in the accuracy. For each of the discretizations, we found that for any non-zero assessment error scale, the μ errors increase as the rank correlation changes from -1.0 to 1.0. The μ errors did not decrease as ρ went from -1 to 0 and then reverse course as ρ continued to increase from 0 to 1. This property held for the each of the discretizations we tested and for each of the assessment error scales we tested. The results for the mean absolute σ^2 error followed the opposite pattern; the error *decreased* as the correlation changed from -1.0 to 1.0. The exception to this pattern is the MCS discretization, which has a consistent mean absolute σ^2 error across all rank correlations. We present the progression for absolute σ^2 error for HB using scale = 0.20 in Figure 5.6. This provides the largest difference in growth.

5.5 Conclusion

In this chapter we propose a new methodology for determining the effect of assessment error on discretization accuracy. This method can account for bias, the scale of variability in the assessments, and the correlation of assessed values. As one would expect, the accuracy of μ and σ^2 of the discretizations decreases with increases in the scale of the assessment error. We also find that for the HB and EPT discretizations which use more extreme discretizations, their accuracy deteriorates more rapidly than that of MCS and ESM. If the scale of the assessment error is going to be greater than 0.10, then it is recommended to switch to ESM or MCS.

A surprising outcome from the simulation and analysis is the effect of correlation on the accuracy of μ and σ^2. Prior to conducting the analysis, it was expected that an increase in the absolute value of the rank correlation would also increase the μ and σ^2 errors. Instead, we found the μ error decreased as correlation increased and σ^2 error decreased as correlation increased. The tables in the Appendix in Section .5 also show that for most correlations, once the scale of assessment error is at least 0.10, the ESM discretization has the lowest μ and lowest σ^2 error for the $I - \cap$ beta area, which is commonly used.

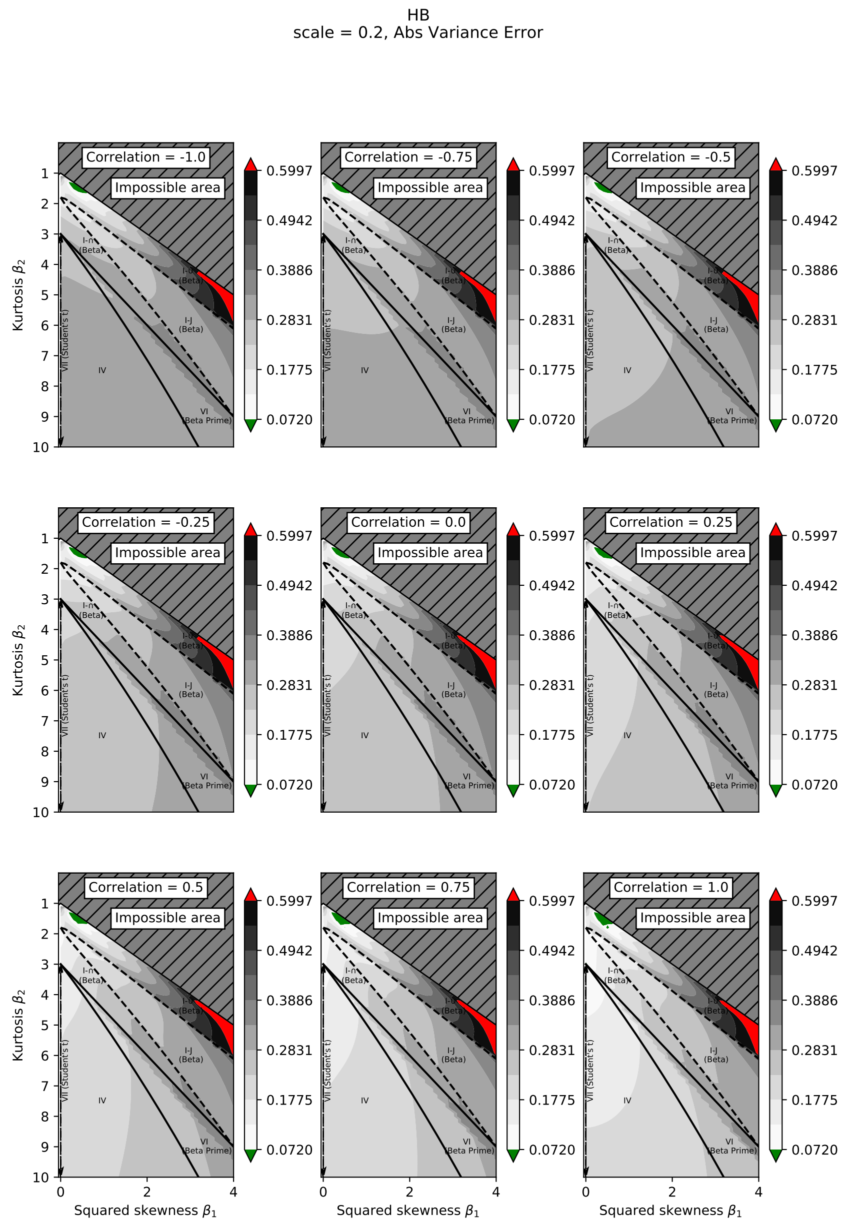

Figure 5.6: The absolute error in σ^2 for the HB discretization with assessment error scale of 0.20 as the rank correlation of the extreme values assessments changes from -1.0 to 1.0.

Chapter 6

Conclusions and Future Work

This dissertation describes three novel techniques that can be applied to furthering the practice of Decision Analysis. In Chapter 3, we introduce a method for improving discretizations for repeated decisions. We find that using less-extreme values for the percentiles results in more accurate estimates of the CE even when all the uncertainties are taken from out of sample distributions. This shows that while discretizations based on the sample distributions are more accurate when more extreme percentiles such as the 5^{th} and 95^{th} are in the discretization, the in-sample errors are minimized. But in order to maintain a discretization that is more effective over a larger set of potential uncertainties, we recommend less-extreme values such at the $P10$ and the $P90$.

In Chapter 4 we borrow from stochastic optimization and introduce the distance. The HB and EPT follow from the previous research of [12] and [19] in finding that these two discretizations have the lowest μ and σ^2 errors. Following the formula for distance in Equation (4.6), HB and EPT have the smallest theoretical distance. But due to the large jumps in probabilities between the extreme percentiles and the $P50$, the theoretical distance does not make as effective a lower bound as it does for ESM and MCS, but most of the time, HB and EPT also have the lowest actual distance. In Figure 6.1 we show a heat map for 12 combined uncertainties using the Pearson region without the Pearson IV distributions. This is just an estimate, but could be indicative of a large decision analysis problem encountered by practitioners. If assessors are assumed to be perfectly calibrated, and there is no correlation between uncertainties, the clear choice is the HB discretization. The HB discretization was created to match the mean and variance, and that accuracy translates to the minimum distance metrics over all regions. The addition of correlation erodes the dominance of the HB discretization. If the $I - \cup beta$ distribution and the Pearson VI distributions are the primary sources of uncertainty, then ESM and EPT are going to be two choices of discretizations.

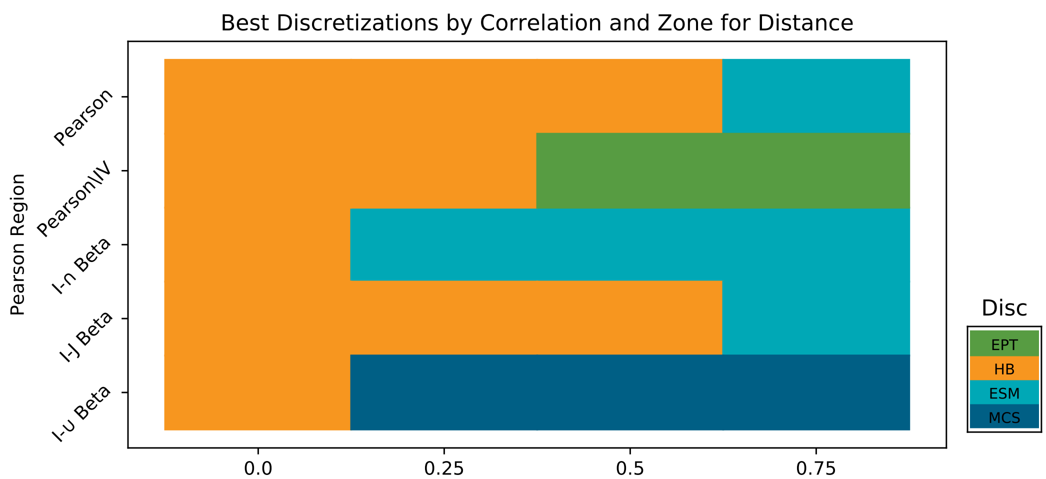

Figure 6.1: For selected correlations and sub-regions of the Pearson system we show the best discretization to use that minimized the total distance in the simulations.

When comparing some specific P values in the value lottery, we find that HB and MCS have the lowest errors at each percentile, as seen in Figures 4.16 and 4.17. What these figures also reveal is that the errors increase as the percentiles increase for ESM and MCS, and that they are more sensitive to increase in rank correlation than are HB and EPT. But if the main concerns are in determining the downside risk of a project, the MCS discretization performs well until the $P50$.

Finally, we provide a novel approach to modeling assessment error. This methodology takes into consideration correlation, bias, and different scales of assessment error. We show that as the scale of the assessment error increases, so do the discretization's errors for μ and σ^2. We also find that, as with problem-specific discretizations, the discretizations with less extreme percentiles are more robust to errors in the assessment. In the literature, [21] and [14] found that assessment error, as defined by the surprise index, increases with more extreme percentiles. So in addition to likely having a larger assessment error scale when using HB or EPT instead than ESM or MCS, the effect the assessment error scale is larger. Figures 6.2 and 6.3 show the best discretizations when applying the discretizations in the different regions of the Pearson system under different assumptions of the scale of the assessment error and the correlation of the errors of the extreme percentiles. For the mean, ESM is the most predominant discretization and could be recommended as long as other metrics are less important. For variance, HB and EPT provide better estimates, even when including assessment error. When shape-matching is included in the decision criteria, then Figure 6.1 provides an estimate for distance when combining multiple uncertainties.

When selecting the proper discretization for a decision analysis problem, we have recommendations. The first is to determine the model which determines which items are uncertainties, parameters, and calculations. It is likely that most calculations will involve both sums and products. This would lead to a using the discretizations that do better for combined areas. The functional form of each uncertainty is unknown. But the benefit of the methodology fol-

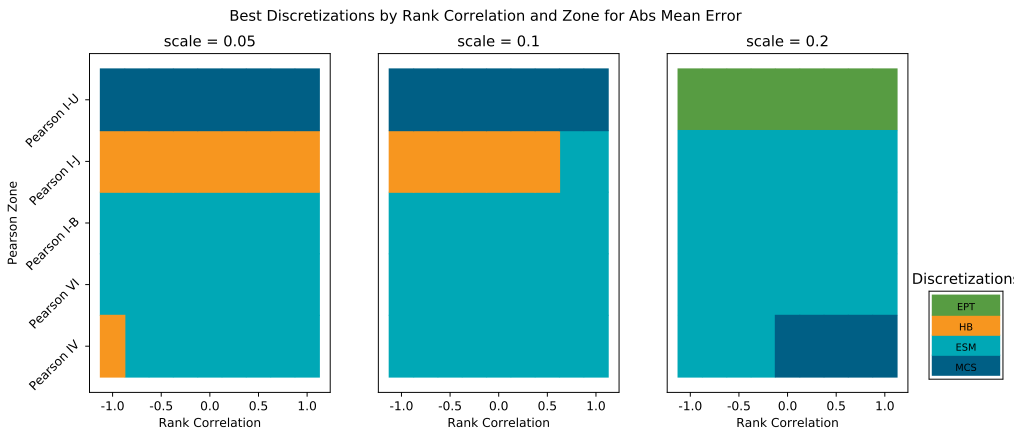

Figure 6.2: For selected correlations and sub-regions of the Pearson system we show the best discretization to use that minimized the absolute error of the mean

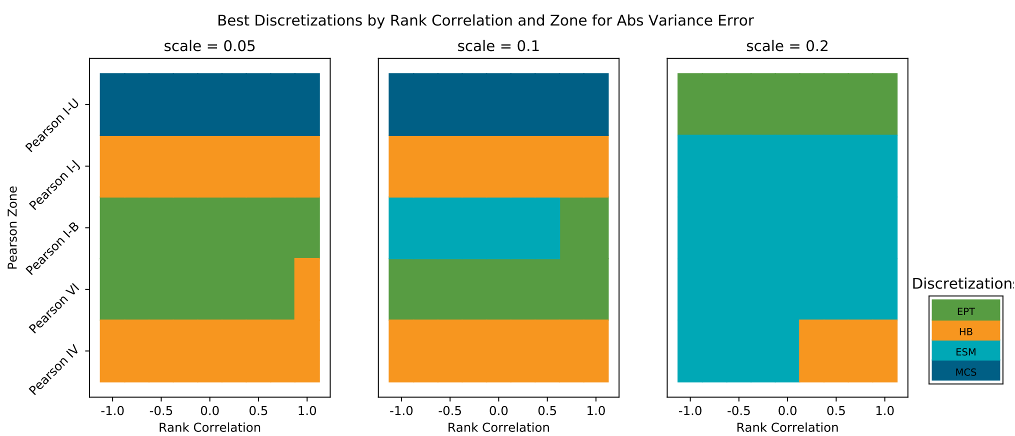

Figure 6.3: For selected correlations and sub-regions of the Pearson system we show the best discretization to use that minimized the absolute error of the variance.

lowed by [12] is that just a few pieces of information are required in order to determine the region of the Pearson system of the uncertainty. For example yes-no outcomes could be though of as $I - \cup$ beta distributions and results that are percentage numbers can be modeled as $I - \cap$ beta distributions. Though lognormal distributions, which are often used to model oil reservoirs, are not part of the Pearson system, their skewness and kurtosis fall in the Pearson VI region. Use the region of the uncertainties that most closely matches a region in Figure 6.1. When estimating calibration, we recommend a test and training similar to that of [14]. Instead of general knowledge questions, we recommend questions about the company and the problem drawn from corporate reports or historical price data. For every question, the subjects should answer for the $P05, P10, P50, P90$, and $P95$. The $P01$ and $P99$ are not necessary as all the examples in the Table 2.1 are badly calibrated at these levels, and are much better calibrated at $P10$ and $P90$. The surprise index for the extreme percentile can be used as a proxy for the scale of the error and the correlation between the high and low percentiles can be used to estimate the rank correlation.

The research presented in this dissertation finds that it is better to err on the side of robustness than to chase accuracy. In general, MCS and ESM each have their regions where they perform better in terms of μ, σ^2, and distance. The region of the uncertainties, the number of uncertainties, and the correlation uncertainties all play a role in the selection of discretizations for a Decision Analysis problem.

While we explored many techniques on their own, we leave it to future research to combine these techniques. For example, instead of finding a problem-specific discretization that minimizes the error of the CE, we can find discretizations that minimize the error of the distance. It is also possible to increase the number of simulations to determine the effect of assessment error on the distance. Another research topic is to develop a methodology to estimate the calibration and the rank correlation of the assessors. If a distribution is fit to the estimated percentiles, then the estimates of q_p yield both a rank correlation and a scale of the error. A final avenue of research is to experiment with the use of assessment error when solving for a problem-specific discretization.

Appendices

.1 Wildcatter Problem Description

This section of the appendix provides the details of the Wildcatter problem described by [40]. We cover the uncertainties and their PDFs, the valuation model, the utility and CE functions, and the sources of risk. We take variants of this basic problem to construct our decision problem sets in the article.

The problem described by [40] is a wildcatting decision problem. A wildcatter is an individual or small group of people who drill for oil. There are four uncertainties that determine the project value. These are the oil price, reservoir volume, recovery rate, and production cost. We refer readers to the source in [40] for a visualization of the influence diagram. The present value of the project given realizations for the four variables is

$$Value = \begin{cases} \frac{1}{\delta} \cdot (p - c) \cdot k \cdot (1 - exp(-\delta \cdot T) - C & \text{if } p > c \\ -C & \text{if } p \leq c, \end{cases} \tag{1}$$

where v is the reservoir volume; r is the recovery rate; p is the oil price; c is the production cost k is a fixed production rate of 100,000 barrels per year; $T = r \cdot v/k$ is the years of production; δ is a fixed discount rate of 5% per year; and C are the initial capital expenditures of \$2.5 million. In the project valuation using Formula (1) the wildcatter will lose money for each barrel pumped if $p \leq c$. Even if the wildatter has already made the decision to expend capital costs C, he or she may choose to not drill when each additional unit of production is not profitable.

The PDFs of the uncertainties defined by [40] are:

$$\begin{array}{rrcll}
\textbf{Reservoir Volume:} & f(\frac{x}{10^6}) & = & \frac{1}{\sqrt{2\pi(x-3.5)}} \cdot \exp(-\frac{(\ln(x-3.5)-0.5)^2}{0.2}) & \frac{x}{10^6} \geq 3.5 \\
\textbf{Recovery:} & f(x \cdot 10^2) & = & \frac{1}{15!} \cdot x^{15} \cdot \exp(-x) & x \geq 0 \\
\textbf{Oil Price:} & f(x) & = & \frac{1}{40} \cdot \frac{6!}{1!4!} \cdot (\frac{x-8}{40})^1 \cdot (\frac{48-x}{40})^4 & 8 \leq x \leq 48 \\
\textbf{Production Cost} \mid \textbf{Oil Price:} & f(x,p) & = & \frac{\sqrt{8}}{\sqrt{p\pi}} \cdot \exp(-\frac{8\cdot(x-p/3-3)^2}{p}) &
\end{array}$$

The PDFs of the uncertainties and are shown in Figure 4. [40] has additional visualizations of the cumulative distribution functions for the uncertainties and the project value. The Wildcatter Problem makes for an interesting problem in Decision Analysis because the distributions may take on many shapes, may be non-symmetrical, and the cost is dependent on the oil price. The reservoir uncertainty follows a lognormal distribution and is bounded from below at 3.5M barrels. The recovery uncertainty is a gamma distributions bounded from below at 0 percent. It is not bounded from above, though in practical terms it should be 100 percent. The oil price uncertainty follows a beta distribution with bounds at 8 and 48 dollars per barrel. Finally, the cost follows a normal distribution with a mean and standard deviation that are functions on the price.

From the project values given by equation (1), we are able to generate the project utility using the equation for utility, (2). From the expected utility we are able to generate a CE. [40] uses an exponential utility function to convert the random project value, x, to a utility, $u(x)$, with a risk tolerance parameter ρ. The expected utilities are converted to a CE. The combination of the uncertainty PDFs, the valuation model, the utility function, and the risk tolerance value ρ combine to make one problem instance $d \in \mathbb{D}$. The functions for the utility and CE are defined as:

$$\textbf{Utility:} \quad u_d(x) = -\,exp\left(-x/\rho_d\right) \tag{2}$$

$$\textbf{Certain Equivalent:} \quad CE_d = -\,\rho_d \cdot ln\left(-E\left[u_d(x)\right]\right) \tag{3}$$

$$\textbf{Target:} \quad T_d = -\,exp\left(-CE_d/\rho_d\right). \tag{4}$$

With the exponential utility function, utility values are between $-\infty$ and 0, and projects with a CE of zero have a utility of -1. Lower risk tolerances penalize losses more. An infinite risk tolerance makes the CE to be equal to the expected value of the project. Given a decision problem $d \in \mathbb{D}$, we can compute a CE by sampling project values based on the uncertainty distributions of$d$, converting values to expected utility, and expected utility to a CE.

.2 Eagle Airlines

Eagle Airlines is a problem described by [6] and further refined by [7] and [?] in the area of fleet expansion. Here we used the information from

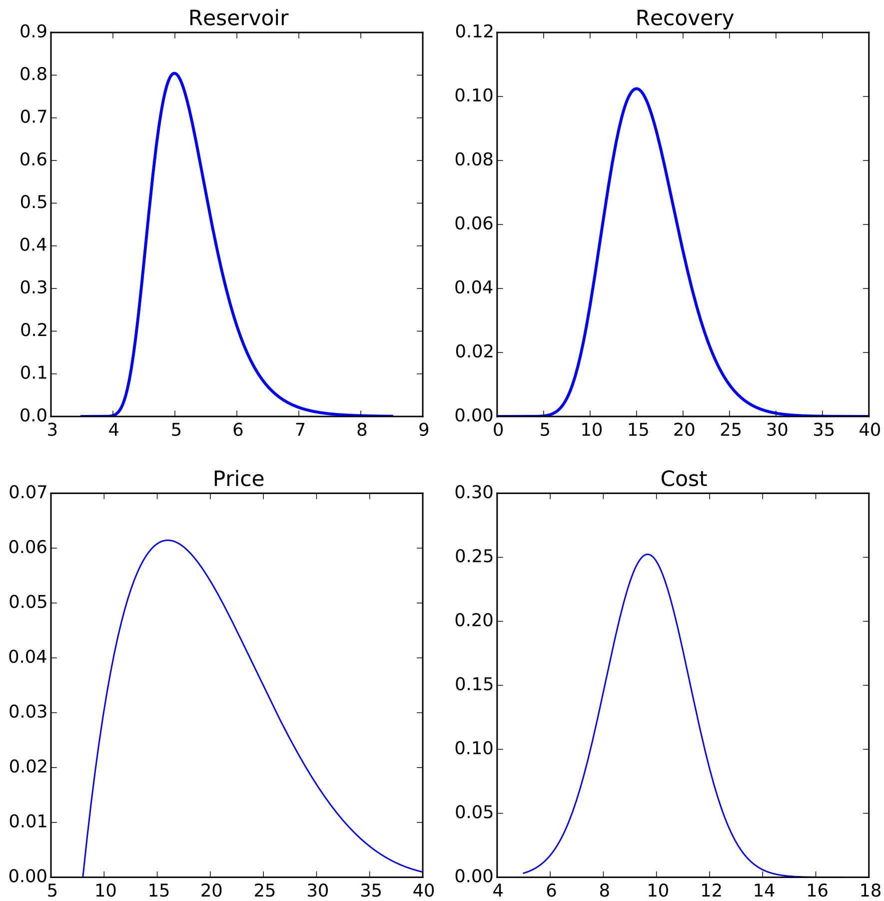

Figure 4: The original distributions are similar to the candidate distributions given in Figure 3.2. As a point of reference, when using the optimal discretizations, the independent worst-case had an error of -0.0369 percent, the best average discretization had an error of -0.0613 percent. The joint best average discretization yields an error of 0.0199 percent and joint worst case discretization yields an error of 0.0823 percent. HB, EPT, ESM, MCS had errors of 0.0357, 0.0411, 0.0337, and -0.6197 percent respectively.

Table 1: Eagle Airlines parameters

Parameter	Value	Description
CR	0.5	Charter ratio
PF	40%	Percentage financed
I	11.5%	Risk-free interest rate
PU	$\$87,500$	Purchase price
IN	$20,000$	Insurance cost
CP	$3.25 \cdot P$	Charter price
N	5	Number of seats

Table 2: Eagle Airlines True Distributions

Uncertainty	Distribution	Parameters	Range
P	Beta	$\alpha = 9, \beta = 15$	$[\$81.94, \$133.96]$
H	Beta	$\alpha = 9, \beta = 15$	$[66.91, 1, 136.26]$
C	Beta	$\alpha = 9, \beta = 15$	$[0, 1]$
O	Normal	$\mu = 245, \sigma = 11.72$	$(-\infty, \infty)$

[?] and the functional forms and rank correlations for the uncertainties given by [26]. In this problem the owner of Eagle Airlines must decide whether or not to expand his fleet with the purchase of one plane. The alternative is to invest the money in a money market earning a certain return. The problem has several uncertainties has determined the uncertainties whose outcomes can affect the decision to go forward with the purchase or not. These uncertainties are are price (P), hours flown (H), capacity (C), and operational cost (O). The owner is risk neutral and will make the decision based on comparing the expected profit to the risk-free return of the money market.

In addition to the uncertainties, the owner uses the following parameters in the profit calculation:

The true distributions for the uncertainties are:

The formulas for revenue, costs and profits are:

$$
\begin{aligned}
Cost &= H \cdot O + IN + PU \cdot PF \cdot I && (5)\\
Revenue &= CR \cdot H \cdot CP + (1 - CR) \cdot H \cdot C \cdot N \cdot P && (6)\\
Profit &= Revenue - Cost && (7)
\end{aligned}
$$

Furthermore, the uncertainties are have a Spearman rank correlation with each other:

Table 3: Eagle Airlines Uncertainty Correlations

	Spearman correlation			
Uncertainty	P	H	C	O
P	1			
H	-0.5	1		
C	-0.25	0.5	1	
O	0	0	0.25	1

In order to calculate the expected mean for this problem we sample using the methods described in [17]. For the discretizations, we generate the correlated uniform values from the percentile discretizations which we then use to generate the Pearson rank correlated uncertainty values. When using rank correlation, the correlation is similar to using a Cholesky decomposition to generate correlated variables, but first, the matrix is adjusted using the following formula:

$$CorrMatrix = 2 \cdot \sin\left(RankCorrMatrix \cdot \frac{\pi}{6}\right). \tag{8}$$

.3 Probability of Normal Tables

This section provides the tables with the probabilities of a sum, or a sum of products of being a normal distribution. As the number of uncertainties increases, so does he probability of normality. Using a fixed mean and variance increases the probability of normality. Taking the product of two uncertainties before summing the products reduces the probability of normality. Increasing the correlation decreases the probability of normality.

Table 4: Probability of Normal in the Pearson Region

		Uncertainties						
		Sum						Combined
ρ	μ, σ^2	1	2	5	10	15	20	10
0.00	variable	0.000	0.000	0.000	0.018	0.103	0.200	0.002
0.00	fixed	0.000	0.000	0.004	0.093	0.306	0.494	0.000
0.25	variable	0.000	0.000	0.000	0.015	0.041	0.087	0.000
0.25	fixed	0.000	0.001	0.005	0.032	0.068	0.125	0.000
0.50	variable	0.000	0.000	0.004	0.009	0.024	0.032	0.000
0.50	fixed	0.000	0.000	0.003	0.013	0.022	0.028	0.000
0.75	variable	0.000	0.000	0.002	0.003	0.005	0.007	0.000
0.75	fixed	0.000	0.001	0.002	0.007	0.004	0.009	0.000
1.00	variable	0.000	0.001	0.002	0.000	0.002	0.000	0.000
1.00	fixed	0.001	0.002	0.002	0.003	0.002	0.001	0.000

.4 Bounding Functions

An example of a a bad bounding function, and an indication the theoretical distance formula will not apply very well is visible for the case of EPT as seen in Table 13. In Figure 4.10 we see the pattern for EPT when summing 20 uncertainties with a fixed μ and σ^2. In this case the slope for the lower bound is negative, indicating the error in the distance *decreases* as the theoretical distance increases. The high initial intercept also indicates the bounding function is inaccurate. Here the lower bound is $lb = 11.315 - 0.1D_{theo}$. The upper bound also indicates the true distance decreases relative to the theoretical distance, $ub = 11.635 - 0.482D_{theo}$.

Table 5: Probability of being normal for the I-$\cap$ region

		Uncertainties						
		Sum						Combined
ρ	μ, σ^2	1	2	5	10	15	20	10
0.00	variable	0.001	0.006	0.037	0.144	0.286	0.453	0.004
0.00	fixed	0.000	0.009	0.056	0.309	0.525	0.665	0.001
0.25	variable	0.001	0.004	0.046	0.162	0.291	0.348	0.000
0.25	fixed	0.002	0.015	0.075	0.230	0.280	0.359	0.000
0.50	variable	0.000	0.012	0.055	0.142	0.199	0.260	0.000
0.50	fixed	0.000	0.014	0.079	0.161	0.221	0.272	0.000
0.75	variable	0.000	0.018	0.073	0.125	0.160	0.203	0.000
0.75	fixed	0.000	0.028	0.070	0.145	0.179	0.202	0.000
1.00	variable	0.002	0.023	0.035	0.074	0.102	0.129	0.000
1.00	fixed	0.000	0.033	0.063	0.083	0.124	0.155	0.000

Table 6: Probability of being normal for the Pearson region, excluding Pearson IV

		Uncertainties						
		Sum						Combined
ρ	μ, σ^2	1	2	5	10	15	20	10
0.00	variable	0.000	0.001	0.004	0.039	0.125	0.236	0.006
0.00	fixed	0.000	0.001	0.007	0.150	0.397	0.558	0.001
0.25	variable	0.000	0.000	0.000	0.030	0.107	0.189	0.002
0.25	fixed	0.000	0.002	0.011	0.087	0.164	0.232	0.000
0.50	variable	0.000	0.002	0.004	0.018	0.065	0.095	0.000
0.50	fixed	0.000	0.002	0.005	0.050	0.088	0.114	0.000
0.75	variable	0.000	0.003	0.002	0.010	0.008	0.022	0.000
0.75	fixed	0.000	0.003	0.004	0.009	0.013	0.019	0.000
1.00	variable	0.002	0.001	0.005	0.002	0.003	0.000	0.000
1.00	fixed	0.000	0.003	0.001	0.002	0.002	0.003	0.000

Table 7: Probability of being normal for the I-J region

		Uncertainties						
		Sum						Combined
ρ	μ, σ^2	1	2	5	10	15	20	10
0.00	variable	0.000	0.000	0.000	0.007	0.046	0.134	0.004
0.00	fixed	0.000	0.000	0.000	0.037	0.250	0.425	0.000
0.25	variable	0.000	0.000	0.001	0.009	0.044	0.088	0.000
0.25	fixed	0.000	0.000	0.003	0.024	0.093	0.159	0.000
0.50	variable	0.000	0.000	0.002	0.011	0.044	0.068	0.000
0.50	fixed	0.000	0.000	0.001	0.026	0.039	0.068	0.000
0.75	variable	0.000	0.000	0.000	0.009	0.023	0.033	0.000
0.75	fixed	0.000	0.000	0.003	0.026	0.019	0.023	0.000
1.00	variable	0.000	0.001	0.004	0.005	0.008	0.016	0.000
1.00	fixed	0.000	0.004	0.002	0.010	0.004	0.004	0.000

Table 8: Probability of being normal for the I- $\cup$ region

		Uncertainties						
		Sum						Combined
ρ	μ, σ^2	1	2	5	10	15	20	10
0.00	variable	0.000	0.000	0.000	0.053	0.226	0.350	0.010
0.00	fixed	0.000	0.000	0.002	0.172	0.488	0.623	0.011
0.25	variable	0.000	0.000	0.000	0.027	0.075	0.120	0.013
0.25	fixed	0.000	0.000	0.000	0.043	0.129	0.160	0.000
0.50	variable	0.000	0.000	0.000	0.000	0.002	0.010	0.001
0.50	fixed	0.000	0.000	0.000	0.000	0.004	0.010	0.000
0.75	variable	0.000	0.000	0.000	0.000	0.000	0.000	0.000
0.75	fixed	0.000	0.000	0.000	0.000	0.000	0.000	0.000
1.00	variable	0.000	0.000	0.000	0.000	0.000	0.000	0.000
1.00	fixed	0.000	0.000	0.000	0.000	0.000	0.000	0.000

Table 9: Bounding for EPT in I-$\cap$ Beta Region with $\rho = 0.0$

Unc.	Agg.	μ and σ^2	Normal?	M_l	b_l	M_u	b_u
5	sum	fixed	False	0.793	0.138	-0.848	0.320
5	sum	fixed	True	0.182	0.147	-1.638	0.285
5	sum	variable	False	2.069	0.261	-0.288	1.095
5	sum	variable	True	1.479	0.343	-0.189	0.847
10	sum	fixed	False	0.629	0.044	-0.735	0.216
10	sum	fixed	True	0.606	0.044	-0.548	0.198
10	sum	variable	False	0.610	0.115	0.004	0.492
10	sum	variable	True	0.721	0.113	0.585	0.280
15	sum	fixed	False	0.358	0.047	0.227	0.126
15	sum	fixed	True	0.599	0.036	-0.307	0.149
15	sum	variable	False	0.574	0.128	0.090	0.457
15	sum	variable	True	0.694	0.102	0.071	0.395
20	combined	fixed	False	0.467	0.077	-0.092	0.272
20	combined	variable	False	0.746	1.001	-1.006	10.869
20	sum	fixed	False	0.512	0.043	0.327	0.101
20	sum	fixed	True	0.631	0.036	0.152	0.106
20	sum	variable	False	0.751	0.110	0.162	0.459
20	sum	variable	True	0.538	0.142	0.412	0.383

Table 10: Bounding for EPT in I-$\cap$ Beta Region with $\rho = 0.25$

Unc.	Agg.	μ and σ^2	Normal?	M_l	b_l	M_u	b_u
5	sum	fixed	False	0.463	0.175	0.391	0.303
5	sum	fixed	True	0.475	0.173	0.863	0.164
5	sum	variable	False	1.061	0.137	0.626	1.012
5	sum	variable	True	1.304	0.037	1.041	0.517
10	sum	fixed	False	0.598	0.141	0.831	0.101
10	sum	fixed	True	0.663	0.126	0.730	0.152
10	sum	variable	False	0.809	0.048	0.994	0.102
10	sum	variable	True	0.943	-0.075	1.017	0.017
15	sum	fixed	False	0.797	0.076	0.801	0.157
15	sum	fixed	True	0.847	0.054	1.014	-0.017
15	sum	variable	False	0.963	-0.263	0.944	0.156
15	sum	variable	True	0.933	-0.098	0.922	0.239
20	combined	fixed	False	0.235	0.655	0.261	0.805
20	combined	variable	False	0.555	2.531	0.395	12.475
20	sum	fixed	False	0.821	0.098	0.808	0.209
20	sum	fixed	True	0.736	0.214	0.942	0.062
20	sum	variable	False	0.904	-0.051	1.034	-0.155
20	sum	variable	True	0.959	-0.198	0.916	0.311

Table 11: Bounding for EPT in I-$\cap$ Beta Region with $\rho = 0.5$

Unc.	Agg.	μ and σ^2	Normal?	M_l	b_l	M_u	b_u
5	sum	fixed	False	0.583	0.237	1.186	0.161
5	sum	fixed	True	0.653	0.228	0.959	0.180
5	sum	variable	False	1.270	0.018	0.878	1.240
5	sum	variable	True	1.396	0.004	0.897	0.934
10	sum	fixed	False	0.462	0.396	0.703	0.346
10	sum	fixed	True	0.748	0.206	1.236	-0.076
10	sum	variable	False	1.041	-0.235	1.081	0.287
10	sum	variable	True	0.992	0.134	1.051	0.294
15	sum	fixed	False	0.611	0.425	0.339	0.937
15	sum	fixed	True	1.031	-0.045	0.895	0.241
15	sum	variable	False	0.916	0.138	1.031	0.354
15	sum	variable	True	1.007	-0.052	1.020	0.345
20	combined	fixed	False	0.146	1.662	0.064	2.333
20	combined	variable	False	0.492	4.182	0.531	14.194
20	sum	fixed	False	0.411	0.942	0.480	1.025
20	sum	fixed	True	1.045	-0.111	1.051	0.043
20	sum	variable	False	0.973	-0.056	1.014	0.455
20	sum	variable	True	0.998	-0.058	1.031	0.310

Table 12: Bounding for EPT in I-$\cap$ Beta Region with $\rho = 0.75$

Unc.	Agg.	μ and σ^2	Normal?	M_l	b_l	M_u	b_u
5	sum	fixed	False	0.540	0.681	0.606	0.753
5	sum	fixed	True	0.437	0.737	0.603	0.714
5	sum	variable	False	2.092	0.149	1.864	1.497
5	sum	variable	True	2.314	0.083	1.920	1.215
10	sum	fixed	False	0.656	0.831	0.400	1.238
10	sum	fixed	True	0.614	0.889	0.376	1.222
10	sum	variable	False	1.532	0.107	1.608	0.817
10	sum	variable	True	1.518	0.246	1.468	1.053
15	sum	fixed	False	0.391	1.518	0.261	1.912
15	sum	fixed	True	0.578	1.264	1.015	0.772
15	sum	variable	False	1.492	-0.297	1.504	0.692
15	sum	variable	True	1.279	0.909	1.390	1.098
20	combined	fixed	False	0.096	3.384	-0.009	4.651
20	combined	variable	False	0.454	8.205	0.578	24.103
20	sum	fixed	False	0.542	1.670	0.412	2.180
20	sum	fixed	True	0.393	1.988	0.940	1.073
20	sum	variable	False	1.340	0.250	1.501	0.392
20	sum	variable	True	1.392	0.049	1.345	1.249

Table 13: Bounding for EPT in I-∩ Beta Region with $\rho = 1.0$

Unc.	Agg.	μ and σ^2	Normal?	M_l	b_l	M_u	b_u
5	sum	fixed	False	0.204	2.784	-0.805	2.971
5	sum	fixed	True	0.764	2.797	-0.758	2.937
5	sum	variable	False	13.854	4.883	-0.743	14.490
5	sum	variable	True	22.642	4.051	-3.939	13.323
10	sum	fixed	False	0.324	5.600	-0.375	5.881
10	sum	fixed	True	0.625	5.623	0.067	5.796
10	sum	variable	False	8.978	12.943	0.710	26.088
10	sum	variable	True	8.274	15.055	2.910	23.149
15	sum	fixed	False	0.201	8.432	-0.323	8.793
15	sum	fixed	True	0.025	8.505	-0.531	8.737
15	sum	variable	False	7.828	21.554	-1.145	38.016
15	sum	variable	True	14.422	20.309	-1.190	35.224
20	combined	fixed	False	0.312	12.498	0.120	15.972
20	combined	variable	False	1.088	56.215	-0.085	206.595
20	sum	fixed	False	0.257	11.257	-0.221	11.691
20	sum	fixed	True	-0.010	11.315	-0.482	11.635
20	sum	variable	False	5.816	30.912	0.269	48.595
20	sum	variable	True	5.129	32.345	-2.809	48.243

Table 14: Bounding for EPT in I-J Beta Region with $\rho = 0.0$

Unc.	Agg.	μ and σ^2	Normal?	M_l	b_l	M_u	b_u
5	sum	fixed	False	1.583	0.152	0.999	0.446
5	sum	variable	False	1.273	0.299	0.798	1.537
10	sum	fixed	False	1.133	0.047	1.300	0.175
10	sum	fixed	True	1.215	0.025	1.365	0.088
10	sum	variable	False	1.034	0.077	0.868	0.617
15	sum	fixed	False	1.008	0.027	1.093	0.090
15	sum	fixed	True	1.041	0.009	1.010	0.091
15	sum	variable	False	0.948	0.103	0.871	0.515
15	sum	variable	True	0.949	0.062	0.799	0.440
20	combined	fixed	False	0.773	0.189	0.763	0.382
20	combined	variable	False	0.826	1.276	0.717	12.873
20	sum	fixed	False	0.958	0.022	0.974	0.075
20	sum	fixed	True	1.001	0.005	0.978	0.069
20	sum	variable	False	0.952	0.083	0.902	0.424
20	sum	variable	True	0.918	0.132	0.977	0.268

Table 15: Bounding for EPT in I-J Beta Region with $\rho = 0.25$

Unc.	Agg.	μ and σ^2	Normal?	M_l	b_l	M_u	b_u
5	sum	fixed	False	-0.250	0.380	-0.178	0.680
5	sum	variable	False	0.833	0.635	0.094	2.394
10	sum	fixed	False	0.255	0.240	-0.293	0.529
10	sum	variable	False	0.624	0.256	0.276	1.066
15	sum	fixed	False	0.694	0.083	0.704	0.161
15	sum	fixed	True	0.845	0.018	0.884	0.061
15	sum	variable	False	0.750	0.001	0.820	0.353
15	sum	variable	True	0.828	-0.012	1.051	-0.057
20	combined	fixed	False	0.276	0.412	0.322	0.630
20	combined	variable	False	0.807	1.095	0.376	19.719
20	sum	fixed	False	0.858	-0.022	0.920	0.030
20	sum	fixed	True	1.053	-0.140	0.964	0.000
20	sum	variable	False	0.897	-0.279	0.932	0.084
20	sum	variable	True	1.093	-0.603	0.945	0.082

Table 16: Bounding for EPT in I-J Beta Region with $\rho = 0.5$

Unc.	Agg.	μ and σ^2	Normal?	M_l	b_l	M_u	b_u
5	sum	fixed	False	-0.165	0.539	-0.532	0.802
5	sum	variable	False	0.740	0.904	-0.259	3.250
10	sum	fixed	False	0.294	0.386	0.404	0.474
10	sum	variable	False	0.745	0.395	0.558	1.524
15	sum	fixed	False	0.748	0.117	0.870	0.183
15	sum	fixed	True	0.923	0.054	1.076	0.020
15	sum	variable	False	0.968	-0.295	0.995	0.458
15	sum	variable	True	1.016	-0.011	1.137	0.074
20	combined	fixed	False	0.240	0.832	0.177	1.645
20	combined	variable	False	0.514	4.946	0.182	31.954
20	sum	fixed	False	0.955	-0.087	1.137	-0.084
20	sum	fixed	True	0.993	-0.035	1.005	0.051
20	sum	variable	False	0.897	-0.177	1.081	0.043
20	sum	variable	True	0.979	-0.122	1.116	-0.075

Table 17: Bounding for EPT in I-J Beta Region with $\rho = 0.75$

Unc.	Agg.	μ and σ^2	Normal?	M_l	b_l	M_u	b_u
5	sum	fixed	False	0.115	0.884	-0.026	1.018
5	sum	variable	False	1.389	1.597	0.168	4.758
10	sum	fixed	False	0.353	1.053	0.521	1.113
10	sum	variable	False	1.169	1.809	0.684	4.560
15	sum	fixed	False	0.567	1.152	0.744	1.206
15	sum	variable	False	1.109	2.068	0.899	4.438
20	combined	fixed	False	0.401	1.624	0.195	3.443
20	combined	variable	False	0.601	5.435	0.286	50.664
20	sum	fixed	False	0.597	1.398	0.736	1.460
20	sum	variable	False	1.088	2.451	1.067	4.244
20	sum	variable	True	1.314	1.507	1.055	3.944

Table 18: Bounding for EPT in I-J Beta Region with $\rho = 1.0$

Unc.	Agg.	μ and σ^2	Normal?	M_l	b_l	M_u	b_u
5	sum	fixed	False	-0.386	2.622	-0.486	2.821
5	sum	variable	False	1.900	4.852	-0.672	13.735
10	sum	fixed	False	-0.426	5.276	-0.531	5.577
10	sum	variable	False	2.311	11.575	-0.282	24.367
15	sum	fixed	False	-0.535	7.969	-0.481	8.301
15	sum	variable	False	2.152	19.171	-0.400	35.234
20	combined	fixed	False	-0.090	11.246	-0.678	17.207
20	combined	variable	False	0.914	38.447	-0.308	220.186
20	sum	fixed	False	-0.503	10.641	-0.500	11.042
20	sum	variable	False	1.912	26.952	-0.104	45.007

Table 19: Bounding for EPT in Pearson Region with $\rho = 0.0$

Unc.	Agg.	μ and σ^2	Normal?	M_l	b_l	M_u	b_u
5	sum	fixed	False	0.833	0.090	0.548	0.323
5	sum	variable	False	0.915	0.231	0.569	1.258
10	sum	fixed	False	0.979	0.004	0.857	0.109
10	sum	fixed	True	0.994	-0.003	0.922	0.079
10	sum	variable	False	0.977	-0.007	0.833	0.551
15	sum	fixed	False	0.994	-0.010	0.914	0.083
15	sum	fixed	True	0.995	-0.006	0.911	0.074
15	sum	variable	False	1.002	-0.047	0.871	0.488
15	sum	variable	True	1.009	-0.054	0.882	0.388
20	combined	fixed	False	0.942	0.022	0.656	0.377
20	combined	variable	False	1.031	-0.902	0.728	10.305
20	sum	fixed	False	0.989	-0.008	0.919	0.085
20	sum	fixed	True	0.975	-0.000	0.935	0.070
20	sum	variable	False	1.002	-0.054	0.890	0.444
20	sum	variable	True	1.002	-0.070	0.928	0.389

Table 20: Bounding for EPT in Pearson Region with $\rho = 0.25$

Unc.	Agg.	μ and σ^2	Normal?	M_l	b_l	M_u	b_u
5	sum	fixed	False	0.807	0.112	0.377	0.440
5	sum	variable	False	0.968	0.163	0.629	1.501
10	sum	fixed	False	0.919	-0.059	0.938	0.089
10	sum	fixed	True	1.226	-0.206	0.906	0.083
10	sum	variable	False	0.974	-0.323	0.958	0.356
15	sum	fixed	False	0.883	-0.069	1.015	-0.002
15	sum	fixed	True	1.157	-0.254	1.045	-0.021
15	sum	variable	False	1.034	-0.675	1.030	0.054
15	sum	variable	True	1.297	-1.326	1.019	0.009
20	combined	fixed	False	0.389	0.209	0.591	0.409
20	combined	variable	False	0.822	-2.712	0.704	12.243
20	sum	fixed	False	0.904	-0.099	1.051	-0.079
20	sum	fixed	True	1.059	-0.202	1.007	-0.024
20	sum	variable	False	0.929	-0.492	1.006	-0.055
20	sum	variable	True	1.130	-1.009	1.060	-0.248

Table 21: Bounding for EPT in Pearson Region with $\rho = 0.5$

Unc.	Agg.	μ and σ^2	Normal?	M_l	b_l	M_u	b_u
5	sum	fixed	False	0.682	0.215	0.486	0.488
5	sum	variable	False	0.891	0.345	0.301	2.540
10	sum	fixed	False	0.733	0.062	0.840	0.210
10	sum	variable	False	0.753	0.159	0.853	0.891
15	sum	fixed	False	0.875	-0.102	1.048	-0.027
15	sum	variable	False	0.830	-0.234	0.983	0.326
20	combined	fixed	False	0.289	0.662	0.313	1.399
20	combined	variable	False	0.333	5.426	0.391	24.663
20	sum	fixed	False	0.883	-0.130	1.055	-0.074
20	sum	variable	False	0.809	-0.129	1.036	-0.053
20	sum	variable	True	0.979	-0.217	0.906	0.694

Table 22: Bounding for EPT in Pearson Region with $\rho = 0.75$

Unc.	Agg.	μ and σ^2	Normal?	M_l	b_l	M_u	b_u
5	sum	fixed	False	0.649	0.574	0.652	0.775
5	sum	variable	False	1.250	0.866	0.596	3.765
10	sum	fixed	False	0.673	0.657	0.726	0.876
10	sum	variable	False	0.832	1.682	0.735	3.826
15	sum	fixed	False	0.600	0.941	0.850	0.927
15	sum	variable	False	0.732	2.625	0.848	3.764
20	combined	fixed	False	0.218	2.340	0.188	3.459
20	combined	variable	False	0.307	8.984	0.238	46.645
20	sum	fixed	False	0.604	1.179	0.879	1.036
20	sum	variable	False	0.802	2.731	0.967	3.599

Table 23: Bounding for EPT in Pearson Region with $\rho = 1.0$

Unc.	Agg.	μ and σ^2	Normal?	M_l	b_l	M_u	b_u
5	sum	fixed	False	-0.388	2.260	-0.332	2.995
5	sum	variable	False	1.291	4.516	-0.796	14.301
10	sum	fixed	False	-0.113	4.803	-0.338	5.875
10	sum	variable	False	0.891	12.667	-1.597	26.448
15	sum	fixed	False	-0.070	7.323	-0.220	8.689
15	sum	variable	False	1.642	19.430	-1.068	37.356
20	combined	fixed	False	0.184	11.459	-0.041	16.638
20	combined	variable	False	0.351	56.178	-0.098	212.717
20	sum	fixed	False	-0.054	9.932	-0.551	11.626
20	sum	variable	False	0.161	30.078	-1.377	48.466

Table 24: Bounding for EPT in Pearson Region without Pearson IV with $\rho = 0.0$

Unc.	Agg.	μ and σ^2	Normal?	M_l	b_l	M_u	b_u
5	sum	fixed	False	0.883	0.098	0.578	0.463
5	sum	variable	False	0.898	0.276	0.578	1.606
10	sum	fixed	False	0.973	0.008	0.833	0.182
10	sum	fixed	True	1.000	-0.008	0.883	0.115
10	sum	variable	False	0.980	-0.005	0.870	0.551
10	sum	variable	True	0.914	-0.011	0.992	0.354
15	sum	fixed	False	1.007	-0.019	0.943	0.081
15	sum	fixed	True	0.990	-0.011	0.951	0.082
15	sum	variable	False	0.983	-0.031	0.924	0.397
15	sum	variable	True	0.997	-0.101	0.943	0.360
20	combined	fixed	False	0.943	0.023	0.807	0.324
20	combined	variable	False	0.956	-1.301	0.739	11.949
20	sum	fixed	False	0.981	-0.008	0.964	0.067
20	sum	fixed	True	1.002	-0.026	0.969	0.064
20	sum	variable	False	0.987	-0.043	0.951	0.355
20	sum	variable	True	0.963	-0.045	1.004	0.232

Table 25: Bounding for EPT in Pearson Region without Pearson IV with $\rho = 0.25$

Unc.	Agg.	μ and σ^2	Normal?	M_l	b_l	M_u	b_u
5	sum	fixed	False	0.852	0.147	0.370	0.604
5	sum	variable	False	0.940	0.342	0.506	2.108
10	sum	fixed	False	0.998	-0.014	0.762	0.271
10	sum	fixed	True	0.946	0.012	0.831	0.193
10	sum	variable	False	1.007	-0.113	0.878	0.696
15	sum	fixed	False	1.048	-0.094	0.939	0.121
15	sum	fixed	True	1.020	-0.058	0.865	0.146
15	sum	variable	False	0.870	-0.011	0.755	0.853
15	sum	variable	True	0.925	-0.042	1.012	0.195
20	combined	fixed	False	0.713	0.007	0.599	0.628
20	combined	variable	False	0.954	-1.017	0.609	17.087
20	sum	fixed	False	1.038	-0.106	1.003	0.079
20	sum	fixed	True	1.113	-0.162	1.035	0.020
20	sum	variable	False	0.900	-0.115	0.816	0.772
20	sum	variable	True	1.065	-0.457	1.033	0.186

Table 26: Bounding for EPT in Pearson Region without Pearson IV with $\rho = 0.5$

Unc.	Agg.	μ and σ^2	Normal?	M_l	b_l	M_u	b_u
5	sum	fixed	False	0.763	0.278	0.375	0.692
5	sum	variable	False	0.968	0.570	0.427	2.757
10	sum	fixed	False	0.895	0.074	0.705	0.420
10	sum	fixed	True	0.914	0.093	0.757	0.291
10	sum	variable	False	0.900	0.255	0.809	1.428
15	sum	fixed	False	0.972	-0.033	1.005	0.187
15	sum	fixed	True	1.110	-0.101	0.910	0.242
15	sum	variable	False	1.016	-0.224	0.961	0.917
15	sum	variable	True	1.123	-0.360	0.983	0.698
20	combined	fixed	False	0.389	0.476	0.495	1.118
20	combined	variable	False	0.819	-1.863	0.544	25.712
20	sum	fixed	False	1.014	-0.105	1.131	0.057
20	sum	fixed	True	1.026	-0.041	0.970	0.192
20	sum	variable	False	0.972	-0.121	1.058	0.621
20	sum	variable	True	0.952	0.070	1.073	0.399

Table 27: Bounding for EPT in Pearson Region without Pearson IV with $\rho = 0.75$

Unc.	Agg.	μ and σ^2	Normal?	M_l	b_l	M_u	b_u
5	sum	fixed	False	0.777	0.588	0.550	0.912
5	sum	variable	False	1.025	1.271	0.352	4.485
10	sum	fixed	False	0.760	0.724	0.805	0.984
10	sum	variable	False	1.006	1.797	0.769	4.453
15	sum	fixed	False	0.828	0.841	0.875	1.123
15	sum	variable	False	1.035	2.159	0.751	5.237
20	combined	fixed	False	0.388	1.694	0.300	3.051
20	combined	variable	False	0.507	7.556	0.445	44.104
20	sum	fixed	False	0.924	0.909	0.938	1.239
20	sum	variable	False	1.088	2.335	0.959	4.991

Table 28: Bounding for EPT in Pearson Region without Pearson IV with $\rho = 1.0$

Unc.	Agg.	μ and σ^2	Normal?	M_l	b_l	M_u	b_u
5	sum	fixed	False	-0.519	2.026	-0.134	2.871
5	sum	variable	False	1.259	3.637	-0.741	13.990
10	sum	fixed	False	-0.722	4.508	-0.734	5.745
10	sum	variable	False	0.392	11.752	-0.500	23.486
15	sum	fixed	False	-0.782	6.987	-0.808	8.504
15	sum	variable	False	0.242	19.157	-1.171	35.468
20	combined	fixed	False	0.052	9.803	-0.523	16.294
20	combined	variable	False	1.110	27.821	-0.080	194.576
20	sum	fixed	False	-0.786	9.446	-1.038	11.368
20	sum	variable	False	-0.361	29.270	-0.883	44.840

Table 29: Bounding for EPT in I-∪ Beta Region with $\rho = 0.0$

Unc.	Agg.	μ and σ^2	Normal?	M_l	b_l	M_u	b_u
5	sum	fixed	False	0.848	0.165	0.578	0.561
5	sum	variable	False	0.882	0.381	0.609	1.962
10	sum	fixed	False	0.965	0.028	0.740	0.445
10	sum	fixed	True	0.973	0.013	0.803	0.337
10	sum	variable	False	0.974	-0.005	0.917	0.594
10	sum	variable	True	0.858	0.179	0.995	0.421
15	sum	fixed	False	0.990	-0.006	0.830	0.334
15	sum	fixed	True	0.956	0.016	0.868	0.265
15	sum	variable	False	1.008	-0.198	0.972	0.317
15	sum	variable	True	0.992	-0.142	0.983	0.246
20	combined	fixed	False	0.961	-0.067	0.994	0.188
20	combined	variable	False	0.972	-4.993	0.945	7.582
20	sum	fixed	False	0.997	-0.019	0.896	0.220
20	sum	fixed	True	1.002	-0.032	0.914	0.202
20	sum	variable	False	1.003	-0.176	0.997	0.232
20	sum	variable	True	1.005	-0.177	1.012	0.170

Table 30: Bounding for EPT in I-$\cup$ Beta Region with $\rho = 0.25$

Unc.	Agg.	μ and σ^2	Normal?	M_l	b_l	M_u	b_u
5	sum	fixed	False	0.771	0.239	0.369	0.705
5	sum	variable	False	0.881	0.482	0.641	2.297
10	sum	fixed	False	0.924	0.078	0.611	0.594
10	sum	fixed	True	0.882	0.100	0.663	0.453
10	sum	variable	False	0.949	0.162	0.823	1.110
15	sum	fixed	False	0.964	0.032	0.750	0.481
15	sum	fixed	True	0.925	0.057	0.729	0.472
15	sum	variable	False	0.974	0.013	0.903	0.765
15	sum	variable	True	0.975	-0.058	0.920	0.503
20	combined	fixed	False	0.896	0.131	0.789	0.668
20	combined	variable	False	0.941	-3.236	0.893	10.706
20	sum	fixed	False	0.967	0.024	0.822	0.380
20	sum	fixed	True	0.947	0.033	0.755	0.419
20	sum	variable	False	0.996	-0.104	0.928	0.729
20	sum	variable	True	0.936	-0.026	0.997	0.475

Table 31: Bounding for EPT in I-$\cup$ Beta Region with $\rho = 0.5$

Unc.	Agg.	μ and σ^2	Normal?	M_l	b_l	M_u	b_u
5	sum	fixed	False	0.739	0.301	0.486	0.736
5	sum	variable	False	0.946	0.499	0.512	3.018
10	sum	fixed	False	0.817	0.253	0.602	0.703
10	sum	variable	False	0.867	0.604	0.795	2.163
15	sum	fixed	False	0.863	0.196	0.734	0.647
15	sum	variable	False	0.928	0.335	0.849	2.000
20	combined	fixed	False	0.879	0.281	0.618	1.270
20	combined	variable	False	1.025	-3.493	0.843	15.832
20	sum	fixed	False	0.909	0.146	0.814	0.619
20	sum	variable	False	0.945	0.222	0.866	2.181

Table 32: Bounding for EPT in I-$\cup$ Beta Region with $\rho = 0.75$

Unc.	Agg.	μ and σ^2	Normal?	M_l	b_l	M_u	b_u
5	sum	fixed	False	0.756	0.367	0.652	0.914
5	sum	variable	False	0.955	0.768	0.488	4.391
10	sum	fixed	False	0.858	0.530	0.733	1.161
10	sum	variable	False	0.858	1.455	0.642	4.947
15	sum	fixed	False	0.698	0.711	0.897	1.324
15	sum	variable	False	0.766	1.994	0.672	6.005
20	combined	fixed	False	0.825	0.908	0.461	2.723
20	combined	variable	False	0.985	0.857	0.763	30.114
20	sum	fixed	False	0.813	0.737	0.796	1.646
20	sum	variable	False	0.764	2.473	0.740	6.665

Table 33: Bounding for EPT in I-$\cup$ Beta Region with $\rho = 1.0$

Unc.	Agg.	μ and σ^2	Normal?	M_l	b_l	M_u	b_u
5	sum	fixed	False	0.265	1.022	-0.292	2.560
5	sum	variable	False	1.308	0.766	-0.046	10.498
10	sum	fixed	False	-0.178	2.905	-0.592	4.952
10	sum	variable	False	0.662	6.307	-0.281	19.126
15	sum	fixed	False	-0.006	4.367	-0.481	7.002
15	sum	variable	False	0.281	12.940	-0.147	26.296
20	combined	fixed	False	0.491	4.786	0.234	9.780
20	combined	variable	False	1.065	-0.126	1.046	67.446
20	sum	fixed	False	-0.440	6.618	-0.573	9.246
20	sum	variable	False	0.137	18.643	-0.348	34.597

Table 34: Bounding for ESM in I-$\cap$ Beta Region with $\rho = 0.0$

Unc.	Agg.	μ and σ^2	Normal?	M_l	b_l	M_u	b_u
5	sum	fixed	False	0.754	0.069	0.400	0.217
5	sum	fixed	True	0.089	0.117	0.868	0.162
5	sum	variable	False	0.791	0.164	0.504	0.789
5	sum	variable	True	0.901	0.227	0.606	0.534
10	sum	fixed	False	0.712	0.021	0.570	0.114
10	sum	fixed	True	0.523	0.033	0.668	0.088
10	sum	variable	False	0.581	0.113	0.528	0.574
10	sum	variable	True	0.515	0.125	0.161	0.468
15	sum	fixed	False	0.667	0.023	0.665	0.087
15	sum	fixed	True	0.679	0.017	0.609	0.076
15	sum	variable	False	0.567	0.120	0.562	0.515
15	sum	variable	True	0.658	0.079	0.461	0.349
20	combined	fixed	False	0.287	0.161	0.125	0.393
20	combined	variable	False	0.620	0.998	0.251	11.133
20	sum	fixed	False	0.764	0.013	0.612	0.098
20	sum	fixed	True	0.692	0.021	0.647	0.076
20	sum	variable	False	0.612	0.111	0.558	0.523
20	sum	variable	True	0.620	0.106	0.527	0.367

Table 35: Bounding for ESM in I-$\cap$ Beta Region with $\rho = 0.25$

Unc.	Agg.	μ and σ^2	Normal?	M_l	b_l	M_u	b_u
5	sum	fixed	False	0.570	0.132	0.696	0.222
5	sum	fixed	True	0.186	0.188	0.221	0.239
5	sum	variable	False	0.825	0.224	0.698	0.835
5	sum	variable	True	0.655	0.372	0.484	0.816
10	sum	fixed	False	0.672	0.036	0.677	0.183
10	sum	fixed	True	0.599	0.059	0.551	0.140
10	sum	variable	False	0.577	0.284	0.826	0.436
10	sum	variable	True	0.650	0.131	0.564	0.545
15	sum	fixed	False	0.744	-0.025	0.582	0.277
15	sum	fixed	True	0.627	0.047	0.697	0.055
15	sum	variable	False	0.667	0.096	0.727	0.641
15	sum	variable	True	0.628	0.169	0.699	0.226
20	combined	fixed	False	0.360	0.399	0.272	0.811
20	combined	variable	False	0.502	1.746	0.385	14.438
20	sum	fixed	False	0.764	-0.059	0.506	0.411
20	sum	fixed	True	0.680	0.011	0.625	0.139
20	sum	variable	False	0.685	0.055	0.855	0.240
20	sum	variable	True	0.679	0.016	0.717	0.173

Table 36: Bounding for ESM in I-$\cap$ Beta Region with $\rho = 0.5$

Unc.	Agg.	μ and σ^2	Normal?	M_l	b_l	M_u	b_u
5	sum	fixed	False	0.536	0.323	0.704	0.362
5	sum	fixed	True	0.312	0.387	0.347	0.416
5	sum	variable	False	1.093	0.396	0.818	1.469
5	sum	variable	True	1.378	0.333	0.889	1.249
10	sum	fixed	False	0.531	0.443	0.651	0.460
10	sum	fixed	True	0.483	0.473	0.469	0.550
10	sum	variable	False	0.958	0.490	0.891	1.372
10	sum	variable	True	1.102	0.288	0.964	1.100
15	sum	fixed	False	0.612	0.515	0.646	0.596
15	sum	fixed	True	0.511	0.608	0.572	0.629
15	sum	variable	False	0.842	0.901	0.821	1.760
15	sum	variable	True	0.997	0.439	0.961	1.120
20	combined	fixed	False	0.344	0.955	0.370	1.116
20	combined	variable	False	0.486	2.323	0.512	19.925
20	sum	fixed	False	0.523	0.755	0.585	0.803
20	sum	fixed	True	0.528	0.745	0.493	0.896
20	sum	variable	False	0.868	0.903	0.864	1.772
20	sum	variable	True	0.919	0.751	0.882	1.509

Table 37: Bounding for ESM in I-$\cap$ Beta Region with $\rho = 0.75$

Unc.	Agg.	μ and σ^2	Normal?	M_l	b_l	M_u	b_u
5	sum	fixed	False	0.490	0.702	0.472	0.803
5	sum	fixed	True	0.466	0.754	0.553	0.779
5	sum	variable	False	1.327	1.006	0.986	3.050
5	sum	variable	True	2.359	0.495	1.708	1.966
10	sum	fixed	False	0.627	1.089	0.537	1.248
10	sum	fixed	True	0.601	1.131	0.589	1.200
10	sum	variable	False	1.221	1.795	1.093	3.925
10	sum	variable	True	1.786	0.817	1.530	2.522
15	sum	fixed	False	0.479	1.734	0.369	1.970
15	sum	fixed	True	0.719	1.486	0.489	1.843
15	sum	variable	False	1.317	2.289	1.234	4.634
15	sum	variable	True	1.612	1.712	1.070	5.088
20	combined	fixed	False	0.277	2.470	0.245	3.152
20	combined	variable	False	0.547	-0.108	0.575	30.486
20	sum	fixed	False	0.574	2.139	0.464	2.439
20	sum	fixed	True	0.564	2.184	0.620	2.206
20	sum	variable	False	1.326	2.962	1.293	5.428
20	sum	variable	True	1.546	2.317	1.259	5.297

Table 38: Bounding for ESM in I-$\cap$ Beta Region with $\rho = 1.0$

Unc.	Agg.	μ and σ^2	Normal?	M_l	b_l	M_u	b_u
5	sum	fixed	False	0.156	2.396	-0.100	2.537
5	sum	fixed	True	0.037	2.442	0.055	2.513
5	sum	variable	False	3.131	4.675	-1.170	12.930
5	sum	variable	True	15.569	3.355	1.813	10.457
10	sum	fixed	False	0.192	4.813	-0.091	5.042
10	sum	fixed	True	0.306	4.860	0.022	5.011
10	sum	variable	False	5.018	10.620	1.352	21.662
10	sum	variable	True	2.952	13.603	0.285	20.852
15	sum	fixed	False	0.263	7.232	0.043	7.516
15	sum	fixed	True	0.661	7.248	0.067	7.508
15	sum	variable	False	1.871	19.933	-1.016	33.059
15	sum	variable	True	4.737	19.753	1.409	28.936
20	combined	fixed	False	0.592	9.156	0.460	12.006
20	combined	variable	False	0.726	26.089	0.504	142.662
20	sum	fixed	False	0.288	9.657	0.034	10.016
20	sum	fixed	True	0.527	9.643	-0.023	10.017
20	sum	variable	False	2.783	26.802	0.274	41.889
20	sum	variable	True	4.526	27.607	0.271	40.277

Table 39: Bounding for ESM in I-J Beta Region with $\rho = 0.0$

Unc.	Agg.	μ and σ^2	Normal?	M_l	b_l	M_u	b_u
5	sum	fixed	False	0.886	0.093	0.298	0.397
5	sum	variable	False	1.084	0.090	0.641	1.164
10	sum	fixed	False	1.063	-0.028	0.882	0.125
10	sum	fixed	True	0.825	0.023	0.700	0.082
10	sum	variable	False	1.004	-0.087	0.908	0.590
15	sum	fixed	False	1.074	-0.038	0.977	0.075
15	sum	fixed	True	1.003	-0.031	0.978	0.044
15	sum	variable	False	1.088	-0.206	0.942	0.447
15	sum	variable	True	0.675	0.119	0.885	0.233
20	combined	fixed	False	0.530	0.143	0.807	0.370
20	combined	variable	False	1.012	-1.111	0.435	16.132
20	sum	fixed	False	1.101	-0.062	0.952	0.081
20	sum	fixed	True	1.094	-0.052	1.010	0.036
20	sum	variable	False	1.058	-0.181	0.972	0.401
20	sum	variable	True	0.941	-0.104	1.014	0.145

Table 40: Bounding for ESM in I-J Beta Region with $\rho = 0.25$

Unc.	Agg.	μ and σ^2	Normal?	M_l	b_l	M_u	b_u
5	sum	fixed	False	0.724	0.165	0.546	0.436
5	sum	variable	False	0.826	0.395	0.954	1.299
10	sum	fixed	False	0.462	0.171	1.425	0.008
10	sum	variable	False	0.560	0.508	1.182	0.547
15	sum	fixed	False	0.526	0.155	1.523	-0.158
15	sum	fixed	True	0.579	0.105	0.441	0.267
15	sum	variable	False	0.653	0.264	1.286	0.158
15	sum	variable	True	0.535	0.544	0.491	0.900
20	combined	fixed	False	0.493	0.226	0.399	0.936
20	combined	variable	False	0.517	2.414	0.481	18.499
20	sum	fixed	False	0.595	0.133	1.504	-0.280
20	sum	fixed	True	0.599	0.097	0.583	0.217
20	sum	variable	False	0.659	0.257	1.254	-0.108
20	sum	variable	True	0.624	0.366	0.576	0.920

Table 41: Bounding for ESM in I-J Beta Region with $\rho = 0.25$

Unc.	Agg.	μ and σ^2	Normal?	M_l	b_l	M_u	b_u
5	sum	fixed	False	0.677	0.350	0.516	0.629
5	sum	variable	False	1.129	0.547	0.693	2.534
10	sum	fixed	False	0.715	0.426	0.874	0.575
10	sum	variable	False	1.024	0.679	0.797	2.512
15	sum	fixed	False	0.445	0.782	0.783	0.751
15	sum	fixed	True	0.255	0.921	0.132	1.136
15	sum	variable	False	0.918	1.073	0.827	2.835
15	sum	variable	True	0.847	1.306	0.366	3.751
20	combined	fixed	False	0.380	0.930	0.427	1.295
20	combined	variable	False	0.519	3.078	0.421	30.643
20	sum	fixed	False	0.410	1.023	0.815	0.838
20	sum	fixed	True	0.246	1.203	0.280	1.295
20	sum	variable	False	0.814	1.750	0.870	3.038
20	sum	variable	True	0.786	1.888	0.785	2.859

Table 42: Bounding for ESM in I-J Beta Region with $\rho = 0.75$

Unc.	Agg.	μ and σ^2	Normal?	M_l	b_l	M_u	b_u
5	sum	fixed	False	0.384	0.796	0.086	1.182
5	sum	variable	False	0.977	1.560	0.473	4.759
10	sum	fixed	False	0.568	1.232	0.305	1.726
10	sum	variable	False	0.964	2.782	0.621	6.435
15	sum	fixed	False	0.591	1.735	0.263	2.419
15	sum	variable	False	1.063	3.946	0.524	8.825
20	combined	fixed	False	0.457	1.600	0.453	2.635
20	combined	variable	False	0.454	10.168	0.611	40.880
20	sum	fixed	False	0.466	2.459	0.326	3.041
20	sum	variable	False	0.979	5.790	0.767	9.825
20	sum	variable	True	0.335	8.906	0.830	9.181

Table 43: Bounding for ESM in I-J Beta Region with $\rho = 1.0$

Unc.	Agg.	μ and σ^2	Normal?	M_l	b_l	M_u	b_u
5	sum	fixed	False	0.046	2.303	0.078	2.405
5	sum	variable	False	3.153	3.761	0.193	11.678
10	sum	fixed	False	0.144	4.612	0.016	4.818
10	sum	variable	False	2.475	10.681	-0.224	21.881
15	sum	fixed	False	0.053	6.964	-0.010	7.224
15	sum	variable	False	2.378	17.813	-0.392	31.245
20	combined	fixed	False	0.803	6.261	0.573	11.043
20	combined	variable	False	0.655	12.530	0.662	134.446
20	sum	fixed	False	0.069	9.287	-0.032	9.639
20	sum	variable	False	2.516	24.451	-0.739	41.544

Table 44: Bounding for ESM in Pearson Region with $\rho = 0.0$

Unc.	Agg.	μ and σ^2	Normal?	M_l	b_l	M_u	b_u
5	sum	fixed	False	1.001	-0.014	0.774	0.192
5	sum	variable	False	1.049	-0.197	0.751	0.916
10	sum	fixed	False	1.030	-0.054	0.944	0.086
10	sum	fixed	True	1.041	-0.043	0.920	0.064
10	sum	variable	False	1.034	-0.248	0.894	0.537
15	sum	fixed	False	1.027	-0.046	0.954	0.081
15	sum	fixed	True	1.011	-0.048	0.975	0.062
15	sum	variable	False	1.039	-0.258	0.928	0.480
15	sum	variable	True	1.023	-0.211	0.964	0.261
20	combined	fixed	False	0.966	-0.111	0.767	0.377
20	combined	variable	False	1.020	-4.316	0.747	10.833
20	sum	fixed	False	1.027	-0.059	0.971	0.075
20	sum	fixed	True	1.027	-0.052	0.979	0.055
20	sum	variable	False	1.035	-0.282	0.954	0.388
20	sum	variable	True	1.027	-0.256	0.963	0.314

Table 45: Bounding for ESM in Pearson Region with $\rho = 0.25$

Unc.	Agg.	μ and σ^2	Normal?	M_l	b_l	M_u	b_u
5	sum	fixed	False	1.022	-0.028	0.691	0.352
5	sum	variable	False	1.056	-0.212	0.785	1.305
10	sum	fixed	False	0.642	0.100	0.792	0.334
10	sum	fixed	True	0.071	0.345	0.454	0.316
10	sum	variable	False	0.852	-0.141	0.794	1.375
15	sum	fixed	False	0.698	0.065	0.738	0.420
15	sum	fixed	True	0.517	0.179	0.397	0.497
15	sum	variable	False	0.911	-0.430	0.908	1.261
15	sum	variable	True	0.242	1.402	0.803	0.637
20	combined	fixed	False	0.282	0.574	0.177	1.453
20	combined	variable	False	0.565	-0.357	0.556	21.265
20	sum	fixed	False	0.698	0.039	0.792	0.441
20	sum	fixed	True	0.511	0.211	0.580	0.442
20	sum	variable	False	0.784	-0.073	0.874	1.524
20	sum	variable	True	0.380	1.414	0.615	1.547

Table 46: Bounding for ESM in Pearson Region with $\rho = 0.5$

Unc.	Agg.	μ and σ^2	Normal?	M_l	b_l	M_u	b_u
5	sum	fixed	False	0.346	0.390	0.392	0.740
5	sum	variable	False	0.910	0.400	0.487	2.976
10	sum	fixed	False	0.237	0.704	0.379	1.025
10	sum	variable	False	0.509	1.539	0.400	3.982
15	sum	fixed	False	0.105	1.121	0.276	1.465
15	sum	variable	False	0.399	2.620	0.152	6.121
20	combined	fixed	False	0.211	1.500	0.185	2.488
20	combined	variable	False	0.318	9.065	0.281	40.629
20	sum	fixed	False	0.190	1.336	0.188	1.900
20	sum	variable	False	0.308	3.962	0.210	7.120
20	sum	variable	True	-0.138	5.548	-0.099	6.844

Table 47: Bounding for ESM in Pearson Region with $\rho = 0.75$

Unc.	Agg.	μ and σ^2	Normal?	M_l	b_l	M_u	b_u
5	sum	fixed	False	0.929	0.458	0.379	1.215
5	sum	variable	False	1.199	0.845	0.498	4.989
10	sum	fixed	False	0.164	1.430	-0.169	2.355
10	sum	variable	False	0.552	3.811	0.255	8.365
15	sum	fixed	False	0.058	2.277	-0.042	3.150
15	sum	variable	False	0.452	5.935	0.155	11.760
20	combined	fixed	False	0.305	2.073	0.171	4.906
20	combined	variable	False	0.358	10.769	0.282	67.771
20	sum	fixed	False	0.083	3.012	-0.063	4.130
20	sum	variable	False	0.332	8.675	0.161	14.987

Table 48: Bounding for ESM in Pearson Region with $\rho = 1.0$

Unc.	Agg.	μ and σ^2	Normal?	M_l	b_l	M_u	b_u
5	sum	fixed	False	0.305	2.051	0.046	2.565
5	sum	variable	False	1.057	4.259	-0.202	12.460
10	sum	fixed	False	0.302	4.364	-0.021	5.156
10	sum	variable	False	1.343	10.810	0.194	21.760
15	sum	fixed	False	0.221	6.787	-0.145	7.780
15	sum	variable	False	1.119	18.607	-0.139	32.310
20	combined	fixed	False	0.194	9.863	0.060	14.810
20	combined	variable	False	0.380	37.937	0.194	178.545
20	sum	fixed	False	0.464	8.992	0.128	10.124
20	sum	variable	False	0.868	26.272	-0.281	42.813

Table 49: Bounding for ESM in Pearson Region without Pearson IV with $\rho = 0.0$

Unc.	Agg.	μ and σ^2	Normal?	M_l	b_l	M_u	b_u
5	sum	fixed	False	0.979	0.020	0.755	0.294
5	sum	variable	False	0.993	0.032	0.817	1.027
10	sum	fixed	False	0.996	-0.019	0.913	0.114
10	sum	fixed	True	0.960	-0.004	0.938	0.073
10	sum	variable	False	1.001	-0.091	0.879	0.686
10	sum	variable	True	0.966	-0.040	0.902	0.433
15	sum	fixed	False	1.006	-0.029	0.945	0.100
15	sum	fixed	True	0.995	-0.026	0.972	0.067
15	sum	variable	False	0.978	-0.033	0.926	0.550
15	sum	variable	True	1.004	-0.179	0.957	0.365
20	combined	fixed	False	0.940	0.062	0.774	0.529
20	combined	variable	False	0.953	-0.690	0.699	16.462
20	sum	fixed	False	0.991	-0.025	0.970	0.090
20	sum	fixed	True	0.968	-0.008	0.977	0.063
20	sum	variable	False	0.992	-0.095	0.954	0.449
20	sum	variable	True	0.985	-0.107	0.975	0.320

Table 50: Bounding for ESM in Pearson Region without Pearson IV with $\rho = 0.25$

Unc.	Agg.	μ and σ^2	Normal?	M_l	b_l	M_u	b_u
5	sum	fixed	False	0.980	0.064	0.673	0.450
5	sum	variable	False	1.003	0.148	0.691	1.917
10	sum	fixed	False	0.947	0.036	0.678	0.478
10	sum	fixed	True	0.899	0.041	0.590	0.371
10	sum	variable	False	1.007	-0.074	0.744	1.862
15	sum	fixed	False	0.968	0.012	0.771	0.519
15	sum	fixed	True	0.928	0.053	0.687	0.450
15	sum	variable	False	0.824	0.297	0.739	2.185
15	sum	variable	True	0.834	0.416	0.679	1.620
20	combined	fixed	False	0.291	0.584	0.244	1.610
20	combined	variable	False	0.864	-1.276	0.593	24.442
20	sum	fixed	False	0.948	0.031	0.801	0.568
20	sum	fixed	True	0.859	0.095	0.702	0.503
20	sum	variable	False	0.895	0.180	0.736	2.544
20	sum	variable	True	0.975	-0.003	0.640	2.249

Table 51: Bounding for ESM in Pearson Region without Pearson IV with $\rho = 0.75$

Unc.	Agg.	μ and σ^2	Normal?	M_l	b_l	M_u	b_u
5	sum	fixed	False	0.914	0.482	0.446	1.272
5	sum	variable	False	0.936	1.393	0.289	5.829
10	sum	fixed	False	0.732	1.045	0.222	2.199
10	sum	variable	False	0.921	3.078	0.324	9.089
15	sum	fixed	False	0.713	1.638	0.255	3.048
15	sum	variable	False	1.066	4.095	0.257	12.467
20	combined	fixed	False	0.416	1.887	0.326	4.702
20	combined	variable	False	0.519	10.183	0.344	76.307
20	sum	fixed	False	0.617	2.363	0.142	3.962
20	sum	variable	False	0.821	6.756	0.206	15.619

Table 52: Bounding for ESM in Pearson Region without Pearson IV with $\rho = 1.0$

Unc.	Agg.	μ and σ^2	Normal?	M_l	b_l	M_u	b_u
5	sum	fixed	False	0.043	1.948	0.055	2.476
5	sum	variable	False	0.876	3.906	-0.067	12.117
10	sum	fixed	False	0.043	4.161	0.037	4.936
10	sum	variable	False	0.613	10.609	-0.206	21.861
15	sum	fixed	False	0.004	6.378	-0.030	7.396
15	sum	variable	False	0.515	17.428	-0.195	31.452
20	combined	fixed	False	0.865	6.543	0.580	12.035
20	combined	variable	False	0.692	19.719	0.496	156.212
20	sum	fixed	False	-0.072	8.692	0.011	9.747
20	sum	variable	False	0.365	25.434	-0.140	40.735

Table 53: Bounding for ESM in I-∪ Beta Region with $\rho = 0.0$

Unc.	Agg.	μ and σ^2	Normal?	M_l	b_l	M_u	b_u
5	sum	fixed	False	0.957	0.050	0.708	0.461
5	sum	variable	False	0.984	0.049	0.821	1.376
10	sum	fixed	False	0.980	0.009	0.892	0.272
10	sum	fixed	True	0.960	0.018	0.803	0.309
10	sum	variable	False	0.983	-0.057	0.955	0.557
10	sum	variable	True	0.984	-0.123	0.914	0.483
15	sum	fixed	False	0.979	-0.007	0.972	0.148
15	sum	fixed	True	0.993	-0.004	0.861	0.261
15	sum	variable	False	0.991	-0.118	0.974	0.452
15	sum	variable	True	0.993	-0.162	0.981	0.367
20	combined	fixed	False	0.955	0.035	0.930	0.363
20	combined	variable	False	0.894	-0.595	0.834	13.973
20	sum	fixed	False	0.988	-0.032	0.979	0.139
20	sum	fixed	True	0.991	-0.018	0.943	0.158
20	sum	variable	False	0.988	-0.123	0.982	0.442
20	sum	variable	True	0.965	-0.014	1.024	0.180

Table 54: Bounding for ESM in I-∪ Beta Region with $\rho = 0.25$

Unc.	Agg.	μ and σ^2	Normal?	M_l	b_l	M_u	b_u
5	sum	fixed	False	0.923	0.110	0.703	0.574
5	sum	variable	False	0.987	0.150	0.815	1.944
10	sum	fixed	False	0.953	0.082	0.859	0.440
10	sum	fixed	True	0.787	0.254	0.713	0.478
10	sum	variable	False	0.979	0.093	0.867	1.719
15	sum	fixed	False	0.951	0.088	0.882	0.454
15	sum	fixed	True	0.894	0.239	0.840	0.480
15	sum	variable	False	0.963	0.211	0.895	1.730
15	sum	variable	True	0.896	0.683	0.945	1.475
20	combined	fixed	False	0.899	0.189	0.844	1.004
20	combined	variable	False	0.916	-2.571	0.802	20.921
20	sum	fixed	False	0.948	0.116	0.875	0.546
20	sum	fixed	True	0.837	0.334	0.906	0.501
20	sum	variable	False	0.959	0.321	0.887	2.071
20	sum	variable	True	0.893	0.951	0.841	2.072

Table 55: Bounding for ESM in I-∪ Beta Region with $\rho = 0.5$

Unc.	Agg.	μ and σ^2	Normal?	M_l	b_l	M_u	b_u
5	sum	fixed	False	0.905	0.182	0.661	0.828
5	sum	variable	False	0.975	0.299	0.662	3.422
10	sum	fixed	False	0.929	0.269	0.703	1.055
10	sum	variable	False	0.970	0.542	0.781	3.930
15	sum	fixed	False	0.883	0.445	0.751	1.244
15	sum	variable	False	0.928	1.130	0.780	4.685
20	combined	fixed	False	0.895	0.478	0.722	2.183
20	combined	variable	False	1.049	-4.965	0.733	41.565
20	sum	fixed	False	0.902	0.544	0.749	1.537
20	sum	variable	False	0.916	1.666	0.758	5.962

Table 56: Bounding for ESM in I-∪ Beta Region with $\rho = 0.75$

Unc.	Agg.	μ and σ^2	Normal?	M_l	b_l	M_u	b_u
5	sum	fixed	False	0.846	0.316	0.552	1.301
5	sum	variable	False	0.974	0.584	0.637	5.132
10	sum	fixed	False	0.970	0.491	0.663	1.900
10	sum	variable	False	0.995	1.391	0.817	6.736
15	sum	fixed	False	0.852	1.037	0.737	2.378
15	sum	variable	False	0.904	2.798	0.898	8.758
20	combined	fixed	False	0.966	0.751	0.856	3.527
20	combined	variable	False	1.126	-1.689	0.684	73.092
20	sum	fixed	False	0.858	1.440	0.861	2.829
20	sum	variable	False	0.997	3.399	0.806	11.635

Table 57: Bounding for ESM in I-∪ Beta Region with $\rho = 1.0$

Unc.	Agg.	μ and σ^2	Normal?	M_l	b_l	M_u	b_u
5	sum	fixed	False	0.450	1.213	0.285	2.162
5	sum	variable	False	0.892	1.779	0.531	8.219
10	sum	fixed	False	0.551	2.494	0.259	4.256
10	sum	variable	False	0.877	5.386	0.560	14.935
15	sum	fixed	False	0.759	3.345	0.497	5.464
15	sum	variable	False	1.025	7.518	0.769	19.492
20	combined	fixed	False	1.056	2.233	0.957	7.606
20	combined	variable	False	1.156	-1.955	1.208	73.565
20	sum	fixed	False	0.549	5.459	0.357	7.815
20	sum	variable	False	1.009	11.441	0.973	22.328

Table 58: Bounding for HB in I-$\cap$ Beta Region with $\rho = 0.0$

Unc.	Agg.	μ and σ^2	Normal?	M_l	b_l	M_u	b_u
5	sum	fixed	False	0.625	0.142	-0.828	0.327
5	sum	fixed	True	0.026	0.153	-1.398	0.286
5	sum	variable	False	1.713	0.283	-0.188	1.097
5	sum	variable	True	1.206	0.359	-0.522	0.869
10	sum	fixed	False	0.582	0.044	-0.684	0.213
10	sum	fixed	True	0.427	0.047	-0.843	0.200
10	sum	variable	False	0.494	0.127	-0.103	0.495
10	sum	variable	True	0.659	0.114	0.305	0.310
15	sum	fixed	False	0.357	0.044	-0.074	0.136
15	sum	fixed	True	0.690	0.032	-0.278	0.145
15	sum	variable	False	0.614	0.109	-0.077	0.470
15	sum	variable	True	0.709	0.096	0.110	0.380
20	combined	fixed	False	0.429	0.070	-0.151	0.264
20	combined	variable	False	0.671	0.868	-1.045	11.362
20	sum	fixed	False	0.415	0.045	0.369	0.097
20	sum	fixed	True	0.590	0.036	0.189	0.107
20	sum	variable	False	0.573	0.126	0.043	0.459
20	sum	variable	True	0.503	0.137	0.230	0.407

Table 59: Bounding for HB in I-$\cap$ Beta Region with $\rho = 0.25$

Unc.	Agg.	μ and σ^2	Normal?	M_l	b_l	M_u	b_u
5	sum	fixed	False	0.371	0.198	0.500	0.280
5	sum	fixed	True	0.666	0.135	0.681	0.205
5	sum	variable	False	1.121	0.077	0.500	1.129
5	sum	variable	True	1.308	0.016	1.023	0.525
10	sum	fixed	False	0.612	0.141	0.862	0.089
10	sum	fixed	True	0.661	0.137	0.873	0.085
10	sum	variable	False	0.821	0.039	1.004	0.087
10	sum	variable	True	0.932	-0.034	1.019	0.026
15	sum	fixed	False	0.740	0.134	0.873	0.104
15	sum	fixed	True	0.942	-0.020	0.965	0.029
15	sum	variable	False	0.915	-0.112	1.008	-0.015
15	sum	variable	True	0.937	-0.089	0.934	0.220
20	combined	fixed	False	0.254	0.645	0.263	0.817
20	combined	variable	False	0.558	2.626	0.458	11.097
20	sum	fixed	False	0.775	0.162	0.759	0.274
20	sum	fixed	True	0.787	0.167	0.868	0.155
20	sum	variable	False	0.897	-0.004	1.035	-0.140
20	sum	variable	True	0.982	-0.275	0.914	0.335

Table 60: Bounding for HB in I-$\cap$ Beta Region with $\rho = 0.5$

Unc.	Agg.	μ and σ^2	Normal?	M_l	b_l	M_u	b_u
5	sum	fixed	False	0.622	0.229	1.121	0.175
5	sum	fixed	True	0.648	0.234	1.096	0.134
5	sum	variable	False	1.238	0.042	1.015	1.043
5	sum	variable	True	1.407	-0.023	0.845	1.014
10	sum	fixed	False	0.524	0.362	0.699	0.366
10	sum	fixed	True	0.831	0.157	1.173	-0.025
10	sum	variable	False	1.021	-0.172	1.105	0.237
10	sum	variable	True	0.983	0.175	1.075	0.265
15	sum	fixed	False	0.621	0.437	0.329	0.985
15	sum	fixed	True	1.172	-0.220	0.970	0.152
15	sum	variable	False	0.934	0.107	1.036	0.366
15	sum	variable	True	0.988	0.051	1.047	0.251
20	combined	fixed	False	0.131	1.759	0.064	2.384
20	combined	variable	False	0.520	3.596	0.538	14.154
20	sum	fixed	False	0.517	0.793	0.427	1.152
20	sum	fixed	True	1.043	-0.097	1.109	-0.056
20	sum	variable	False	0.980	-0.058	1.007	0.531
20	sum	variable	True	1.009	-0.118	1.031	0.340

Table 61: Bounding for HB in I-∩ Beta Region with $\rho = 0.75$

Unc.	Agg.	μ and σ^2	Normal?	M_l	b_l	M_u	b_u
5	sum	fixed	False	0.584	0.665	0.591	0.765
5	sum	fixed	True	0.459	0.733	0.637	0.704
5	sum	variable	False	2.049	0.145	1.877	1.413
5	sum	variable	True	2.293	0.030	1.879	1.235
10	sum	fixed	False	0.543	0.948	0.526	1.134
10	sum	fixed	True	0.600	0.910	0.377	1.240
10	sum	variable	False	1.511	0.125	1.619	0.696
10	sum	variable	True	1.467	0.341	1.526	0.794
15	sum	fixed	False	0.410	1.513	0.234	1.989
15	sum	fixed	True	0.606	1.243	1.096	0.658
15	sum	variable	False	1.487	-0.339	1.503	0.636
15	sum	variable	True	1.232	1.146	1.432	0.815
20	combined	fixed	False	0.094	3.434	-0.014	4.753
20	combined	variable	False	0.462	7.846	0.585	23.443
20	sum	fixed	False	0.608	1.564	0.357	2.339
20	sum	fixed	True	0.407	2.002	0.955	1.058
20	sum	variable	False	1.359	0.092	1.471	0.528
20	sum	variable	True	1.372	0.138	1.360	1.107

Table 62: Bounding for HB in I-$\cap$ Beta Region with $\rho = 1.0$

Unc.	Agg.	μ and σ^2	Normal?	M_l	b_l	M_u	b_u
5	sum	fixed	False	0.187	2.786	-0.617	2.970
5	sum	fixed	True	0.567	2.808	-0.558	2.934
5	sum	variable	False	9.027	5.589	1.538	14.020
5	sum	variable	True	20.769	4.371	0.507	12.557
10	sum	fixed	False	0.298	5.605	-0.294	5.873
10	sum	fixed	True	0.666	5.615	0.017	5.804
10	sum	variable	False	8.766	12.710	1.624	25.453
10	sum	variable	True	7.261	15.405	1.180	24.342
15	sum	fixed	False	0.240	8.429	-0.110	8.782
15	sum	fixed	True	0.188	8.484	-0.359	8.739
15	sum	variable	False	7.534	21.647	0.026	37.622
15	sum	variable	True	14.151	20.016	1.348	33.833
20	combined	fixed	False	0.267	12.572	0.128	15.924
20	combined	variable	False	1.009	57.117	-0.045	204.014
20	sum	fixed	False	0.229	11.255	-0.096	11.682
20	sum	fixed	True	0.243	11.290	-0.318	11.634
20	sum	variable	False	5.729	30.834	-0.430	49.171
20	sum	variable	True	6.630	30.785	-2.773	49.319

Table 63: Bounding for HB in I-J Beta Region with $\rho = 0.0$

Unc.	Agg.	μ and σ^2	Normal?	M_l	b_l	M_u	b_u
5	sum	fixed	False	1.648	0.171	0.728	0.497
5	sum	variable	False	1.339	0.345	0.543	1.625
10	sum	fixed	False	1.298	0.048	0.937	0.279
10	sum	fixed	True	1.159	0.067	1.287	0.168
10	sum	variable	False	1.133	0.080	0.683	0.724
15	sum	fixed	False	0.997	0.031	0.881	0.151
15	sum	fixed	True	0.846	0.047	0.958	0.123
15	sum	variable	False	1.055	0.064	0.665	0.618
15	sum	variable	True	0.986	0.117	0.491	0.524
20	combined	fixed	False	0.802	0.177	0.473	0.492
20	combined	variable	False	1.117	1.106	0.435	14.136
20	sum	fixed	False	0.937	0.032	0.691	0.124
20	sum	fixed	True	0.866	0.035	0.718	0.112
20	sum	variable	False	1.017	0.073	0.667	0.591
20	sum	variable	True	0.914	0.126	0.814	0.390

Table 64: Bounding for HB in I-J Beta Region with $\rho = 0.25$

Unc.	Agg.	μ and σ^2	Normal?	M_l	b_l	M_u	b_u
5	sum	fixed	False	-0.122	0.357	-0.813	0.702
5	sum	variable	False	0.513	0.610	-0.297	2.313
10	sum	fixed	False	0.383	0.203	-0.075	0.502
10	sum	variable	False	0.585	0.236	0.407	0.875
15	sum	fixed	False	0.736	0.043	0.802	0.080
15	sum	fixed	True	0.867	-0.026	0.798	0.080
15	sum	variable	False	0.726	0.017	0.816	0.207
15	sum	variable	True	0.830	-0.047	0.902	0.081
20	combined	fixed	False	0.244	0.424	0.218	0.724
20	combined	variable	False	0.495	3.160	-0.003	21.858
20	sum	fixed	False	0.834	-0.028	0.938	-0.021
20	sum	fixed	True	0.957	-0.118	1.014	-0.085
20	sum	variable	False	0.933	-0.536	0.918	-0.046
20	sum	variable	True	0.895	-0.243	0.948	-0.107

Table 65: Bounding for HB in I-J Beta Region with $\rho = 0.5$

Unc.	Agg.	μ and σ^2	Normal?	M_l	b_l	M_u	b_u
5	sum	fixed	False	-0.056	0.485	-0.405	0.783
5	sum	variable	False	0.583	0.786	-0.043	2.904
10	sum	fixed	False	0.453	0.267	0.408	0.423
10	sum	variable	False	0.722	0.166	0.591	1.125
15	sum	fixed	False	0.729	0.055	0.760	0.194
15	sum	fixed	True	0.833	0.035	1.075	-0.100
15	sum	variable	False	0.760	-0.077	0.935	0.162
15	sum	variable	True	1.066	-0.691	0.848	0.569
20	combined	fixed	False	0.236	0.751	0.160	1.614
20	combined	variable	False	0.405	5.439	0.209	29.208
20	sum	fixed	False	0.848	-0.086	0.984	-0.058
20	sum	fixed	True	1.021	-0.226	0.796	0.190
20	sum	variable	False	0.807	-0.263	0.897	0.289
20	sum	variable	True	0.758	0.471	1.055	-0.390

Table 66: Bounding for HB in I-J Beta Region with $\rho = 0.75$

Unc.	Agg.	μ and σ^2	Normal?	M_l	b_l	M_u	b_u
5	sum	fixed	False	0.067	0.816	-0.004	0.952
5	sum	variable	False	1.112	1.267	0.134	4.347
10	sum	fixed	False	0.403	0.810	0.561	0.859
10	sum	variable	False	0.998	1.196	0.722	3.313
15	sum	fixed	False	0.563	0.854	0.735	0.868
15	sum	variable	False	0.958	1.313	0.877	2.975
20	combined	fixed	False	0.345	1.349	0.151	3.416
20	combined	variable	False	0.398	9.435	0.412	38.552
20	sum	fixed	False	0.605	0.993	0.852	0.852
20	sum	variable	False	0.918	1.694	1.081	2.139
20	sum	variable	True	1.139	0.688	0.981	2.457

Table 67: Bounding for HB in I-J Beta Region with $\rho = 1.0$

Unc.	Agg.	μ and σ^2	Normal?	M_l	b_l	M_u	b_u
5	sum	fixed	False	-0.154	2.398	-0.544	2.669
5	sum	variable	False	2.715	4.803	-1.352	12.993
10	sum	fixed	False	-0.171	4.822	-0.607	5.194
10	sum	variable	False	3.197	11.532	-1.151	23.279
15	sum	fixed	False	-0.251	7.277	-0.370	7.670
15	sum	variable	False	3.498	18.801	-0.660	32.973
20	combined	fixed	False	0.162	10.609	0.076	15.384
20	combined	variable	False	0.707	31.593	-0.010	199.925
20	sum	fixed	False	-0.260	9.709	-0.179	10.165
20	sum	variable	False	3.764	25.807	-0.052	42.523

Table 68: Bounding for HB in Pearson Region with $\rho = 0.0$

Unc.	Agg.	μ and σ^2	Normal?	M_l	b_l	M_u	b_u
5	sum	fixed	False	0.840	0.062	0.542	0.252
5	sum	variable	False	0.860	0.133	0.551	1.018
10	sum	fixed	False	0.986	-0.027	0.886	0.078
10	sum	fixed	True	1.007	-0.017	0.928	0.059
10	sum	variable	False	0.970	-0.140	0.836	0.482
15	sum	fixed	False	0.995	-0.028	0.919	0.064
15	sum	fixed	True	1.006	-0.027	0.953	0.048
15	sum	variable	False	0.984	-0.165	0.899	0.385
15	sum	variable	True	0.898	-0.028	0.947	0.208
20	combined	fixed	False	0.502	0.087	0.665	0.321
20	combined	variable	False	0.924	-2.009	0.591	10.214
20	sum	fixed	False	1.001	-0.026	0.929	0.068
20	sum	fixed	True	1.013	-0.029	0.946	0.059
20	sum	variable	False	0.998	-0.157	0.908	0.362
20	sum	variable	True	1.012	-0.129	0.925	0.269

Table 69: Bounding for HB in Pearson Region with $\rho = 0.25$

Unc.	Agg.	μ and σ^2	Normal?	M_l	b_l	M_u	b_u
5	sum	fixed	False	0.710	0.085	0.580	0.302
5	sum	variable	False	0.756	0.148	0.645	1.243
10	sum	fixed	False	0.771	-0.042	0.525	0.295
10	sum	fixed	True	0.571	0.103	0.643	0.144
10	sum	variable	False	0.685	-0.006	0.674	0.845
15	sum	fixed	False	0.787	-0.053	0.648	0.260
15	sum	fixed	True	0.714	0.050	0.856	0.032
15	sum	variable	False	0.776	-0.216	0.672	1.108
15	sum	variable	True	0.740	-0.031	0.793	0.354
20	combined	fixed	False	0.345	0.203	0.374	0.658
20	combined	variable	False	0.444	1.984	0.385	15.060
20	sum	fixed	False	0.856	-0.138	0.645	0.319
20	sum	fixed	True	0.888	-0.126	0.940	-0.054
20	sum	variable	False	0.837	-0.451	0.694	1.139
20	sum	variable	True	0.940	-0.738	0.790	0.506

Table 70: Bounding for HB in Pearson Region with $\rho = 0.5$

Unc.	Agg.	μ and σ^2	Normal?	M_l	b_l	M_u	b_u
5	sum	fixed	False	0.704	0.105	0.542	0.407
5	sum	variable	False	0.713	0.296	0.380	2.166
10	sum	fixed	False	0.450	0.162	0.342	0.538
10	sum	variable	False	0.567	0.264	0.359	2.005
15	sum	fixed	False	0.723	-0.079	0.418	0.627
15	sum	variable	False	0.643	-0.064	0.472	2.174
20	combined	fixed	False	0.259	0.536	0.250	1.344
20	combined	variable	False	0.325	5.453	0.287	26.142
20	sum	fixed	False	0.676	-0.029	0.570	0.499
20	sum	variable	False	0.616	0.152	0.421	2.890
20	sum	variable	True	0.822	-0.487	0.755	0.449

Table 71: Bounding for HB in Pearson Region with $\rho = 0.75$

Unc.	Agg.	μ and σ^2	Normal?	M_l	b_l	M_u	b_u
5	sum	fixed	False	0.266	0.516	0.182	0.833
5	sum	variable	False	0.487	1.321	0.368	3.421
10	sum	fixed	False	0.368	0.525	0.235	0.978
10	sum	variable	False	0.419	1.647	0.370	3.704
15	sum	fixed	False	0.319	0.771	0.338	1.145
15	sum	variable	False	0.532	1.545	0.433	4.253
20	combined	fixed	False	0.253	1.402	0.163	2.937
20	combined	variable	False	0.283	9.940	0.276	41.059
20	sum	fixed	False	0.394	0.865	0.426	1.257
20	sum	variable	False	0.522	2.010	0.532	4.234

Table 72: Bounding for HB in Pearson Region with $\rho = 1.0$

Unc.	Agg.	μ and σ^2	Normal?	M_l	b_l	M_u	b_u
5	sum	fixed	False	-0.408	1.761	-0.982	2.825
5	sum	variable	False	0.867	3.645	-1.097	12.953
10	sum	fixed	False	0.166	3.237	-1.267	5.590
10	sum	variable	False	0.891	8.880	-0.639	21.966
15	sum	fixed	False	-0.133	5.392	-1.128	8.099
15	sum	variable	False	0.531	14.968	-1.157	33.099
20	combined	fixed	False	0.234	8.673	0.037	14.471
20	combined	variable	False	0.435	26.607	0.056	175.686
20	sum	fixed	False	-0.539	7.753	-0.662	10.241
20	sum	variable	False	0.287	21.498	-0.990	42.376

Table 73: Bounding for HB in Pearson Region without Pearson IV with $\rho = 0.0$

Unc.	Agg.	μ and σ^2	Normal?	M_l	b_l	M_u	b_u
5	sum	fixed	False	0.824	0.086	0.403	0.411
5	sum	variable	False	0.901	0.151	0.642	1.362
10	sum	fixed	False	0.981	-0.019	0.864	0.117
10	sum	fixed	True	0.898	0.007	0.884	0.083
10	sum	variable	False	0.950	-0.126	0.858	0.488
10	sum	variable	True	1.002	-0.097	0.908	0.308
15	sum	fixed	False	1.000	-0.028	0.946	0.065
15	sum	fixed	True	1.011	-0.029	0.950	0.058
15	sum	variable	False	1.010	-0.198	0.919	0.361
15	sum	variable	True	0.952	-0.036	0.985	0.226
20	combined	fixed	False	0.843	-0.037	0.720	0.307
20	combined	variable	False	0.801	-0.908	0.564	12.806
20	sum	fixed	False	0.981	-0.020	0.984	0.050
20	sum	fixed	True	0.996	-0.022	0.979	0.042
20	sum	variable	False	1.009	-0.172	0.950	0.300
20	sum	variable	True	0.999	-0.124	0.958	0.233

Table 74: Bounding for HB in Pearson Region without Pearson IV with $\rho = 0.25$

Unc.	Agg.	μ and σ^2	Normal?	M_l	b_l	M_u	b_u
5	sum	fixed	False	0.579	0.174	0.289	0.508
5	sum	variable	False	0.764	0.349	0.447	1.888
10	sum	fixed	False	0.694	0.065	0.765	0.203
10	sum	fixed	True	0.943	-0.042	0.748	0.160
10	sum	variable	False	0.779	-0.035	0.932	0.550
15	sum	fixed	False	0.820	-0.020	0.932	0.097
15	sum	fixed	True	0.930	-0.075	0.947	0.028
15	sum	variable	False	0.550	0.632	0.516	1.540
15	sum	variable	True	0.977	-0.390	0.852	0.427
20	combined	fixed	False	0.449	0.099	0.537	0.519
20	combined	variable	False	0.519	1.607	0.393	15.523
20	sum	fixed	False	0.953	-0.143	0.862	0.157
20	sum	fixed	True	0.988	-0.145	0.868	0.125
20	sum	variable	False	0.680	0.454	0.611	1.619
20	sum	variable	True	0.895	-0.188	0.816	0.692

Table 75: Bounding for HB in Pearson Region without Pearson IV with $\rho = 0.5$

Unc.	Agg.	μ and σ^2	Normal?	M_l	b_l	M_u	b_u
5	sum	fixed	False	0.380	0.318	0.338	0.604
5	sum	variable	False	0.578	0.608	0.481	2.293
10	sum	fixed	False	0.594	0.155	0.648	0.377
10	sum	fixed	True	0.776	0.085	0.698	0.270
10	sum	variable	False	0.664	0.288	0.717	1.295
15	sum	fixed	False	0.762	-0.011	0.680	0.427
15	sum	fixed	True	1.016	-0.203	0.802	0.227
15	sum	variable	False	0.775	-0.180	0.704	1.666
15	sum	variable	True	0.851	0.006	0.946	0.269
20	combined	fixed	False	0.393	0.226	0.355	1.205
20	combined	variable	False	0.516	1.157	0.360	24.579
20	sum	fixed	False	0.857	-0.119	0.822	0.279
20	sum	fixed	True	0.906	-0.150	1.012	-0.040
20	sum	variable	False	0.775	-0.017	0.767	1.556
20	sum	variable	True	0.978	-0.865	0.917	0.617

Table 76: Bounding for HB in Pearson Region without Pearson IV with $\rho = 0.75$

Unc.	Agg.	μ and σ^2	Normal?	M_l	b_l	M_u	b_u
5	sum	fixed	False	0.177	0.596	0.204	0.892
5	sum	variable	False	0.587	1.100	0.170	4.044
10	sum	fixed	False	0.419	0.498	0.563	0.833
10	sum	variable	False	0.535	1.347	0.467	3.906
15	sum	fixed	False	0.635	0.301	0.589	0.956
15	sum	variable	False	0.642	0.961	0.533	4.201
20	combined	fixed	False	0.296	0.998	0.317	2.512
20	combined	variable	False	0.427	5.846	0.289	41.892
20	sum	fixed	False	0.660	0.375	0.684	1.025
20	sum	variable	False	0.666	1.071	0.700	3.892

Table 77: Bounding for HB in Pearson Region without Pearson IV with $\rho = 1.0$

Unc.	Agg.	μ and σ^2	Normal?	M_l	b_l	M_u	b_u
5	sum	fixed	False	0.242	1.253	-1.079	2.766
5	sum	variable	False	0.863	2.788	-0.956	12.194
10	sum	fixed	False	0.144	2.606	-1.420	5.424
10	sum	variable	False	0.251	8.155	-1.239	21.466
15	sum	fixed	False	-0.005	4.053	-1.445	7.913
15	sum	variable	False	0.175	12.881	-1.251	30.943
20	combined	fixed	False	0.375	5.557	-0.114	13.426
20	combined	variable	False	0.584	22.179	0.062	158.151
20	sum	fixed	False	-0.291	5.936	-1.451	10.349
20	sum	variable	False	0.232	17.422	-1.140	39.006

Table 78: Bounding for HB in I-∪ Beta Region with $\rho = 0.0$

Unc.	Agg.	μ and σ^2	Normal?	M_l	b_l	M_u	b_u
5	sum	fixed	False	0.867	0.066	0.547	0.423
5	sum	variable	False	0.817	0.089	0.759	1.148
10	sum	fixed	False	0.950	-0.022	0.847	0.178
10	sum	fixed	True	0.998	-0.033	0.891	0.132
10	sum	variable	False	0.975	-0.291	0.927	0.468
10	sum	variable	True	1.094	-0.426	0.980	0.185
15	sum	fixed	False	0.996	-0.059	0.982	0.061
15	sum	fixed	True	1.005	-0.046	0.986	0.054
15	sum	variable	False	0.987	-0.317	0.948	0.460
15	sum	variable	True	0.987	-0.213	1.006	0.171
20	combined	fixed	False	0.782	-0.026	0.930	0.173
20	combined	variable	False	0.875	-4.788	0.784	9.223
20	sum	fixed	False	1.006	-0.068	0.985	0.064
20	sum	fixed	True	1.008	-0.057	0.995	0.047
20	sum	variable	False	1.008	-0.328	0.980	0.308
20	sum	variable	True	0.983	-0.186	0.998	0.196

Table 79: Bounding for HB in I-∪ Beta Region with $\rho = 0.25$

Unc.	Agg.	μ and σ^2	Normal?	M_l	b_l	M_u	b_u
5	sum	fixed	False	0.717	0.158	0.558	0.473
5	sum	variable	False	0.700	0.312	0.608	1.710
10	sum	fixed	False	0.801	0.026	0.802	0.300
10	sum	fixed	True	0.886	-0.022	0.807	0.198
10	sum	variable	False	0.850	-0.232	0.889	0.902
15	sum	fixed	False	0.818	-0.030	0.834	0.306
15	sum	fixed	True	0.770	0.093	0.912	0.121
15	sum	variable	False	0.829	-0.215	0.840	1.183
15	sum	variable	True	0.984	-0.806	0.827	0.786
20	combined	fixed	False	0.531	0.117	0.477	0.980
20	combined	variable	False	0.498	2.283	0.512	17.603
20	sum	fixed	False	0.951	-0.187	0.899	0.270
20	sum	fixed	True	0.843	0.005	0.945	0.091
20	sum	variable	False	0.814	-0.123	0.926	0.880
20	sum	variable	True	0.839	-0.017	0.896	0.722

Table 80: Bounding for HB in I-∪ Beta Region with $\rho = 0.5$

Unc.	Agg.	μ and σ^2	Normal?	M_l	b_l	M_u	b_u
5	sum	fixed	False	0.580	0.245	0.461	0.674
5	sum	variable	False	0.615	0.536	0.466	2.742
10	sum	fixed	False	0.656	0.168	0.541	0.714
10	sum	variable	False	0.654	0.434	0.544	2.933
15	sum	fixed	False	0.535	0.336	0.589	0.811
15	sum	variable	False	0.688	0.411	0.568	3.286
20	combined	fixed	False	0.413	0.496	0.324	1.785
20	combined	variable	False	0.489	2.896	0.428	27.896
20	sum	fixed	False	0.664	0.211	0.583	0.970
20	sum	variable	False	0.465	1.980	0.637	3.555

Table 81: Bounding for HB in I-∪ Beta Region with $\rho = 0.75$

Unc.	Agg.	μ and σ^2	Normal?	M_l	b_l	M_u	b_u
5	sum	fixed	False	0.481	0.397	0.115	1.215
5	sum	variable	False	0.629	0.802	0.135	5.083
10	sum	fixed	False	0.309	0.699	0.250	1.610
10	sum	variable	False	0.663	0.868	0.181	6.720
15	sum	fixed	False	0.480	0.676	0.137	2.219
15	sum	variable	False	0.560	1.909	0.146	9.138
20	combined	fixed	False	0.445	0.814	0.295	3.219
20	combined	variable	False	0.484	6.540	0.386	47.838
20	sum	fixed	False	0.379	1.087	0.221	2.622
20	sum	variable	False	0.564	2.207	0.165	10.864

Table 82: Bounding for HB in I-∪ Beta Region with $\rho = 1.0$

Unc.	Agg.	μ and σ^2	Normal?	M_l	b_l	M_u	b_u
5	sum	fixed	False	0.646	1.144	0.267	1.998
5	sum	variable	False	1.040	2.342	0.483	8.319
10	sum	fixed	False	0.529	2.737	0.217	3.976
10	sum	variable	False	0.788	7.645	0.311	16.250
15	sum	fixed	False	0.700	4.035	0.221	5.816
15	sum	variable	False	1.089	10.600	0.522	22.343
20	combined	fixed	False	0.811	3.256	0.534	8.971
20	combined	variable	False	0.789	-3.883	0.638	109.102
20	sum	fixed	False	0.563	5.802	0.217	7.696
20	sum	variable	False	0.859	16.792	0.314	30.527

Table 83: Bounding for MCS in I-$\cap$ Beta Region with $\rho = 0.0$

Unc.	Agg.	μ and σ^2	Normal?	M_l	b_l	M_u	b_u
5	sum	fixed	False	0.594	0.078	0.678	0.135
5	sum	fixed	True	0.431	0.129	0.149	0.243
5	sum	variable	False	0.646	0.086	0.722	0.235
5	sum	variable	True	0.959	-0.109	0.745	0.236
10	sum	fixed	False	0.842	0.004	0.804	0.064
10	sum	fixed	True	0.883	0.000	0.966	0.006
10	sum	variable	False	0.811	-0.064	0.805	0.182
10	sum	variable	True	0.931	-0.103	0.867	0.116
15	sum	fixed	False	0.912	-0.013	0.900	0.035
15	sum	fixed	True	0.967	-0.028	0.886	0.047
15	sum	variable	False	0.852	-0.038	0.817	0.251
15	sum	variable	True	0.931	-0.092	0.836	0.251
20	combined	fixed	False	0.647	0.137	0.664	0.232
20	combined	variable	False	0.639	0.175	0.763	2.330
20	sum	fixed	False	0.894	0.000	0.957	0.013
20	sum	fixed	True	0.970	-0.033	0.922	0.044
20	sum	variable	False	0.913	-0.111	0.874	0.200
20	sum	variable	True	0.941	-0.102	0.956	0.072

Table 84: Bounding for MCS in I-$\cap$ Beta Region with $\rho = 0.25$

Unc.	Agg.	μ and σ^2	Normal?	M_l	b_l	M_u	b_u
5	sum	fixed	False	0.571	0.116	0.471	0.238
5	sum	fixed	True	0.731	0.060	0.454	0.215
5	sum	variable	False	0.700	0.011	0.736	0.265
5	sum	variable	True	0.846	-0.066	0.900	0.026
10	sum	fixed	False	0.523	0.285	0.586	0.278
10	sum	fixed	True	0.714	0.120	0.718	0.156
10	sum	variable	False	0.751	0.089	0.808	0.228
10	sum	variable	True	0.870	-0.188	0.837	0.154
15	sum	fixed	False	0.629	0.307	0.637	0.361
15	sum	fixed	True	0.807	0.074	0.725	0.242
15	sum	variable	False	0.792	0.096	0.875	0.058
15	sum	variable	True	0.870	-0.151	0.848	0.227
20	combined	fixed	False	0.350	0.697	0.321	0.980
20	combined	variable	False	0.492	2.138	0.573	6.981
20	sum	fixed	False	0.632	0.430	0.676	0.424
20	sum	fixed	True	0.770	0.189	0.717	0.349
20	sum	variable	False	0.810	0.166	0.857	0.258
20	sum	variable	True	0.889	-0.256	0.845	0.392

Table 85: Bounding for MCS in I-$\cap$ Beta Region with $\rho = 0.5$

Unc.	Agg.	μ and σ^2	Normal?	M_l	b_l	M_u	b_u
5	sum	fixed	False	0.502	0.190	0.510	0.237
5	sum	fixed	True	0.619	0.125	0.500	0.232
5	sum	variable	False	0.628	0.181	0.721	0.349
5	sum	variable	True	0.819	-0.085	0.741	0.307
10	sum	fixed	False	0.408	0.464	0.496	0.414
10	sum	fixed	True	0.535	0.327	0.564	0.329
10	sum	variable	False	0.697	0.094	0.739	0.408
10	sum	variable	True	0.790	-0.097	0.746	0.362
15	sum	fixed	False	0.456	0.640	0.470	0.689
15	sum	fixed	True	0.475	0.629	0.530	0.572
15	sum	variable	False	0.739	0.109	0.704	0.871
15	sum	variable	True	0.762	0.120	0.811	0.130
20	combined	fixed	False	0.233	1.604	0.236	1.909
20	combined	variable	False	0.423	5.713	0.505	12.415
20	sum	fixed	False	0.472	0.839	0.485	0.898
20	sum	fixed	True	0.610	0.500	0.586	0.632
20	sum	variable	False	0.734	0.343	0.760	0.665
20	sum	variable	True	0.776	0.126	0.785	0.395

Table 86: Bounding for MCS in I-$\cap$ Beta Region with $\rho = 0.75$

Unc.	Agg.	μ and σ^2	Normal?	M_l	b_l	M_u	b_u
5	sum	fixed	False	0.464	0.324	0.455	0.398
5	sum	fixed	True	0.378	0.380	0.492	0.336
5	sum	variable	False	0.727	0.219	0.656	1.078
5	sum	variable	True	0.845	0.105	0.719	0.863
10	sum	fixed	False	0.311	0.726	0.288	0.842
10	sum	fixed	True	0.299	0.767	0.467	0.563
10	sum	variable	False	0.682	0.280	0.729	0.811
10	sum	variable	True	0.773	0.079	0.795	0.310
15	sum	fixed	False	0.263	1.207	0.200	1.461
15	sum	fixed	True	0.330	1.088	0.340	1.140
15	sum	variable	False	0.734	0.147	0.755	0.834
15	sum	variable	True	0.790	-0.043	0.719	1.012
20	combined	fixed	False	0.145	2.959	0.105	3.856
20	combined	variable	False	0.422	4.363	0.393	26.936
20	sum	fixed	False	0.288	1.554	0.291	1.680
20	sum	fixed	True	0.384	1.296	0.493	1.043
20	sum	variable	False	0.708	0.566	0.801	0.574
20	sum	variable	True	0.760	0.299	0.785	0.628

Table 87: Bounding for MCS in I-$\cap$ Beta Region with $\rho = 1.0$

Unc.	Agg.	μ and σ^2	Normal?	M_l	b_l	M_u	b_u
5	sum	fixed	False	0.026	2.355	-0.057	2.499
5	sum	fixed	True	0.001	2.386	0.055	2.432
5	sum	variable	False	2.408	2.064	2.242	6.698
5	sum	variable	True	4.140	0.110	4.245	1.838
10	sum	fixed	False	0.025	4.725	0.051	4.862
10	sum	fixed	True	0.024	4.768	0.254	4.654
10	sum	variable	False	3.209	2.884	2.054	12.922
10	sum	variable	True	3.273	4.124	3.924	4.880
15	sum	fixed	False	0.066	7.042	0.111	7.194
15	sum	fixed	True	0.516	6.405	0.284	6.900
15	sum	variable	False	2.881	6.750	2.154	18.075
15	sum	variable	True	3.120	6.797	3.650	7.715
20	combined	fixed	False	0.447	8.975	0.354	11.101
20	combined	variable	False	0.754	2.243	0.389	131.149
20	sum	fixed	False	0.123	9.293	0.090	9.627
20	sum	fixed	True	0.323	8.907	0.193	9.399
20	sum	variable	False	2.684	11.537	2.255	22.947
20	sum	variable	True	3.087	9.406	3.123	15.250

Table 88: Bounding for MCS in I-J Beta Region with $\rho = 0.0$

Unc.	Agg.	μ and σ^2	Normal?	M_l	b_l	M_u	b_u
5	sum	fixed	False	0.716	0.059	0.162	0.412
5	sum	variable	False	0.670	0.059	0.611	0.752
10	sum	fixed	False	0.831	0.000	0.727	0.106
10	sum	fixed	True	0.934	-0.020	0.836	0.040
10	sum	variable	False	0.759	-0.068	0.775	0.193
15	sum	fixed	False	0.907	-0.025	0.860	0.047
15	sum	fixed	True	0.930	-0.021	0.879	0.044
15	sum	variable	False	0.850	-0.122	0.875	0.097
15	sum	variable	True	0.983	-0.232	0.867	0.149
20	combined	fixed	False	0.604	0.073	0.699	0.136
20	combined	variable	False	0.588	0.016	0.597	5.748
20	sum	fixed	False	0.944	-0.036	0.875	0.057
20	sum	fixed	True	0.920	-0.011	0.936	0.026
20	sum	variable	False	0.869	-0.075	0.855	0.198
20	sum	variable	True	0.947	-0.161	0.970	-0.002

Table 89: Bounding for MCS in I-J Beta Region with $\rho = 0.25$

Unc.	Agg.	μ and σ^2	Normal?	M_l	b_l	M_u	b_u
5	sum	fixed	False	0.519	0.137	0.127	0.500
5	sum	variable	False	0.678	0.018	0.609	0.793
10	sum	fixed	False	0.542	0.184	0.624	0.188
10	sum	variable	False	0.726	-0.087	0.747	0.255
15	sum	fixed	False	0.553	0.300	0.790	0.090
15	sum	fixed	True	0.769	0.072	0.833	0.042
15	sum	variable	False	0.754	0.011	0.783	0.326
15	sum	variable	True	0.822	-0.032	0.780	0.404
20	combined	fixed	False	0.319	0.650	0.311	0.934
20	combined	variable	False	0.454	1.607	0.479	10.062
20	sum	fixed	False	0.579	0.400	0.667	0.359
20	sum	fixed	True	0.806	0.057	0.814	0.104
20	sum	variable	False	0.743	0.267	0.844	0.123
20	sum	variable	True	0.851	-0.143	0.811	0.398

Table 90: Bounding for MCS in I-J Beta Region with $\rho = 0.5$

Unc.	Agg.	μ and σ^2	Normal?	M_l	b_l	M_u	b_u
5	sum	fixed	False	0.472	0.197	-0.048	0.702
5	sum	variable	False	0.597	0.198	0.618	1.073
10	sum	fixed	False	0.428	0.325	0.483	0.343
10	sum	variable	False	0.595	0.217	0.624	0.637
15	sum	fixed	False	0.550	0.292	0.516	0.483
15	sum	fixed	True	0.900	-0.258	0.821	-0.041
15	sum	variable	False	0.665	0.111	0.691	0.611
15	sum	variable	True	0.803	-0.373	0.682	0.743
20	combined	fixed	False	0.272	1.033	0.220	1.862
20	combined	variable	False	0.386	4.989	0.411	16.140
20	sum	fixed	False	0.548	0.431	0.574	0.527
20	sum	fixed	True	0.786	-0.061	0.785	0.020
20	sum	variable	False	0.656	0.429	0.717	0.632
20	sum	variable	True	0.724	0.239	0.701	0.867

Table 91: Bounding for MCS in I-J Beta Region with $\rho = 0.75$

Unc.	Agg.	μ and σ^2	Normal?	M_l	b_l	M_u	b_u
5	sum	fixed	False	0.388	0.402	-0.018	0.874
5	sum	variable	False	0.651	0.460	0.431	2.523
10	sum	fixed	False	0.448	0.415	0.387	0.599
10	sum	variable	False	0.562	0.775	0.622	1.160
15	sum	fixed	False	0.532	0.381	0.370	0.895
15	sum	variable	False	0.616	0.656	0.602	1.507
20	combined	fixed	False	0.291	1.127	0.206	2.867
20	combined	variable	False	0.368	7.507	0.431	25.097
20	sum	fixed	False	0.534	0.493	0.416	1.047
20	sum	variable	False	0.628	0.761	0.627	1.654
20	sum	variable	True	0.831	-0.785	0.884	-0.729

Table 92: Bounding for MCS in I-J Beta Region with $\rho = 1.0$

Unc.	Agg.	μ and σ^2	Normal?	M_l	b_l	M_u	b_u
5	sum	fixed	False	0.172	2.114	0.104	2.282
5	sum	variable	False	1.791	2.783	1.597	7.875
10	sum	fixed	False	0.192	4.241	0.047	4.583
10	sum	variable	False	2.174	5.695	1.368	15.116
15	sum	fixed	False	0.215	6.365	0.139	6.722
15	sum	variable	False	1.660	12.527	1.392	21.527
20	combined	fixed	False	0.578	6.504	0.451	9.659
20	combined	variable	False	0.615	6.554	0.536	116.051
20	sum	fixed	False	0.236	8.468	0.098	9.040
20	sum	variable	False	1.946	15.402	1.214	29.079

Table 93: Bounding for MCS in Pearson Region with $\rho = 0.0$

Unc.	Agg.	μ and σ^2	Normal?	M_l	b_l	M_u	b_u
5	sum	fixed	False	0.839	0.007	0.630	0.212
5	sum	variable	False	0.689	0.067	0.676	0.742
10	sum	fixed	False	0.994	-0.073	0.981	0.026
10	sum	fixed	True	0.920	-0.022	1.072	-0.007
10	sum	variable	False	0.971	-0.349	0.903	0.308
15	sum	fixed	False	0.975	-0.055	1.013	0.005
15	sum	fixed	True	1.029	-0.072	1.017	-0.008
15	sum	variable	False	1.010	-0.379	0.966	0.183
15	sum	variable	True	1.010	-0.288	0.973	0.105
20	combined	fixed	False	0.702	0.006	0.729	0.218
20	combined	variable	False	0.578	0.923	0.708	7.306
20	sum	fixed	False	1.027	-0.092	0.973	0.028
20	sum	fixed	True	1.056	-0.091	0.996	0.013
20	sum	variable	False	1.013	-0.361	0.971	0.169
20	sum	variable	True	1.009	-0.278	1.009	0.054

Table 94: Bounding for MCS in Pearson Region with $\rho = 0.25$

Unc.	Agg.	μ and σ^2	Normal?	M_l	b_l	M_u	b_u
5	sum	fixed	False	0.423	0.171	0.574	0.284
5	sum	variable	False	0.715	0.020	0.646	1.040
10	sum	fixed	False	0.724	0.036	0.648	0.268
10	sum	fixed	True	0.904	-0.095	0.985	-0.053
10	sum	variable	False	0.802	-0.224	0.667	1.082
15	sum	fixed	False	0.853	-0.095	0.761	0.193
15	sum	fixed	True	0.952	-0.199	0.788	0.185
15	sum	variable	False	0.845	-0.361	0.743	0.991
15	sum	variable	True	0.863	-0.252	0.973	-0.330
20	combined	fixed	False	0.468	0.084	0.454	0.713
20	combined	variable	False	0.493	0.529	0.564	12.161
20	sum	fixed	False	0.852	-0.086	0.849	0.073
20	sum	fixed	True	0.960	-0.252	0.849	0.096
20	sum	variable	False	0.809	-0.008	0.702	1.525
20	sum	variable	True	0.892	-0.494	0.927	-0.236

Table 95: Bounding for MCS in Pearson Region with $\rho = 0.5$

Unc.	Agg.	μ and σ^2	Normal?	M_l	b_l	M_u	b_u
5	sum	fixed	False	0.217	0.356	0.215	0.554
5	sum	variable	False	0.554	0.366	0.194	2.371
10	sum	fixed	False	0.618	0.095	0.589	0.379
10	sum	variable	False	0.659	0.119	0.491	1.973
15	sum	fixed	False	0.631	0.138	0.569	0.567
15	sum	variable	False	0.695	0.008	0.631	1.671
20	combined	fixed	False	0.323	0.578	0.279	1.774
20	combined	variable	False	0.391	3.119	0.438	19.719
20	sum	fixed	False	0.654	0.150	0.629	0.530
20	sum	variable	False	0.754	-0.536	0.600	2.324
20	sum	variable	True	0.833	-0.719	0.751	0.573

Table 96: Bounding for MCS in Pearson Region with $\rho = 0.75$

Unc.	Agg.	μ and σ^2	Normal?	M_l	b_l	M_u	b_u
5	sum	fixed	False	0.143	0.563	0.034	0.890
5	sum	variable	False	0.522	0.738	0.104	3.676
10	sum	fixed	False	0.415	0.457	0.235	1.036
10	sum	variable	False	0.562	0.753	0.203	4.413
15	sum	fixed	False	0.514	0.404	0.409	1.030
15	sum	variable	False	0.503	1.631	0.415	4.071
20	combined	fixed	False	0.258	1.465	0.208	3.068
20	combined	variable	False	0.326	7.711	0.292	38.264
20	sum	fixed	False	0.555	0.411	0.426	1.236
20	sum	variable	False	0.580	1.138	0.471	4.275

Table 97: Bounding for MCS in Pearson Region with $\rho = 1.0$

Unc.	Agg.	μ and σ^2	Normal?	M_l	b_l	M_u	b_u
5	sum	fixed	False	0.765	1.679	0.379	2.208
5	sum	variable	False	1.874	2.319	0.890	9.082
10	sum	fixed	False	0.605	3.684	0.364	4.429
10	sum	variable	False	1.171	9.043	0.857	17.349
15	sum	fixed	False	0.472	5.891	0.425	6.520
15	sum	variable	False	1.377	13.127	0.925	24.391
20	combined	fixed	False	0.163	9.750	0.107	12.662
20	combined	variable	False	0.341	31.713	0.175	151.773
20	sum	fixed	False	0.470	7.943	0.431	8.683
20	sum	variable	False	1.102	20.431	1.045	30.441

Table 98: Bounding for MCS in Pearson Region without Pearson IV with $\rho = 0.0$

Unc.	Agg.	μ and σ^2	Normal?	M_l	b_l	M_u	b_u
5	sum	fixed	False	0.927	0.006	0.577	0.317
5	sum	variable	False	1.025	-0.201	0.667	1.063
10	sum	fixed	False	1.005	-0.053	0.920	0.080
10	sum	fixed	True	1.018	-0.035	0.956	0.052
10	sum	variable	False	1.019	-0.325	0.880	0.437
10	sum	variable	True	0.971	-0.134	0.981	0.196
15	sum	fixed	False	1.019	-0.052	0.963	0.056
15	sum	fixed	True	1.025	-0.053	0.978	0.043
15	sum	variable	False	1.033	-0.308	0.930	0.334
15	sum	variable	True	1.026	-0.211	0.966	0.236
20	combined	fixed	False	0.740	-0.029	0.819	0.242
20	combined	variable	False	0.841	-2.969	0.727	9.224
20	sum	fixed	False	1.029	-0.065	0.975	0.055
20	sum	fixed	True	1.002	-0.039	0.997	0.037
20	sum	variable	False	1.030	-0.317	0.955	0.310
20	sum	variable	True	1.012	-0.205	0.996	0.176

Table 99: Bounding for MCS in Pearson Region without Pearson IV with $\rho = 0.25$

Unc.	Agg.	μ and σ^2	Normal?	M_l	b_l	M_u	b_u
5	sum	fixed	False	0.672	0.104	0.500	0.408
5	sum	variable	False	0.831	-0.032	0.656	1.340
10	sum	fixed	False	0.610	0.077	0.861	0.176
10	sum	fixed	True	0.778	0.011	0.895	0.093
10	sum	variable	False	0.650	0.186	0.787	0.960
15	sum	fixed	False	0.758	-0.005	0.900	0.147
15	sum	fixed	True	0.852	-0.058	0.847	0.141
15	sum	variable	False	0.497	0.788	0.497	2.003
15	sum	variable	True	0.818	-0.119	0.920	0.202
20	combined	fixed	False	0.425	0.171	0.444	0.756
20	combined	variable	False	0.435	1.658	0.517	14.639
20	sum	fixed	False	0.806	-0.037	0.888	0.159
20	sum	fixed	True	0.906	-0.120	0.805	0.228
20	sum	variable	False	0.661	0.360	0.612	1.894
20	sum	variable	True	0.925	-0.598	0.994	0.005

Table 100: Bounding for MCS in Pearson Region without Pearson IV with $\rho = 0.5$

Unc.	Agg.	μ and σ^2	Normal?	M_l	b_l	M_u	b_u
5	sum	fixed	False	0.231	0.311	0.132	0.682
5	sum	variable	False	0.409	0.658	0.295	2.467
10	sum	fixed	False	0.386	0.295	0.397	0.656
10	sum	fixed	True	0.670	0.070	0.631	0.267
10	sum	variable	False	0.503	0.560	0.558	2.003
15	sum	fixed	False	0.583	0.155	0.448	0.753
15	sum	fixed	True	0.692	0.063	0.755	0.210
15	sum	variable	False	0.610	0.414	0.667	1.914
15	sum	variable	True	0.745	-0.074	0.799	0.590
20	combined	fixed	False	0.373	0.356	0.279	1.531
20	combined	variable	False	0.420	3.474	0.363	26.514
20	sum	fixed	False	0.526	0.349	0.463	0.937
20	sum	fixed	True	0.701	0.083	0.781	0.239
20	sum	variable	False	0.585	0.743	0.580	2.790
20	sum	variable	True	0.732	-0.007	0.888	0.119

Table 101: Bounding for MCS in Pearson Region without Pearson IV with $\rho = 0.75$

Unc.	Agg.	μ and σ^2	Normal?	M_l	b_l	M_u	b_u
5	sum	fixed	False	0.249	0.494	0.026	0.967
5	sum	variable	False	0.534	0.896	-0.032	4.260
10	sum	fixed	False	0.082	0.821	0.011	1.286
10	sum	variable	False	0.448	1.421	0.064	5.317
15	sum	fixed	False	0.230	0.889	0.172	1.487
15	sum	variable	False	0.367	2.416	0.095	6.533
20	combined	fixed	False	0.326	0.884	0.248	2.395
20	combined	variable	False	0.365	8.210	0.240	48.616
20	sum	fixed	False	0.277	1.044	0.265	1.653
20	sum	variable	False	0.509	1.878	0.177	7.355

Table 102: Bounding for MCS in Pearson Region without Pearson IV with $\rho = 1.0$

Unc.	Agg.	μ and σ^2	Normal?	M_l	b_l	M_u	b_u
5	sum	fixed	False	0.498	1.536	0.265	2.238
5	sum	variable	False	1.037	3.674	-0.191	11.257
10	sum	fixed	False	0.725	3.423	0.299	4.413
10	sum	variable	False	1.115	9.075	0.835	17.495
15	sum	fixed	False	0.549	5.487	0.300	6.590
15	sum	variable	False	0.958	15.484	0.594	26.641
20	combined	fixed	False	0.572	7.110	0.352	11.379
20	combined	variable	False	0.524	20.892	0.362	142.230
20	sum	fixed	False	0.660	7.372	0.386	8.683
20	sum	variable	False	1.256	21.046	0.467	35.028

Table 103: Bounding for MCS in I-$\cup$ Beta Region with $\rho = 0.0$

Unc.	Agg.	μ and σ^2	Normal?	M_l	b_l	M_u	b_u
5	sum	fixed	False	0.896	0.091	0.455	0.578
5	sum	variable	False	0.961	0.153	0.697	1.552
10	sum	fixed	False	0.973	0.016	0.705	0.439
10	sum	fixed	True	0.928	0.033	0.686	0.393
10	sum	variable	False	0.981	-0.020	0.931	0.468
10	sum	variable	True	1.022	-0.139	0.920	0.365
15	sum	fixed	False	0.969	0.003	0.859	0.280
15	sum	fixed	True	0.982	-0.003	0.785	0.318
15	sum	variable	False	0.991	-0.097	0.984	0.292
15	sum	variable	True	0.996	-0.159	0.976	0.275
20	combined	fixed	False	0.940	0.024	0.865	0.364
20	combined	variable	False	0.900	-1.134	0.812	10.619
20	sum	fixed	False	0.976	-0.009	0.924	0.190
20	sum	fixed	True	0.977	-0.008	0.891	0.214
20	sum	variable	False	0.996	-0.119	0.975	0.328
20	sum	variable	True	1.005	-0.171	0.974	0.287

Table 104: Bounding for MCS in I-$\cup$ Beta Region with $\rho = 0.25$

Unc.	Agg.	μ and σ^2	Normal?	M_l	b_l	M_u	b_u
5	sum	fixed	False	0.916	0.109	0.479	0.635
5	sum	variable	False	0.897	0.330	0.648	1.951
10	sum	fixed	False	0.980	0.022	0.678	0.549
10	sum	fixed	True	0.882	0.121	0.523	0.503
10	sum	variable	False	0.985	-0.007	0.807	1.329
15	sum	fixed	False	0.962	0.031	0.735	0.483
15	sum	fixed	True	0.856	0.125	0.713	0.461
15	sum	variable	False	0.999	-0.054	0.826	1.354
15	sum	variable	True	0.929	0.115	0.685	1.435
20	combined	fixed	False	0.918	0.071	0.666	0.972
20	combined	variable	False	0.881	-0.636	0.749	15.945
20	sum	fixed	False	0.978	0.000	0.804	0.440
20	sum	fixed	True	0.905	0.090	0.758	0.441
20	sum	variable	False	0.994	-0.090	0.841	1.479
20	sum	variable	True	0.962	0.064	0.822	1.343

.5 Errors of μ and σ^2 with Assessment Error

Table 105: Bounding for MCS in I-∪ Beta Region with $\rho = 0.5$

Unc.	Agg.	μ and σ^2	Normal?	M_l	b_l	M_u	b_u
5	sum	fixed	False	0.853	0.197	0.480	0.766
5	sum	variable	False	0.914	0.485	0.476	2.996
10	sum	fixed	False	0.966	0.091	0.561	0.839
10	sum	variable	False	1.014	0.100	0.642	2.954
15	sum	fixed	False	0.977	0.076	0.585	0.969
15	sum	variable	False	0.996	0.088	0.654	3.344
20	combined	fixed	False	0.869	0.118	0.555	1.680
20	combined	variable	False	0.989	-1.362	0.615	31.600
20	sum	fixed	False	0.966	0.086	0.561	1.136
20	sum	variable	False	1.041	-0.043	0.617	4.162

Table 106: Bounding for MCS in I-∪ Beta Region with $\rho = 0.75$

Unc.	Agg.	μ and σ^2	Normal?	M_l	b_l	M_u	b_u
5	sum	fixed	False	0.678	0.391	0.296	1.074
5	sum	variable	False	0.945	0.702	0.373	4.350
10	sum	fixed	False	0.941	0.297	0.475	1.416
10	sum	variable	False	0.964	0.933	0.527	5.386
15	sum	fixed	False	0.899	0.370	0.391	1.827
15	sum	variable	False	0.939	1.045	0.576	6.753
20	combined	fixed	False	0.719	0.620	0.706	2.662
20	combined	variable	False	0.942	2.733	0.621	49.912
20	sum	fixed	False	0.948	0.426	0.454	2.128
20	sum	variable	False	0.975	1.255	0.488	8.163

Table 107: Bounding for MCS in I-∪ Beta Region with $\rho = 1.0$

Unc.	Agg.	μ and σ^2	Normal?	M_l	b_l	M_u	b_u
5	sum	fixed	False	0.050	1.336	-0.168	2.142
5	sum	variable	False	0.700	2.461	-0.034	9.306
10	sum	fixed	False	0.167	2.769	-0.254	4.216
10	sum	variable	False	0.445	7.410	-0.107	17.171
15	sum	fixed	False	0.125	4.268	-0.219	6.145
15	sum	variable	False	0.644	11.161	0.088	23.448
20	combined	fixed	False	0.576	4.996	0.600	9.851
20	combined	variable	False	1.183	3.136	0.648	127.876
20	sum	fixed	False	-0.084	6.303	-0.300	8.212
20	sum	variable	False	0.591	15.930	0.191	29.600

Table 108: Assessment Error: Absolute μ error, $\rho = -1.0$

Zone	Scale	HB	EPT	ESM	MCS
I-∪ Beta Region	0.05	0.074	0.079	0.150	0.073
	0.10	0.087	0.084	0.143	0.079
	0.20	0.121	0.097	0.145	0.101
I-J Beta Region	0.05	0.022	0.024	0.033	0.043
	0.10	0.042	0.045	0.044	0.053
	0.20	0.080	0.086	0.076	0.080
I-∩ Beta Region	0.05	0.017	0.017	0.013	0.035
	0.10	0.034	0.034	0.025	0.041
	0.20	0.068	0.068	0.049	0.059
Pearson VI	0.05	0.021	0.019	0.015	0.046
	0.10	0.041	0.037	0.028	0.051
	0.20	0.077	0.075	0.054	0.066
Pearson IV	0.05	0.012	0.014	0.012	0.029
	0.10	0.024	0.026	0.020	0.033
	0.20	0.048	0.053	0.036	0.046

Table 109: Assessment Error: Absolute μ error, $\rho = -0.75$

Zone	Scale	HB	EPT	ESM	MCS
I-∪ Beta Region	0.05	0.074	0.079	0.150	0.073
	0.10	0.087	0.084	0.143	0.079
	0.20	0.122	0.097	0.145	0.101
I-J Beta Region	0.05	0.022	0.025	0.033	0.043
	0.10	0.042	0.045	0.044	0.053
	0.20	0.081	0.086	0.077	0.080
I-∩ Beta Region	0.05	0.018	0.018	0.015	0.035
	0.10	0.036	0.035	0.028	0.042
	0.20	0.071	0.071	0.054	0.062
Pearson VI	0.05	0.022	0.020	0.016	0.046
	0.10	0.042	0.039	0.031	0.051
	0.20	0.079	0.078	0.058	0.068
Pearson IV	0.05	0.015	0.016	0.014	0.030
	0.10	0.029	0.031	0.025	0.035
	0.20	0.058	0.063	0.046	0.051

Table 110: Assessment Error: Absolute μ error, $\rho = -0.5$

Zone	Scale	HB	EPT	ESM	MCS
I-∪ Beta Region	0.05	0.074	0.079	0.150	0.073
	0.10	0.087	0.084	0.142	0.079
	0.20	0.122	0.098	0.145	0.101
I-J Beta Region	0.05	0.022	0.025	0.033	0.043
	0.10	0.042	0.046	0.045	0.054
	0.20	0.082	0.088	0.078	0.082
I-∩ Beta Region	0.05	0.019	0.019	0.016	0.036
	0.10	0.037	0.037	0.031	0.044
	0.20	0.075	0.075	0.060	0.065
Pearson VI	0.05	0.023	0.021	0.017	0.046
	0.10	0.044	0.041	0.033	0.052
	0.20	0.083	0.082	0.064	0.072
Pearson IV	0.05	0.017	0.018	0.016	0.030
	0.10	0.033	0.035	0.029	0.037
	0.20	0.066	0.073	0.054	0.057

Table 111: Assessment Error: Absolute μ error, $\rho = -0.25$

Zone	Scale	HB	EPT	ESM	MCS
I-$\cup$ Beta Region	0.05	0.074	0.079	0.149	0.073
	0.10	0.088	0.084	0.142	0.079
	0.20	0.123	0.098	0.145	0.102
I-J Beta Region	0.05	0.022	0.025	0.033	0.044
	0.10	0.043	0.046	0.046	0.055
	0.20	0.083	0.090	0.080	0.083
I-$\cap$ Beta Region	0.05	0.020	0.020	0.017	0.036
	0.10	0.039	0.039	0.033	0.045
	0.20	0.079	0.079	0.065	0.069
Pearson VI	0.05	0.024	0.022	0.019	0.047
	0.10	0.046	0.043	0.036	0.053
	0.20	0.086	0.087	0.068	0.075
Pearson IV	0.05	0.019	0.020	0.018	0.031
	0.10	0.037	0.039	0.033	0.039
	0.20	0.074	0.081	0.062	0.062

Table 112: Assessment Error: Absolute μ error, $\rho = 0.0$

Zone	Scale	HB	EPT	ESM	MCS
I-$\cup$ Beta Region	0.05	0.074	0.080	0.149	0.073
	0.10	0.088	0.084	0.142	0.080
	0.20	0.124	0.098	0.145	0.102
I-J Beta Region	0.05	0.023	0.026	0.033	0.044
	0.10	0.044	0.047	0.046	0.055
	0.20	0.085	0.091	0.082	0.085
I-$\cap$ Beta Region	0.05	0.021	0.021	0.018	0.037
	0.10	0.041	0.041	0.036	0.046
	0.20	0.083	0.083	0.069	0.072
Pearson VI	0.05	0.025	0.023	0.020	0.047
	0.10	0.048	0.045	0.038	0.054
	0.20	0.089	0.090	0.073	0.078
Pearson IV	0.05	0.021	0.022	0.020	0.032
	0.10	0.040	0.042	0.036	0.041
	0.20	0.080	0.088	0.068	0.067

Table 113: Assessment Error: Absolute μ error, $\rho = 0.25$

Zone	Scale	HB	EPT	ESM	MCS
I-$\cup$ Beta Region	0.05	0.074	0.080	0.149	0.074
	0.10	0.089	0.085	0.142	0.080
	0.20	0.127	0.100	0.147	0.104
I-J Beta Region	0.05	0.025	0.028	0.034	0.044
	0.10	0.048	0.051	0.050	0.058
	0.20	0.093	0.100	0.089	0.092
I-$\cap$ Beta Region	0.05	0.024	0.024	0.021	0.038
	0.10	0.047	0.047	0.041	0.050
	0.20	0.095	0.095	0.081	0.082
Pearson VI	0.05	0.028	0.026	0.022	0.047
	0.10	0.055	0.051	0.043	0.057
	0.20	0.101	0.103	0.083	0.087
Pearson IV	0.05	0.025	0.026	0.023	0.033
	0.10	0.048	0.050	0.042	0.046
	0.20	0.095	0.103	0.081	0.078

Table 114: Assessment Error: Absolute μ error, $\rho = 0.5$

Zone	Scale	HB	EPT	ESM	MCS
I-$\cup$ Beta Region	0.05	0.075	0.080	0.149	0.074
	0.10	0.090	0.085	0.142	0.081
	0.20	0.129	0.102	0.148	0.107
I-J Beta Region	0.05	0.027	0.030	0.035	0.045
	0.10	0.052	0.055	0.052	0.060
	0.20	0.101	0.108	0.095	0.098
I-$\cap$ Beta Region	0.05	0.027	0.027	0.024	0.039
	0.10	0.053	0.053	0.046	0.054
	0.20	0.106	0.106	0.090	0.092
Pearson VI	0.05	0.031	0.029	0.025	0.048
	0.10	0.060	0.056	0.047	0.060
	0.20	0.111	0.113	0.092	0.095
Pearson IV	0.05	0.028	0.030	0.025	0.035
	0.10	0.054	0.057	0.048	0.051
	0.20	0.107	0.117	0.092	0.088

Table 115: Assessment Error: Absolute μ error, $\rho = 0.75$

Zone	Scale	HB	EPT	ESM	MCS
I-$\cup$ Beta Region	0.05	0.075	0.080	0.149	0.074
	0.10	0.091	0.086	0.143	0.082
	0.20	0.131	0.103	0.149	0.108
I-J Beta Region	0.05	0.028	0.031	0.036	0.045
	0.10	0.055	0.059	0.055	0.062
	0.20	0.108	0.114	0.100	0.104
I-$\cap$ Beta Region	0.05	0.030	0.030	0.026	0.040
	0.10	0.058	0.058	0.050	0.057
	0.20	0.115	0.115	0.099	0.099
Pearson VI	0.05	0.033	0.031	0.026	0.048
	0.10	0.065	0.061	0.051	0.063
	0.20	0.120	0.122	0.100	0.102
Pearson IV	0.05	0.031	0.032	0.027	0.036
	0.10	0.060	0.063	0.052	0.055
	0.20	0.118	0.127	0.101	0.097

Table 116: Assessment Error: Absolute μ error, $\rho = 1.0$

Zone	Scale	HB	EPT	ESM	MCS
I-$\cup$ Beta Region	0.05	0.075	0.080	0.149	0.075
	0.10	0.091	0.086	0.143	0.082
	0.20	0.131	0.103	0.150	0.109
I-J Beta Region	0.05	0.029	0.032	0.037	0.046
	0.10	0.057	0.061	0.056	0.063
	0.20	0.112	0.118	0.103	0.107
I-$\cap$ Beta Region	0.05	0.031	0.031	0.027	0.040
	0.10	0.061	0.061	0.053	0.060
	0.20	0.122	0.122	0.104	0.105
Pearson VI	0.05	0.035	0.033	0.028	0.049
	0.10	0.069	0.064	0.054	0.065
	0.20	0.125	0.128	0.105	0.107
Pearson IV	0.05	0.033	0.035	0.029	0.037
	0.10	0.064	0.067	0.056	0.058
	0.20	0.125	0.135	0.107	0.103

Table 117: Assessment Error: Absolute σ^2 error, $\rho = -1.0$

Zone	Scale	HB	EPT	ESM	MCS
I-$\cup$ Beta Region	0.05	0.302	0.264	0.286	0.179
	0.10	0.325	0.252	0.287	0.199
	0.20	0.375	0.262	0.335	0.267
I-J Beta Region	0.05	0.103	0.122	0.128	0.222
	0.10	0.163	0.183	0.166	0.244
	0.20	0.300	0.340	0.257	0.298
I-$\cap$ Beta Region	0.05	0.080	0.079	0.106	0.227
	0.10	0.150	0.149	0.142	0.243
	0.20	0.300	0.301	0.227	0.282
Pearson VI	0.05	0.100	0.096	0.170	0.300
	0.10	0.194	0.173	0.194	0.314
	0.20	0.352	0.348	0.263	0.338
Pearson IV	0.05	0.104	0.115	0.196	0.328
	0.10	0.167	0.185	0.215	0.341
	0.20	0.306	0.362	0.276	0.359

Table 118: Assessment Error: Absolute σ^2 error, $\rho = -0.75$

Zone	Scale	HB	EPT	ESM	MCS
I-$\cup$ Beta Region	0.05	0.302	0.264	0.286	0.179
	0.10	0.326	0.252	0.287	0.199
	0.20	0.375	0.262	0.334	0.267
I-J Beta Region	0.05	0.103	0.122	0.128	0.222
	0.10	0.163	0.182	0.165	0.244
	0.20	0.299	0.339	0.256	0.298
I-$\cap$ Beta Region	0.05	0.078	0.077	0.106	0.227
	0.10	0.146	0.146	0.140	0.243
	0.20	0.294	0.294	0.221	0.279
Pearson VI	0.05	0.098	0.095	0.170	0.301
	0.10	0.190	0.170	0.193	0.315
	0.20	0.347	0.343	0.259	0.337
Pearson IV	0.05	0.103	0.113	0.196	0.328
	0.10	0.161	0.179	0.215	0.341
	0.20	0.292	0.346	0.269	0.359

Table 119: Assessment Error: Absolute σ^2 error, $\rho = -0.5$

Zone	Scale	HB	EPT	ESM	MCS
I-$\cup$ Beta Region	0.05	0.302	0.264	0.285	0.179
	0.10	0.327	0.251	0.286	0.199
	0.20	0.377	0.262	0.334	0.268
I-J Beta Region	0.05	0.103	0.122	0.128	0.222
	0.10	0.164	0.183	0.166	0.245
	0.20	0.301	0.342	0.257	0.299
I-$\cap$ Beta Region	0.05	0.077	0.076	0.105	0.228
	0.10	0.144	0.144	0.138	0.244
	0.20	0.290	0.290	0.216	0.278
Pearson VI	0.05	0.098	0.094	0.171	0.301
	0.10	0.189	0.169	0.193	0.316
	0.20	0.347	0.341	0.256	0.337
Pearson IV	0.05	0.102	0.111	0.197	0.328
	0.10	0.157	0.173	0.215	0.342
	0.20	0.281	0.334	0.264	0.358

Table 120: Assessment Error: Absolute σ^2 error, $\rho = -0.25$

Zone	Scale	HB	EPT	ESM	MCS
I-$\cup$ Beta Region	0.05	0.303	0.264	0.285	0.179
	0.10	0.327	0.250	0.286	0.199
	0.20	0.379	0.262	0.335	0.269
I-J Beta Region	0.05	0.103	0.122	0.129	0.223
	0.10	0.164	0.183	0.167	0.246
	0.20	0.303	0.344	0.258	0.301
I-$\cap$ Beta Region	0.05	0.076	0.075	0.104	0.228
	0.10	0.142	0.141	0.136	0.244
	0.20	0.286	0.286	0.210	0.277
Pearson VI	0.05	0.097	0.094	0.171	0.301
	0.10	0.187	0.167	0.193	0.316
	0.20	0.346	0.339	0.253	0.337
Pearson IV	0.05	0.100	0.110	0.197	0.328
	0.10	0.152	0.168	0.215	0.343
	0.20	0.270	0.320	0.259	0.359

Table 121: Assessment Error: Absolute σ^2 error, $\rho = 0.0$

Zone	Scale	HB	EPT	ESM	MCS
I-$\cup$ Beta Region	0.05	0.303	0.263	0.285	0.179
	0.10	0.328	0.250	0.285	0.200
	0.20	0.380	0.261	0.335	0.270
I-J Beta Region	0.05	0.103	0.122	0.129	0.223
	0.10	0.165	0.184	0.167	0.246
	0.20	0.304	0.346	0.258	0.302
I-$\cap$ Beta Region	0.05	0.075	0.074	0.104	0.228
	0.10	0.139	0.138	0.133	0.245
	0.20	0.281	0.280	0.204	0.276
Pearson VI	0.05	0.096	0.093	0.171	0.302
	0.10	0.185	0.166	0.193	0.317
	0.20	0.345	0.335	0.250	0.337
Pearson IV	0.05	0.099	0.108	0.197	0.329
	0.10	0.148	0.162	0.216	0.343
	0.20	0.257	0.305	0.255	0.359

Table 122: Assessment Error: Absolute σ^2 error, $\rho = 0.25$

Zone	Scale	HB	EPT	ESM	MCS
I-$\cup$ Beta Region	0.05	0.303	0.263	0.284	0.179
	0.10	0.328	0.249	0.284	0.199
	0.20	0.380	0.259	0.333	0.268
I-J Beta Region	0.05	0.102	0.120	0.129	0.223
	0.10	0.162	0.181	0.166	0.247
	0.20	0.298	0.339	0.254	0.300
I-$\cap$ Beta Region	0.05	0.073	0.071	0.103	0.229
	0.10	0.134	0.133	0.130	0.246
	0.20	0.270	0.270	0.195	0.274
Pearson VI	0.05	0.093	0.091	0.172	0.302
	0.10	0.181	0.162	0.192	0.318
	0.20	0.337	0.326	0.245	0.338
Pearson IV	0.05	0.098	0.107	0.198	0.329
	0.10	0.142	0.155	0.216	0.344
	0.20	0.242	0.285	0.251	0.361

Table 123: Assessment Error: Absolute σ^2 error, $\rho = 0.5$

Zone	Scale	HB	EPT	ESM	MCS
I-$\cup$ Beta Region	0.05	0.304	0.263	0.284	0.178
	0.10	0.329	0.248	0.284	0.197
	0.20	0.380	0.257	0.330	0.266
I-J Beta Region	0.05	0.101	0.119	0.128	0.224
	0.10	0.159	0.177	0.164	0.247
	0.20	0.291	0.331	0.249	0.298
I-$\cap$ Beta Region	0.05	0.070	0.068	0.102	0.229
	0.10	0.129	0.128	0.126	0.246
	0.20	0.257	0.257	0.186	0.273
Pearson VI	0.05	0.090	0.089	0.172	0.302
	0.10	0.175	0.156	0.192	0.319
	0.20	0.328	0.313	0.240	0.339
Pearson IV	0.05	0.097	0.105	0.198	0.329
	0.10	0.137	0.148	0.217	0.345
	0.20	0.226	0.264	0.248	0.363

Table 124: Assessment Error: Absolute σ^2 error, $\rho = 0.75$

Zone	Scale	HB	EPT	ESM	MCS
I-$\cup$ Beta Region	0.05	0.304	0.262	0.284	0.178
	0.10	0.329	0.247	0.283	0.196
	0.20	0.379	0.254	0.328	0.263
I-J Beta Region	0.05	0.099	0.117	0.128	0.224
	0.10	0.156	0.173	0.162	0.247
	0.20	0.283	0.321	0.244	0.295
I-$\cap$ Beta Region	0.05	0.067	0.065	0.101	0.229
	0.10	0.123	0.121	0.123	0.247
	0.20	0.242	0.242	0.175	0.273
Pearson VI	0.05	0.087	0.086	0.172	0.303
	0.10	0.169	0.151	0.192	0.319
	0.20	0.317	0.298	0.234	0.340
Pearson IV	0.05	0.095	0.104	0.198	0.330
	0.10	0.131	0.141	0.218	0.346
	0.20	0.209	0.240	0.246	0.366

Table 125: Assessment Error: Absolute σ^2 error, $\rho = 1.0$

Zone	Scale	HB	EPT	ESM	MCS
I-$\cup$ Beta Region	0.05	0.303	0.262	0.283	0.177
	0.10	0.328	0.247	0.281	0.194
	0.20	0.377	0.251	0.322	0.257
I-J Beta Region	0.05	0.097	0.114	0.127	0.224
	0.10	0.149	0.166	0.160	0.247
	0.20	0.269	0.305	0.235	0.292
I-$\cap$ Beta Region	0.05	0.063	0.061	0.099	0.230
	0.10	0.114	0.112	0.119	0.248
	0.20	0.223	0.222	0.162	0.274
Pearson VI	0.05	0.082	0.083	0.172	0.303
	0.10	0.159	0.143	0.193	0.320
	0.20	0.302	0.279	0.228	0.343
Pearson IV	0.05	0.094	0.103	0.199	0.330
	0.10	0.125	0.136	0.219	0.347
	0.20	0.191	0.217	0.247	0.369

Bibliography

[1] Petroleum and other liquids. `https://www.eia.gov/dnav/pet/hist/RCLC1D.htm`. Accessed: 2017-09-13.

[2] A Alpert and H Raiffa. *Judgement under uncertainty: Heuristics and biases*, chapter A progress report on the training of probability assessors., pages 294–305. Cambridge University Press, Cambridge, England, 1982.

[3] J Eric Bickel, Larry W Lake, John Lehman, et al. Discretization, simulation, and swanson's (inaccurate) mean. *Society of Petroleum Engineers Economics and Management*, 3(03):128–140, 2011.

[4] Patrick L Brockett and Yehuda Kahane. Risk, return, skewness and preference. *Management Science*, 38(6):851–866, 1992.

[5] Rex V Brown, Andrew S Kahr, and Cameron Peterson. *Decision analysis for the manager*. Holt, Rinehart, and Winston, 1974.

[6] R. T. Clemen. *Making hard decisions: an introduction to decision analysis, 2nd edition.* Duxbury Press, 1996.

[7] R. T. Clemen and T. Reilly. Correlations and copulas for decision and risk analysis. *Management Science*, 45(2):208–224, 1999.

[8] J.L Coolidge. The gambler's ruin. *Annals of Mathematics*, 10(4):181–192, 1909.

[9] Jitka Dupačová, Nicole Gröwe-Kuska, and Werner Römisch. Scenario reduction in stochastic programming. *Mathematical Programming*, 95(3):493–511, 2003.

[10] R. K. Hammond. *Discrete Approximations to Continuous Distributions in Decision Analysis*. PhD thesis, University of Texas, Austin, 2014.

[11] Robert K Hammond and J Eric Bickel. Approximating continuous probability distributions using the 10th, 50th, and 90th percentiles. *The Engineering Economist*, 58(3):189–208, 2013.

[12] Robert K Hammond and J Eric Bickel. Reexamining discrete approximations to continuous distributions. *Decision Analysis*, 10(1):6–25, 2013.

[13] Robert K Hammond and J Eric Bickel. Discretization precision and assessment error. *Decision Analysis*, 14(1):21–34, 2017.

[14] Ronald A. Howard. Decision alaysis: Practice and promises. *Management Science*, 34(6):679–695, 1988.

[15] A Hurst, GC Brown, and RI Swanson. Swanson's 30-40-30 rule. *American Association of Petroleum Geologists bulletin*, 84(12):1883–1891, 2000.

[16] Christiaan Huygens. *De ratiociniis in ludo aleae*. Ex officinia J. Elsevirii, 1980.

[17] Ronald L Iman and William-Jay Conover. A distribution-free approach to inducing rank correlation among input variables. *Communications in Statistics-Simulation and Computation*, 11(3):311–334, 1982.

[18] Donald L Keefer. Certainty equivalents for three-point discrete-distribution approximations. *Management Science*, 40(6):760–773, 1994.

[19] Donald L Keefer and Samuel E Bodily. Three-point approximations for continuous random variables. *Management Science*, 29(5):595–609, 1983.

[20] Sarah Lichtenstein and Baruch Fischhoff. Do those who know more also know more about how much they know? *Organizational behavior and human performance*, 20(2):159–183, 1977.

[21] Sarah Lichtenstein, Baruch Fischhoff, and Lawrence D Phillips. Calibration of probabilities: The state of the art to 1980. Technical report, DECISION RESEARCH EUGENE OR, 1981.

[22] M.D. McKay, R.J Beckman, and W.J. Conover. A comparison of three methods for selecting values of input variables in the analysis of output from a computer code. *Technometrics*, 21(2):239–245, 1979.

[23] Peter McNamee and John Celona. *Decision Analysis with Supertree*. San Francisco, CA: Scientific Press, 1990.

[24] Robert E Megill. *An introduction to risk analysis*. Penwell Books, Tulsa, OK, 1977.

[25] Allen C Miller III and Thomas R Rice. Discrete approximations of probability distributions. *Management Science*, 29(3):352–362, 1983.

[26] Luis V Montiel and J Eric Bickel. A simulation-based approach to decision making with partial information. *Decision Analysis*, 9(4):329–347, 2012.

[27] Allan H Murphy and Robert L Winkler. Subjective probability forecasting experiments in meteorology: Some preliminary results. *Bulletin of the American Meteorological Society*, 55(10):1206–1216, 1974.

[28] Allan H Murphy and Robert L Winkler. The use of credible intervals in temperature forecasting: some experimental results. In *Decision making and change in human affairs*, pages 45–56. Springer, 1977.

[29] E. S. Pearson and J. W. Tukey. Approximate means and standard deviations based on distances between percentage points of frequency curves. *Biometrika*, 52(3/4):533–546, December 1965.

[30] Karl Pearson. Contributions to the mathematical theory of evolution. ii. skew variation in homogeneous material. *Philosophical Transactions of the Royal Society of London*, 186(Part I):343–424, 1895.

[31] Karl Pearson. Mathematical contributions to the theory of evolution. x. supplement to a memoir on skew variation. *Philosophical Trans. Royal Soc. London*, 197:443–459, 1916.

[32] Karl Pearson. Mathematical contributions to the theory of evolution. xix. second supplement to a memoir on skew variation. *Philosophical Trans. Royal Soc. London*, 216:429–457, 1916.

[33] Svetlovar T. Rachev. *Probability Metrics and the Stability of Stochastic Models*. John Wiley and Sons, 1991.

[34] Svetlozar T Rachev and Werner Römisch. Quantitative stability in stochastic programming: The method of probability metrics. *Mathematics of Operations Research*, 27(4):792–818, 2002.

[35] Svetlozar T Rachev and Ludger Rüschendorf. *Mass Transportation Problems: Applications*. Springer Science and Business Media, 2006.

[36] Terence Reilly. Sensitivity analysis for dependent variables. *Decision Sciences*, 31(3):551–572, 2000.

[37] Ralf E Schaefer and Katrin Borcherding. The assessment of subjective probability distributions: A training experiment. *Acta Psychologica*, 37(2):117–129, 1973.

[38] Antonio Seijas-Macías and Amílcar Oliveira. An approach to distribution of the product of two normal variables. *Discussiones Mathematicae Probability and Statistics*, 32(1-2):87–99, 2012.

[39] JE Selvidge. Experimental comparison of different methods for assessing the extremes of probability distributions by the fractile method. *Management Science Report Series*, 1975.

[40] James E Smith. Moment methods for decision analysis. *Management Science*, 39(3):340–358, 1993.

[41] Lawrence A Tomassini, Ira Solomon, Marshall B Romney, and Jack L Krogstad. Calibration of auditors' probabilistic judgments: Some empirical evidence. *Organizational Behavior and Human Performance*, 30(3):391–406, 1982.

[42] Amos Tversky and Daniel Kahneman. Judgment under uncertainty: Heuristics and biases. *Science*, 185(4157):1124–1131, 1974.

[43] Thomas S Wallsten and David V Budescu. State of the art-encoding subjective probabilities: A psychological and psychometric review. *Management Science*, 29(2):151–173, 1983.